Doctoral Thesis

MICROFLUIDIC APPROACHES FOR QUANTITATIVE ANALYSIS AND SCREENING OF SYNTHETICALLY ENGINEERED MICROBES

Ji Won Lim

Department of Biomedical Engineering

Graduate School of UNIST

2018

MICROFLUIDIC APPROACHES FOR QUANTITATIVE ANALYSIS AND SCREENING OF SYNTHETICALLY ENGINEERED MICROBES

Ji Won Lim

Department of Biomedical Engineering

Graduate School of UNIST

MICROFLUIDIC APPROACHES FOR QUANTITATIVE ANALYSIS AND SCREENING OF SYNTHETICALLY ENGINEERED MICROBES

A thesis
submitted to the Graduate School of UNIST
in partial fulfillment of the
requirements for the degree of
Doctor of Philosophy

Ji Won Lim

December. 21. 2017
Approved by

Advisor
Taesung Kim

MICROFLUIDIC APPROACHES FOR QUANTITATIVE ANALYSIS AND SCREENING OF SYNTHETICALLY ENGINEERED MICROBES

Ji Won Lim

This certifies that the thesis/dissertation of Ji Won Lim is approved.

December. 21. 2017

Advisor: Taesung Kim

Sung Kuk Lee

Cheol-min Ghim

Jaesung Jang

Soon Ho Hong

Table of Contents

List of Figures

List of Tables

Nomenclature

Amp: ampicillin

AQDS: anthraquinone disulfide

BSA: bovine serum albumin

CCD: charge coupled device

Cm: Chloramphenicol

CNT: carbon nanotube

C2C: cell-to-cell

DNA: deoxyribonucleic acid

DC: donor cell

***E. coli*:** *Escherichia coli*

exFAB: extracellular fatty acid biosensor (plasmid)

FAB: fatty acid biosensor (plasmid)

FACS: fluorescent activated cell sorting

FFA: free fatty acid

FITC: fluorescein isothiocyanate

GC: gas chromatography

GFP: green fluorescent protein

HMI: heavy metal ions

HTS: high-throughput screening

Km: kanamycin

LB: Luria-Bertani broth

MEMS: microelectromechanical system

MIC: minimal inhibition concentration

M9: minimal broth

OD_{600}: optical density at 600 nm

PAH: polyallylamine hydrochloride

PBS: phosphate buffered saline

PCR: polymerase chain reaction

PDMS: polydimethylsiloxane

RFP: red fluorescent protein

RNA: ribonucleic acid

RC: reciever cell

SC: sender cell

SEM: scanning electron microscope

SG: specific gravity

TB: tryptone broth

Tet: tetracycline

WT: wild type

UV: ultraviolet

Abstract

Recently, our understanding of complex genomes, proteomes, bio-molecules, and even many metabolic pathways has been developed significantly as growing a fundamental knowledge of the biochemistry of life. These newly revealed findings have incredibly influenced in recent bio-technologies, such as synthetic biology having massive potential to solve the missing connected dots. To have better understanding of microbe, microfluidic approaches were innovatively introduced to the field with the potential to revolutionize high-throughput biological assays.

In this study, suggested approach to address limitations of conventional microbiology is microfluidics integrated with synthetic biology. At first, the microbial biosensors will be introduced into microfluidic ratchet platform for a quantitative analysis of microbial bio-signal. The microfluidic device using microfabricated arrowhead-shaped ratchet structures has an intrinsic function that concentrates motile microbes in a microchamber array. Additionally, the ratchet structure provides the concentrated microbes to grow better in a continuous-feed mode. A continuous exposure of detection analytes leads the amplification of fluorescence signal from microbes in a microchamber. Therefore, it was noted that the substantial amplification of bio-signal was achieved from the microfluidic device and measured signals were analyzed in quantitative manner.

As a second practical application of the microfluidic approach, for high-throughput screening (HTS) application, a fluid array will be developed by using immiscible character between water and oil for microbial incubation, analysis, selective extraction, recovery process and the demonstration of practical applications. From the characterization of the fluid array platform, HTS will be demonstrated based on two different categories: reporter-gene basis and growth complementation basis. The fluid array device showed not only demonstrations of high-throughput screening, but also advanced screening applications were also demonstrated with higher mutant library screening with 10^6 and C2C communication screening system. Outstanding mutants were sophisticatedly screened among 10^6 of a mutant library based on the hybrid type screening method. Also, the proposed C2C screening approach has enabled high-throughput compartmentalization and resulted in 10 possible mutants showing higher extracellular biomolecule secretion performance.

The proposed microfluidic approaches can be practically useful combinations showing many advantages: 1) economical and reduced time requirement for real application without complex

instruments, 2) facile potentials to enable a multiplex quantitative analysis in a high-throughput manner, and 3) selective, direct and convenient measurement without pre- or post-treatment of sample solutions in near future the entire processes could be fully automated. In this dissertation, different type of microfluidic devices was developed for various collaborative purposes for the bottleneck of conventional microbiology. Therefore, the microfluidic devices have knocked a new door for high-throughput screening application for synthetically engineered microorganisms and quantitative approaches for microbial biosensors. Thus, the research contributions in this doctoral dissertation are the microfluidic approaches to popularize and overcome conventional constraints from biological experimental tools by integration of total analysis system for synthetically engineered microbe cases.

Chapter 1. Introduction

1.1 From basic microbiology to microfluidics

Microorganisms are an attractive platform for both a biosensory platform that detects various intra/extracellular biochemicals [1] and a microbial factory that produces various valuable products including many enzymes [2, 3], antibiotics [4, 5], or chemicals [6, 7]. Our understanding of complex biological systems including genomes, proteomes, and metabolic pathways has been broadened with newly revealed knowledge of the biochemistry of the life. As increasing demand both for theoretical and practical application of microorganism, many experimental approaches, from conventional test tubes to the-state-of-arts instruments, have been introduced to the field to investigate better understanding of the biosystem as the useful platform [8]. When its early research phase of using only conventional experimental tools such as test tubes, handmade pipettes, and glass-based apparatuses, it was considerably difficult to examine complex biological system, especially cellular inside. However, due to the increasing use of powerful Micro-Electro-Mechanical Systems (MEMS) tools becoming easily accessible, microbiology researchers and bioengineers begun to use ‘bioMEMS’ as an experimental platform to answer more practical and complex biological questions [9].

1.2 Motivation of microfluidic approaches 1 : Integrative microbial biosensors

Second practical application of the bioMEMS approach in this dissertation was a microfluidic device integrated with a microbial biosensor for heavy metal ion detection [10]. Most of the time, detection of toxic compounds and heavy metals is an important matter for our health issue. In particular, heavy metals such as cadmium, mercury, and lead are found in many industrial wastes, including vehicle emissions, lead-acid batteries, and chemical fertilizers, and they are generally denser than iron. Heavy metals are toxic to cells mostly via oxidative stress [11, 12] and also can accumulate over time in animal bodies, causing lung cancer [13], brain dysfunction [14], softening of bones [15], and kidney disease [16]. Generally, detection of heavy metal ions (HMIs) using conventional methods requires

skilled operation and methods requiring expensive instruments such as atomic absorption spectroscopy [17] and coupled plasma-atomic emission/mass spectroscopy [18], in addition to complex configuration of electrochemical instruments [19].

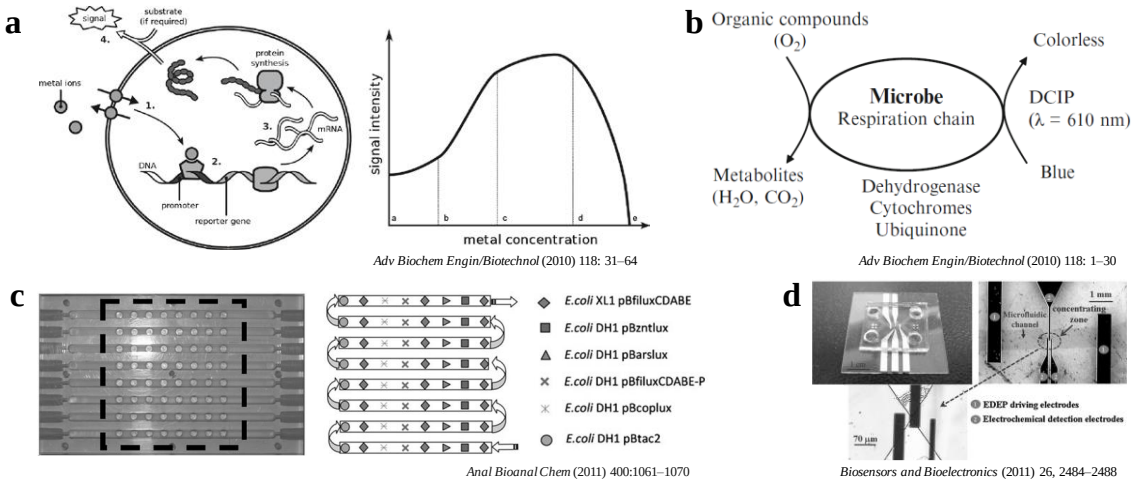

Figure 1. Fundamental mechanism of heavy metal ion biosensor. (a) Whole-cell bioreporters for the detection of bioavailable metals [20]. (b) Applications of microbial cell sensors [21]. (c) A multi-channel bioluminescent bacterial biosensor for the on-line detection of metals and toxicity [22]. (d) Rapid cell sensing chip for low-level arsenite detection [23].

To overcome the limitations of the conventional methods, microbial biosensors, which utilize pre-engineered genetic circuits of live microbes, have been generated with the rapid growth of synthetic biology [24-26]. The microbial biosensors offer considerable advantages: they provide inexpensive and facile detection without complex equipment and provide flexibility for various analyses, and pre- and/or post- processes such as purification and separation are not required. For example, microbial fluorescence-based [27] and luminescence-based biosensors [28, 29] utilize the expression of reporter genes that can be specifically switched on by biochemical interaction events between cellular receptors and inducer molecules (*e.g.* HMIs). The optical or fluorescent signals produced by the microbes can be directly quantified during incubation of the microbes with test solutions, thereby enabling detection of target analytes with unknown concentrations.

Recently, bioreactor systems have been miniaturized to not only shorten diffusion distances and enhance reaction kinetics but also to reduce the labor involved and sample consumption. For example, Gu *et al*. introduced a milliliter-scale bioreactor (58 mL working volume) that can be operated in a continuous and repeatable manner for testing toxic compounds in an aqueous solution. They found that higher growth rates and/or dilution rates enhanced the performance of microbial biosensors [30]. Additionally, Charrier *et al*. reported a bioreactor system with multiple wells that had a diameter of several millimeters and were connected in series. They immobilized microbial biosensors in the multiple wells and then applied a sample solution containing several heavy metals to utilize the

biosensors to express bioluminescence in response to the target analytes [22]. For further miniaturization, several research groups developed microfluidic devices and combined them with microbial biosensors for detecting toxic compounds and HMIs. For instance, Rothert *et al*. used a microbial whole-cell biosensor in a centrifugal microfluidic device to detect six different conditions of HMIs such as arsenite and antimonite by generating selective fluorescence signals from the biosensors [31].

In addition, Garcia-Alonso *et al*. prepared a microfluidic device that had several microchannels in parallel and could screen multiple toxic compounds or a single compound at different concentrations on a chip by using chemical gradients and recombinant yeast cells [32, 33]. These approaches combining a microbial biosensor and a miniaturized device/system provided many advantages, including small sample volume consumption and short analysis time [31-33], high throughput [22, 31-33], and enhanced sensitivity and selectivity, compared to conventional methods [30, 31]. However, most of these approaches appeared to rely on conventional batch-mode culture environments. Basically, the batch-type mixing of microbes and target analytes in a confined solution not only limits the maximum cell growth because of depletion of nutrients but also gradually reduces the number of target analytes available for additional induction over time. In contrast, it is advantageous to provide a continuous nutrient environment for microbes to enable high cell growth rates in a microchamber on a chip [34]. For this reason, a continuous culture and induction environment is essential to enhance detection sensitivity because continuous feeding of nutrients and target analytes (target HMIs) helps enhance the gene expression in the microbial biosensor.[10]

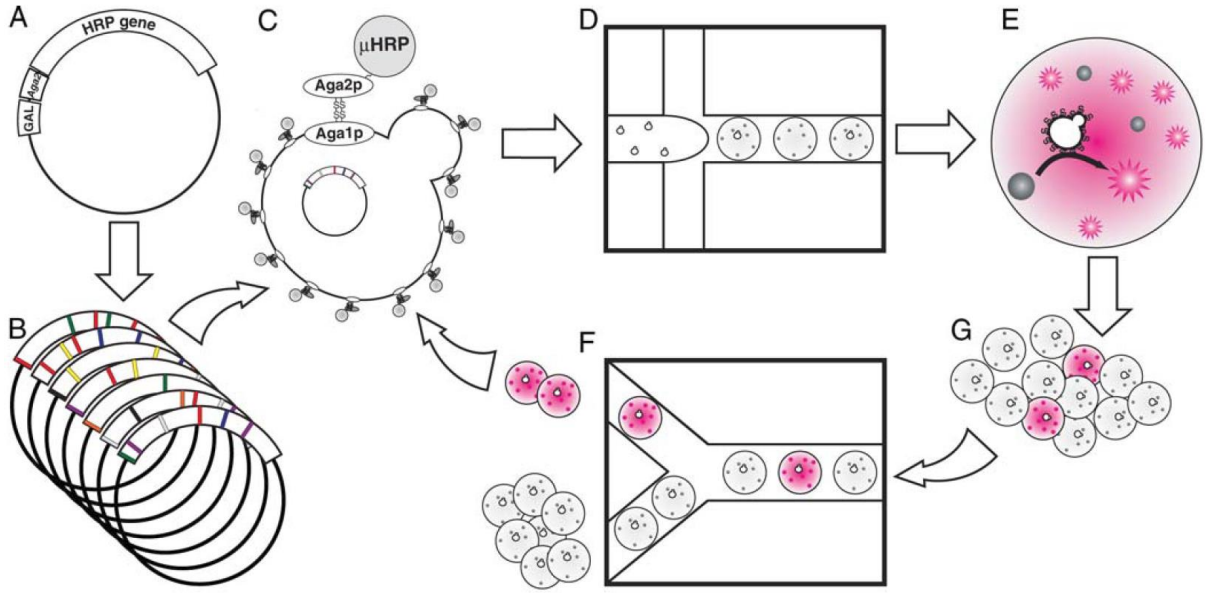

Figure 2. Schematic diagram. The directed evolution of the yeast platform experiment integrated with microfluidic approach. The microdroplet emulsions were broken and released the cells from the microdroplets allowing the cells for recovery, induction, and sorting process. [35]**.**

1.3 Motivation of microfluidic approaches 2 : High-throughput screening

In this dissertation, the bioMEMS integrative approach is suggested and described as an experimental platform to overcome such limitations of the conventional microbiology. Especially, microfluidics was used for the following research projects as the representative platform to realize advanced challenges of microbiology. For the first practical application, a microfluidic fluid array was developed and suggested to apply microbial high-throughput screening (HTS) [36]. Basically wild-type microorganisms do not meet a sufficient level of yield rates for valuable bio-refineries but, with the help of synthetic biology and metabolic engineering, it became possible to make engineered microorganisms produce useful bio-refineries at an economic level. In a microorganism system, enhanced production of bio-refineries may require the alteration of its genotype involved in biosynthesis, regulation, or precursor forming reactions [37-39].

Table 1. Comparison of various conventional screening methods

	Method	Screening performance (Throughput)	Noted	
			Advantages	Disadvantages
Conventional hand-based equipment	Test tubes, flasks	$10^{1\sim3}$	Massive absolute sample number (good for mutation)	Require for many labor
	Petri dishes	$10^{2\sim4}$	Detectable with single colony-based growth and expression	Require for many labor
Conventional instrumental based equipment	Microplate reader	$10^{3\sim4}$	Most widely used	Limited by a plate reading instrument
	GC / LC	$10^{2\sim3}$	Available for post product assay	Low-throughput / limited by analysis instrument
	FACS	$10^{4\sim7}$	High-throughput	Only detectable with fluorescence intensity

Since the rational design of a biological system presents challenges due to the biological complexity, directed evolution and random mutagenic approaches have emerged to create the desired mutants [40-

43]. These approaches easily generate large mutant libraries, making a high-throughput screening (HTS) process unavoidable for the selection of desired mutants. However, it is difficult to analyze a large number of mutants by using conventional laboratory instruments such as culture tubes and a microplate reader. Therefore, an efficient HTS technology is inevitably required to achieve the selection of target cells out of the mutant libraries [36].

For the past decade, microfluidics has achieved great improvements with the potential to revolutionize high throughput biological assays [35, 44-46]. Since this microfluidic technique is a suitable platform for patterning liquid with a fully compartmentalized environment and high-throughput performance, many applications were developed to be an appropriate candidate for a biological assay, for example droplet-based microfluidics [47-50], small bioreactors using complex pneumatic valves [51] and liquid patterning of aqueous phase by immiscible oil separation [52-54]. These microfluidic platforms provide the enormous benefit of compatibility with fully automated experimental systems, minimized scaling of dimensions, reduced reagent consumption and shortened reaction time. Because of the advantages listed above, some researchers developed novel microfluidic devices for liquid patterning, in other words, digitization of sample [52, 54], self-priming [55, 56], and droplet patterning [35, 44-46, 57-63]. Since these liquid patterning technologies fulfill many requirements of the directed evolution by random mutation method, the device can provide a high-throughput screening technique as well as a fully compartmentalized environment for the detection of microbial secreted chemical products [36].

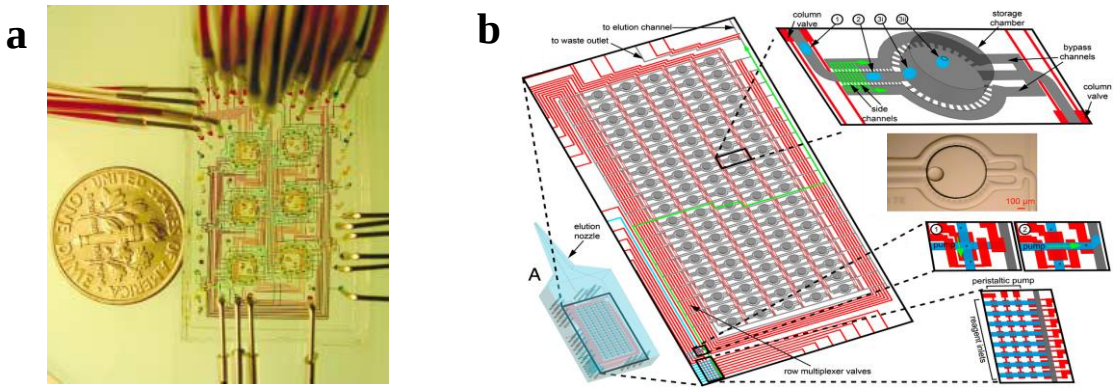

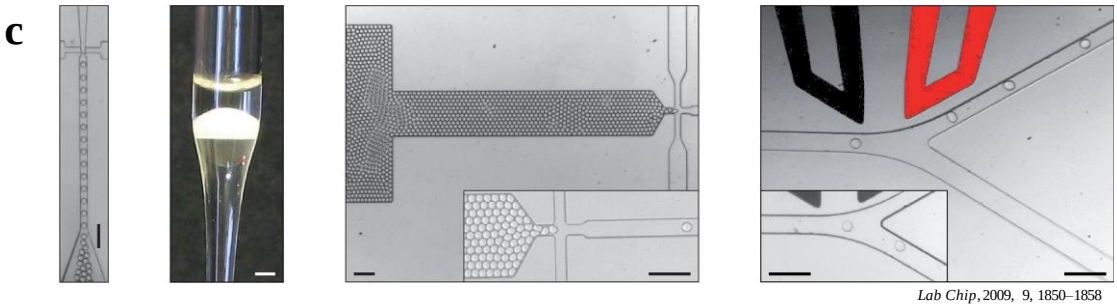

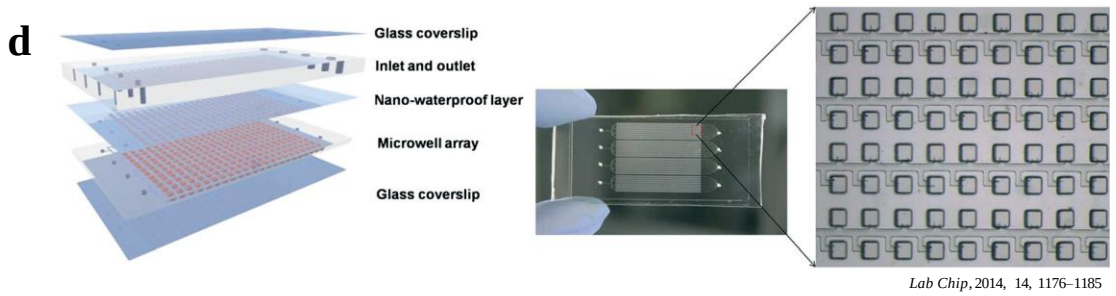

Figure 3. Representative microfluidic devices for various biological applications. (a) Long-term monitoring of bacteria undergoing programmed population control in a microchemostat environment for a small microbial bioreactor [51]. (b) Programmable droplet manipulation device with concentration dilution, separation functions [49]. (c) Fluorescence-activated droplet sorting (FADS) for efficient microfluidic cell sorting based on enzymatic activity [50]. (d) Digital PCR on an integrated self-priming compartmentalization chip [56].

Chapter 2. Theory : Microbial Biosensors in Micro-/Nanofluidic Technologies

2.1 Introduction of microbial biosensors

Biosensors are analytical tools that are generally used to detect or recognize specific elements. Since the first biosensor was developed by Clark in 1962 [64], biosensors, with their great potential, have been widely studied and extensively applied in many situations. Typically, biosensors can be categorized by their fundamental platforms, including antibodies [65], protein receptors [66], enzymes [67, 68], and microorganisms [24-26]. Most of the biosensors in practical and clinical use in recent decades rely on enzymes [69] and nucleic acid oligonucleotides with an array platform [70, 71] due to their high specificity and sensitivity [68]. In parallel, microorganisms have been developed as biosensors and provide many advantages such as the ability to detect a wide range of substrates, reduced cost, mass production, and easier genetic modification compared to other platforms utilizing enzymes and mammalian cells [24-26].

However, determination of target compounds or environmental factors using microbial biosensors seems to be imprecise as it requires traditional analytical methods including test tubes or hand-pipettes, making it highly dependent on the technical skill of the researchers. In addition to such instrumental limitations, the relatively poor sensitivity and selectivity of microbial biosensors are still critical issues and this can be attributed to the nature of biological sensing mechanisms. Another intrinsic limitation of microbial biosensors is the slow response caused by decelerated diffusion of substrates and products through the cell wall [25].

In this research review, not only the academic applications of microbial biosensor development were discussed, but also many cutting-edge micro/nanotechnologies developed for microbial biosensors. First of all, the basic principles of microbial biosensors was discussed. Micro/nanotechnologies categorized by read-out method was then introduced. Many recently developed technologies, instruments, or miniaturization systems with automation functions that have been integrated with microbial biosensors are discussed. In particular, it was focused on recent micro/nanotechnologies as a promising strategy to improve the sensitivity, selectivity, portability, and multiplexity of such microbial biosensors. The advantages of the incorporation of micro/nanotechnologies into microbial biosensors

also were reviewed over conventional methods to overcome the aforementioned limitations. Finally, recent biological technologies for enhancing the performance of microbial biosensors and several future perspectives were discussed [1].

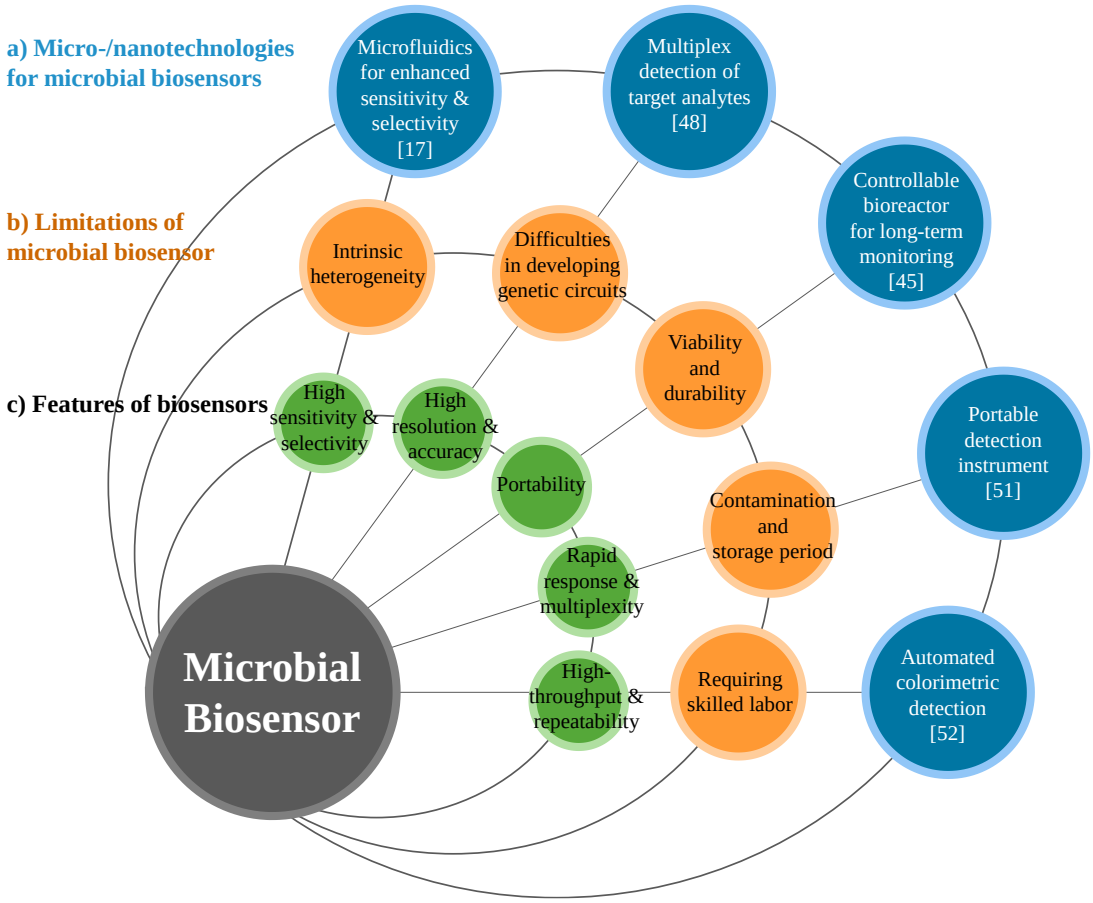

Figure 4. Schematic diagram of microbial biosensor integration with micro-/nanotechnologies. (a) Micro/nanotechnolgies enhancing the performance of microbial biosensors, (b) limitations of conventional microbial biosensors, and (c) general features of biosensors.

2.2 Microbial biosensors in recent decades

2.2.1 Working mechanisms as biosensors

In recent decades, many improved microbial biosensors have been reported, which show promise for a wide variety of applications (*Figure 4.* Schematic diagram of microbial biosensor integration with micro-/nanotechnologies. (a) Micro/nanotechnolgies enhancing the performance of microbial biosensors, (b) limitations of conventional microbial biosensors, and (c) general features of biosensors.). Microbial biosensors are generally defined as analytical devices composed of a microorganism that detects a target substrate and converts the detected signal to a quantifiable response in a physiological, electrical, or biochemical manner. The sensing and recognition mechanisms of microbial biosensors

include various types of conventional optical (*e.g.* fluorescence or bioluminescence) [24, 26], electrochemical [25], and sensory-regulated devices [72]. Prior to delving into the conventional sensing mechanisms, sensory-regulated genetic devices that are classified as emerging biotechnology for microbial sensing mechanisms were briefly reviewed.

Recently, novel molecular biological techniques have significantly improved microbial genetic manipulation and precise metabolic engineering for enhanced production of many useful biochemical signals. To regulate and optimize cell growth, behavior, and transduction of certain biochemicals, all biological systems have evolved with delicate sensory mechanisms. Sensory-regulative biosensors and their mechanisms can detect various cellular signals, and then transduce the signals in optical or electrochemical manner. Also, the regulation of cell behavior or metabolic pathways can be represented in other detectable manners because microorganisms detect not only environmental factors including nutrients, temperature, and pH, but also sense their own metabolic status [72]. In order to sense both intracellular and extracellular signals and then regulate the behavior of cell growth and responses, synthetically engineered biosensors including riboswitches [8], metabolite-responsive transcription factor (MTF)-based biosensors, and other RNA biosensors [73] have been developed in genetic circuit forms with recent progress in synthetic biology. These newly developed biosensors and their mechanisms provide an opportunity to sense other interesting metabolites/analytes with high sensitivity by allosterically regulating the metabolic pathways of microorganisms. The details of biotechnological approaches to microbial biosensors seem to be beyond the scope of this review.

2.2.2 Advantages and limitations

As mentioned earlier, microorganisms such as bacteria and yeast offer a promising strategy for developing microbial biosensors that possess various advantages from many perspectives. First, biosensors based on microorganisms offer an analysis cost for sensing elements that is considerably lower than that of other methods requiring conventional instruments such as gas chromatography, liquid chromatography, mass spectrophotometry, and other methods [74]. Since microorganisms can be produced in massive numbers using a simple culture process and cheap liquid nutrient media, the analysis cost can be dramatically reduced. Second, microbial biosensors show the potential to detect various target elements, and the engineering of such microbial biosensors for specific substrates appears to be easily achieved by using recent molecular biological techniques [72]. Genetic manipulation of microorganisms seems to be better controlled and tailored than engineering mammalian, plant, or other types of biosensors [75]. Third, other types of representative biosensors such as those based on enzymes

or antibodies are comparably unstable and very sensitive to pH and temperature. However, microbial biosensors that can be more robust show an excellent capacity to endure various environmental conditions. Despite the multiple advantages of microbial biosensor over conventional sensing instruments, the widespread use of microbial biosensors is hampered by a few intrinsic limitations of microorganisms such as comparably low sensitivity, which is closely coupled with both cell population size and optical signal [10, 76], poor selectivity in multiplex detection [77], intrinsic cellular heterogeneity both genotypically and phenotypically [78], and stochastic protein expression [79].

2.3 Conventional detection methods

2.3.1 Optical detection methods

Optics has played an important role in biosensor development as a fundamental tool for sensing signals. Microbial biosensors that detect interactions between microorganisms and analytes are no exception. Such interaction induces an engineered genetic circuit in a microorganism to activate a reporter gene for expression of a measurable signal. To quantify the optical signal which is sensitive enough to figure out the interaction between the reporter and inducer molecules, diverse detection systems have been developed. In the early days of development, a photon detector which absorbs photons using a semiconductor film to form electrons and holes for creating a current was used to detect luminescent signals in response to pathogens [80]. Fluorescence microscopy is also used for its wide range of applicability, which can not only measure signal but also provide in situ imaging [81]. Chromatography techniques such as high pressure liquid chromatography are very simple tools that are widely used for detecting colorimetric signals, because the signal can be even observed with the naked eye [82-85]. Following the introduction of microwell plates, use of conventional optical technologies in microbial biosensors became popular, and has led to the use of microbial biosensors in many applications. In particular, microwell plates have been successfully integrated with luminometers, which measure the intensity of luminescent light, to estimate adenosine triphosphate or luciferase and then used for most luminescence-based biosensor experiments [86-88]. Also, fluorescence spectrometers, which are composed of a diffraction grating structure to make a light source monochromatic and a photomultiplier tube to quantify the fluorescent light, are used for fluorescence-based experiments [89-91].

2.3.2 Electrochemical detection methods

Electrochemical microbial biosensors are one of the most widely used platforms for microbial biosensors because of their high sensing accuracy [26] and possible applications such as point-of-care testing devices [92]. Therefore, many researchers and industries have introduced electrochemical microbial biosensors that can detect many types of target materials such as glucose [93, 94], heavy metal ions [95, 96], phenol [97, 98], and other chemicals [24, 99-101]. Electrochemical microbial biosensors generally consist of a working electrode, a transducer layer for detection (microorganisms), and recording equipment. The signal from the transducers, produced by the electrochemical reaction, is recorded and correlated with the concentration and composition of the chemical compounds present, and displayed as an electrical expression. These systems can be classified according to the mechanism used to detect the signal from the transducer: 1) conductometric- 2) amperometric-, 3) potentiometric-, and 4) voltammetric microbial biosensors [25].

Conductometric microbial biosensors detect chemicals by the variation in conductivity of a sample solution via the consumption or production of ions by transducers. They can rapidly detect target chemicals with high sensitivity. In particular, they can easily be miniaturized because they do not require a reference electrode [102]. However, they have a low selectivity for chemical compounds because the variation in conductivity can be affected by electrical charges [103]. Amperometric microbial biosensors express the chemical concentration by recording the current signal through a sample [104]. In particular, amperometric microbial biosensors can provide outstanding sensitivity, owing to the advances made in the current measuring device (< pA) [25]. Potentiometric approaches use the potential difference from a reference (or grounded) electrode, and thus require three electrodes, two working electrodes and a reference electrode. Two major advantages of potentiometric electrochemical microbial sensors are their selectivity for target chemicals and their remarkable sensitivity. However, they are limited by their requirement for a reference electrode for stable and accurate sensing [25]. Voltammetric microbial biosensors are a comparably versatile platform for detection of chemical compounds; they record and correlate each electric signal (electric current and potential difference) with a corresponding sample [105]. Voltammetric approaches can provide high selectivity and measurability *via* the position and density of the peak current signal. However, they require complex components and their detection speed is low.

Currently, micro/nanotechnologies are being rapidly applied to and integrated with electrochemical detection technologies that employ microbial biosensors [106, 107]. The principal goals of such integration of micro/nanotechnologies with electrochemical microbial biosensors are for: 1) miniaturization and portability, 2) high-throughput screening, 3) enhanced sensitivity and selectivity, and 4) simple and rapid immobilization of microorganisms (transducers) which replaces conventional transducers [108].

2.3.3 Detection equipment

Conventional detection equipment for microbial biosensor like microplate readers has been used for establishing the fundamental methods for selecting superior microorganisms, detecting toxic compounds, or monitoring environmental conditions [83, 87, 88]. However, such microplate readers could not completely fulfill the requirement of microbial biosensors. In fact, not only do they show weaknesses in throughput, portability, sensitivity and selectivity, but they also still require the skilled labor to implement the biosensing process. Although microwell plate-based detection has proven useful for enhancing throughput and reducing the consumption of resources, these endeavors did not overcome the limitations of even higher sensitivity, full automation, or provide a portable usage environment. These unsolved complications became the motivation for novel integration with micro/nanotechnology, which is attracting attention from both the scientific and industrial communities.

2.4 Micro/nanotechnological detection methods

To overcome the limitations of conventional detection methods, several examples of innovative integration of microbial biosensors with recent micro/nanotechnologies have been proposed in the past decade. For instance, microfluidic systems showed many advantages by minimizing the sample and reagent volumes required, shortening analysis time with high resolution and repeatability, and demonstrating multiple assays on a chip in a high-throughput manner [10]. In addition, it was demonstrated that microfluidic systems can not only provide microorganisms with an ideal cell culture microenvironment that is close to in vivo one [80], but also enable high portability and more rapid analysis compared to conventional methods [81]. Moreover, micro/nanofabrication showed remarkable potential for microbial biosensors from the viewpoint of 1) enhanced optical and electrochemical measurements, 2) improved immobilization and automated culture environments, and 3) high portability and more practical applications. In the following sections, various micro/nanotechnologies that can effectively improve microbial biosensors will be discussed in comparison with conventional analytical methods [82].

2.4.1 Microfluidics

Microfluidic technology has been used for a broad range of biological assays. Especially microfluidic technology provides various, miniaturized cell-culture environments in a small scale, which facilitate not only sensitive [10, 109] and parallel analysis [110] of cell cultivation and/or fermentation in a high-throughput manner but also the concentration gradient generation for multiplex analysis [10, 111]. It is noted that this feature is appropriate for the microbial biosensor because microfluidics technology reduces cost and labor and improves sensitivity and selectivity with high resolution. For example, Biran *et al.* fabricated a novel microwell by using optical fiber to improve the sensitivity [112]. A different etching rate between the core and the cladding in the optical fiber was used to form a well on the core part and a wall on the cladding part. Since the core size was appropriate for immobilizing a single cell in each microwell, it facilitated multiple individual microbial biosensors with high sensitivity. Using this method, the mercury concentration was able to be detected by measuring the fluorescent signal from individually immobilized *E. coli* RBE27-13 harboring pECFP. Also, Rothert *et al.* reported a centrifugal microfluidic platform integrated with the microbial biosensor to reduce time and resource consumption, and increase portability [113]. Computerized numeric control machining was used to fabricate poly(methyl methacrylate) in the shape of a compact disk, and centrifugal forces made the mixing process efficient between the reagent and E. coli AW10 harboring pSD10. This microfluidic platform reduced the resources consumed but the analytical performance of the microbial biosensor for detecting arsenite and antimonite was not affected, showing the advantage of microfluidic integration with microbial biosensor.

Additional miniaturization was incorporated by using micro/nanofabrication technologies and was further facilitated by soft-lithography [114]. In particular, microfluidic devices are made of polydimethylsiloxane (PDMS), which is a representative material for microfluidics, is transparent and biocompatible, and is appropriate for a biosensor platform. Because soft-lithography allows flexible channel design, microfluidic devices can be used for microbial biosensors to screen different toxic compounds in separated and parallel channels, enabling a high-throughput assay on a chip. For instance, García-Alonso *et al*. reported eight parallel microfluidic channels used for detecting methyl-methanesulfonate, depending on its concentration [115]. This tool facilitates a rapid qualitative measurement of the harmfulness of the toxic material on the Saccharomyces cerevisiae RAD54.

A PDMS microfluidic device for a microbial biosensor has been developed to improve sensitivity by magnetically controlling position or increasing the number of bacterial cells. For example, a microfluidic device integrated with magnetically functionalized reagents was developed by García-Alonso *et al.*, which facilitated removal and relocation of microbial biosensors conveniently [116]. The yeast cell was magnetized for easy handling of its position by coating polyallylamine hydrochloride(PAH)-stabilized magnetic particles, which are positively charged (*e.g.* 15 nm in

diameter). Since the used cells can be easily discarded by the flow of culture media without external magnets, the device can be reused with good reproducibility. The technique appears to resolve the problem of cell retention, which is a major hurdle in the development of microfluidic devices, and make it easy to control the nutrient conditions and analyte input. Also, a novel magnetotactic bacterium, Magnetospirillum gryphiswaldense MSR-1, has been developed by Roda *et al*. (*Figure 5a*) [117].

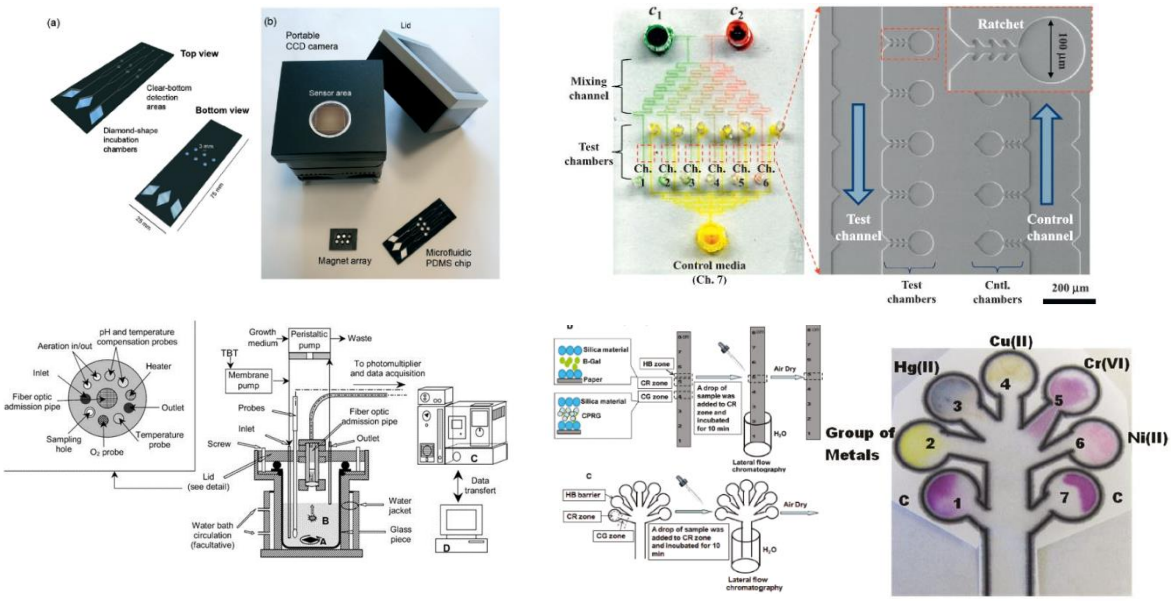

Figure 5. Various micro/nanotechnologies for enhancing the performance of microbial biosensors. (a) A magnetotacic array device was introduced that can improve the positioning of microbial biosensor by separating a detection area from a cultivation area [117]. (b) A microfluidic device was developed for multiplex detection of small volume samples [10]. (c) Miniaturized bioreactor facilitates not only the cultivation of bacterial cells but also the real-time monitoring of toxic material at a practical level [118]. (d) An inkjet-printed paper based liquid chromatography method facilitates the multiplex detection with naked eye [119].

A permanent magnet trapped the bacteria in a detection area that was in contact with a charge coupled device sensor. Since the position of the bacteria could easily be controlled, not only it was easy to wash them out and reuse the instrument but it also increased sensitivity by decreasing the noise-to-signal ratio because the culturing and detecting positions were placed far apart. In addition, a novel microfluidic device was introduced that allowed continuous supply of nutrient for increasing cell growth rates and the number density in a microchamber (*Figure 5b*) [10]. Because the device implemented a microfabricated ratchet structure to prevent motile bacterial cells, *E. coli* HK621 and HK622, from escaping from a culture microchamber, the accumulated fluorescent signals were significantly amplified over time. The microfluidic device increased the sensitivity of microbial

biosensors over three orders of magnitude compared to conventional methods in heavy metal detection. In addition, it showed high potential for a high-selective microbial biosensor platform.

2.4.2 Microbioreactors

For various biological assays, optimization studies for initial environmental conditions are typically performed in miniaturized-scale under several conditions as similar as possible to the actual large-scale conditions for industrial cultivation and fermentation. These optimization approaches are often called the scale-down approach [120]. Gu *et al.* developed a miniaturized bioreactor for reducing the working volume while retaining the main function of the conventional bioreactor [121]. This bioreactor was composed of a culturing chamber, injected air, a water-based temperature controller, cell inoculation, and chemical injection parts. This instrument made it possible to conduct long-term continuous experiments using only a small amount of medium; it required approximately 4 L per week by using *E.coli* TV1061 harboring pGrpELux5. Based on the initial miniaturized bioreactor mentioned earlier, a multi-channel bioreactor has also been developed for detecting multiple components [122]. Four different bioluminescent bacteria, *E.coli* DPD2794, DPD2540, TV1061, and GC2, were placed in each channel for testing, for example, water samples. Since the small size allowed minimal media consumption and easy setup, this instrument was very economical. Thousand *et al*. have improved a bioreactor through the addition of oxygen and a pH controller (*Figure 5c*) [118]. These additions allowed more sensitive detection due to stricter regulation, which is basically important for cell growth rates.

2.4.3 Micro/nanofabrication

Micro/nanofabrication processes have been actively developed and applied to various research and industrial fields during the last two decades. This seems to be possible because of numerous developments in machining tools and measuring equipment [123]. In this context, micro/nanofabrication techniques are also applied to and integrated with electrochemical detection using microbial biosensors. Typically, micro/nanofabrication is combined with microbial biosensors for several improvements such as a stable and simple process for transducer immobilization and miniaturization for high-throughput screening [124].

The photolithography technique is a fundamental micro/nanofabrication process for fabrication of miniaturization systems. Micropatterned electrodes can easily be fabricated on a silicon wafer using a

photo mask and vacuum evaporation of metallic ions such as gold and platinum [125]. Therefore, a miniaturized electrode can dramatically increase the reaction speed of sensors when applied to electrochemical microbial biosensors. For example, Popovtzer *et al*. suggested using photolithography for detection of water toxicity by microbial biosensors (*Figure 6a*) [126]. Eight miniaturized sensor cells were integrated on a single disposable chip with a partial gold coating, allowing individual operation. Each chamber consisted of three embedded electrodes: a gold working electrode, a counter electrode, and a reference electrode, respectively. Using the fabricated chip, they measured the potentiostatic signal from microbial biosensors and then determined the presence of ethanol and phenol in water.

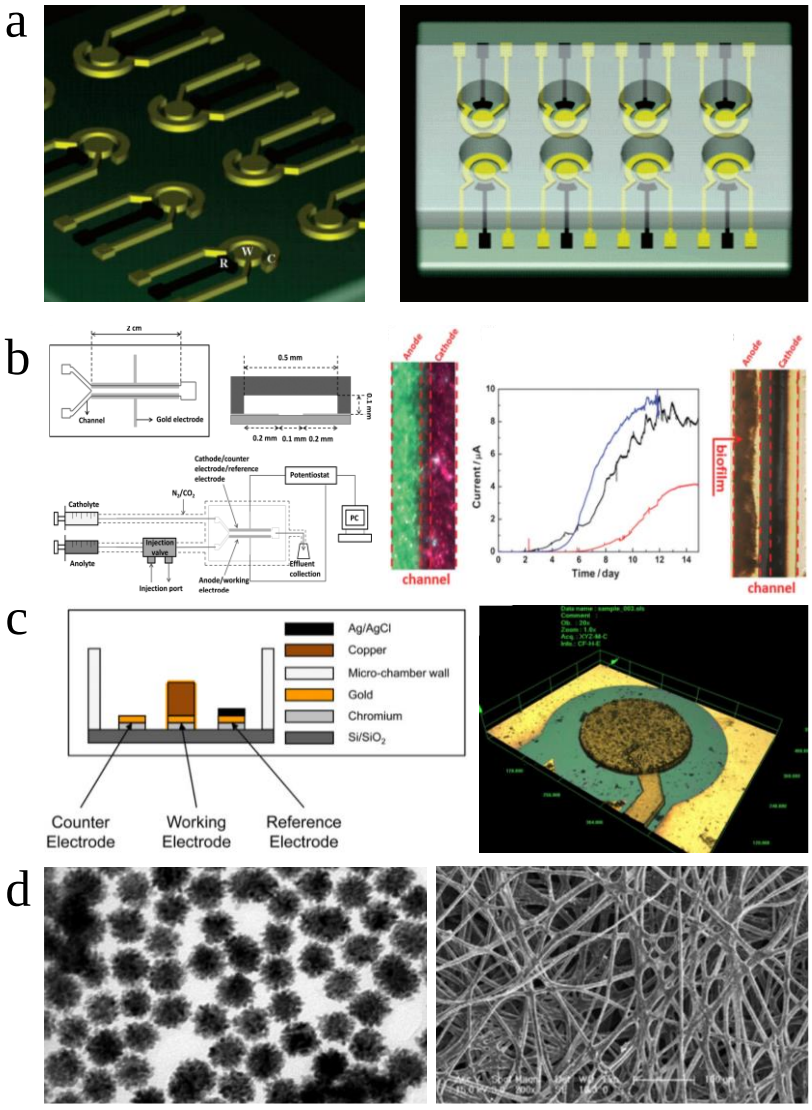

Figure 6. Novel micro/nanoscale structures and materials for enhancing the performance of electrochemical detection of microbial biosensors. (a) A miniaturized microbial biosensor was integrated with eight electrochemical sensing cells fabricated by photolithography techniques. Toxic materials such as phenol and ethanol in water were detected in a high throughput manner [126]. (b) A microfluidic device enabled microbial biosensors to conduct quantitative analysis and live monitoring

of AQDS. Laminar flows generated by a Y-shape microfluidic channel network made it possible to reduce reaction and response time in electrochemical detection [127]. (c) Electrodes were fabricated by using microfabrication techniques including deep reactive ion etching and then applied to microbial biosensors. Since the microstructured electrodes enhanced electric signal from microbial biosensors, the induction factor improved over two times [128]. (d) Metallic nano-particles integrated with silk microfibers showed remarkable sensing ability for the detection glucose in various concentrations [129].

In addition, with recent advances in photolithography techniques, many microfluidic devices have also been combined with electrochemical microbial biosensors. The integration of microfluidic devices provides numerous advantages for high-throughput screening via miniaturization. Li *et al*. reported a laminar-flow based microfluidic device for live monitoring and quantitative analysis of anthraquinone disulfide (AQDS) in solution (*Figure 6b*) [127]. In particular, they used laminar flow in microchannels for elimination of the separation membrane, which was an essential element in previous microfluidic devices. Furthermore, it can provide a short hydraulic retention time (*e.g.* 2 min) and a rapid response time (< 21 min) for Geobacter sulfurreducens cells by continuous provision of substrate.

When combined with electrochemical microbial biosensors, screen-printed electrodes (SPEs) provided several improvements such as a low detection limit, a simple fabrication process, and a wide range of printing materials. Additionally, SPEs were used for enhanced immobilization of microorganisms on the working electrode [130]. Shitanda *et al*. fabricated an amperometric microbial biosensor using a carbon electrode on which biomaterials had been printed [131]. The ink suspension (algae, sodium alginate solution, and cells) was printed onto the screen-printed carbon electrode and directly immobilized there via cross-linking using a $CaCl_2$ solution. Hence, the microbial biosensor could amperometrically detect atrazine, using Chlorella vulgaris cells. This device introduced a simple immobilization process and demonstrated cost-effectiveness and high portability compared with previous algal biosensors. Another miniaturized electrochemical microbial biosensor was developed by Ben-Yoav *et al*. (*Figure 6c*) [128]. They integrated a pillar structure on a silicon wafer and coated a metallic substrate with three-dimensional (3D) nanostructures, using the deep reactive ion etching process, electrodeposition, and electro-polymerization of a conducting polymer (polypyrrole, PPy). They confirmed the effects of electrode materials such as copper and gold. Additionally, they investigated the effect of increasing the surface area using an electrodeposited and PPy-coated 3D micro/nanostructure. Finally, they successfully showed that surface-modified electrodes can significantly increase the signal from microorganisms.

2.4.4 Micro/nanomaterials

Micro/nanomaterials have been drawing significant attention for electrical and chemical modification of substrates because they possess outstanding electrochemical properties derived from the large surface-to-volume ratio and the rapid transport of electrons. For this reason, many researchers attempted to employ micro/nanomaterials to modify and/or functionalize electrodes and then integrate them with microbial biosensors. As a result, the sensitivity of electrochemical microbial biosensors significantly improved. The most popular micro/nanomaterial seems to be carbon nanotubes (CNTs) [132] because addition of CNTs can easily modify electrodes. For example, they can increase electrical conductivity, functionalize cationic surfactant to stabilize certain molecules, and improve response time towards, thereby resulting in the improvement of microbial biosensors. Of course, conventional CNT-based electrodes have some weaknesses such as high background current (noise) and a decreased electron diffusion rate during operation due to overlapping of the diffusion layer. Timur *et al*. introduced a method for modifying CNT-based electrodes using a mixture of CNT and redox osmium (Os-redox) polymer solution to overcome the noise-to-signal ratio limitations [133, 134]. They optimized the required conditions for phenol detection using Pseudomonas putida cells. This was possible by using a mixture of CNT and Os-redox polymer and manipulating pH and temperature as well.

In addition, some different and integrative approaches were taken for modifying electrodes with nanoparticles and microfibers. In particular, Deng *et al.* developed a novel device for electrochemical microbial biosensors by using a silk-derived (S-derived) carbon fibrous mat with metallic nanoparticles (Au-Pt) (*Figure 6d*) [129]. The micro/nanomaterial used in their work contained amino groups in the fibrous component, allowing self-assembly of nanoparticles on the carbon fibrous mat. The immobilization of S-derived carbon fibers on nanoparticles allowed the efficient electron tunneling that in turn amplified the electrical communication between the microbial biosensor and the electrode surface. This resulted in a novel microenvironment that sustained the bioactivity of microbial biosensors, showing high sensitivity and a low detection limit compared with commercialized carbon paper-based biosensors.

2.5 Micro/nanotechnological platforms for microbial biosensors

2.5.1 Automation, portability, and multiplexity platforms

Micro/nanotechnology has contributed to the development of new instruments for 1) fully automated processes [135], 2) miniaturization for portability [136], and 3) complexed multicomponent detection [137]. First, a semi-automated system has been developed by Knight *et al*. to reduce the time

required for measuring the fluorescent signal of RAD54 protein in Saccharomyces cerevisiae [138]. The combination of a laser light source, a detector, and an automated cell culture chamber enabled continuous measurements of fluorescent signals, which in turn were rapidly processed in real-time. Although it was a prototypic semi-automated instrument, a reliable result could be acquired 6 times as fast as using a standard colony-based growth test. An instrument has also been developed by Cho *et al*. for automated and continuous detection systems with low cost, which was composed of robot arms, multiple microwell plates, a temperature controller, and a photo-multiplier tube sensor used for measuring the intensity of light with a photoelectron [135]. The robot arms made it possible to conduct experiments continuously, without manual control, enabling real-time toxicity monitoring at 10-min intervals for up to a month. By using this instrument, the toxicity of wastewater samples without further purification was detected by Janthinobacterium lividum YH9.

Second, significant research efforts have been made for portable detectors because portability became an important issue for practical applications of microbial biosensors and the demand for in situ testing had led to the improvement of portable microbial biosensors. Most recognition and detection systems are composed of a biosensing chamber, a light-proof chamber, and a luminometer. For example, a freeze-drying method was developed by Choi *et al*. to extend the period of use of the portable biosensor so that sensor cells, E.coli DPD2794, DPD2540, TV1061, and GC2, can easily be transported and used for environmental detection and monitoring after rehydration of lyophilized cell [136]. This portable biosensor kit showed remarkable potential for practical application; it was achieved by increasing the retention period. Also, a portable microbial biosensor was reported by Berno *et al*., which detects benzene not only in laboratory samples but also in outdoor samples for in situ testing [139].

Third, basically the multiplexity of a biosensor determines practicality because the performance of the biosensor is decided not only by its portability but also by its capability to deal with multiple components in a single process. For example, Charrier *et al*. reported that integration of removable multi-well cards, an optical setup for bioluminescence monitoring, a fluidic channel network for media and sample loading, and a computer interface for full automation, allowed the detection of multiple components [137]. Four bacterial cells, *E. coli* DH1 pBzntlux, pBarslux, pBcoplux, and XL1 pBfiluxCDABE, were immobilized in an agarose matrix on a multi-well card, media and samples were flown along the fluidic channels, bioluminescent signals from *E. coli* were measured by a CCD camera, and all experiments were controlled and all data processing were automated by a computer. Although the microbial biosensors showed intrinsic weaknesses in cross-talk and synergistic effects for a heavy metal mixture, it was well demonstrated that a multiplex detection using microbial biosensors can be incorporated.

Table 2 Comparison of microbial biosensors integrated with micro-/nanotechnologies

Integrated technology	Microorganism	Detection method	Substrate	Dynamic range/(LOD)	Improvements
Instrument					
Automated	*S. cerevisiae*	Fluorescence	Methylmethan sulfonate (MMS)	0.01%	Reducing time compared with Ames Test (6 times faster) [138]
Automated	*J. lividum*	Luminescence	EC_{50}		Real-time automated toxicity monitoring for a month [135]
Portable	*E. coli*	Luminescence	Phenol	0.15 mM ~ 5 mM	Increasing the retention period by using freeze-drying method [136]
			Mitomycin C	0.27 ppm ~ 2 ppm	
			H_2O_2	0.0006% ~ 0.0025%	
			Ethanol	1% ~ 3%	
Portable	*E. coli*	Luminescence	Benzene	0.5 ppm	Introduction of battery for in situ test [139]
Multiplexed	*E. coli*	Luminescence	Arsenic / Cd	5 μM / 0.5 μM	Multiplexed detection by immobilization in multi-well kit [137]
Multiplexed	*E. coli*	Colorimetry	Hg / Ag	0.002 ppm	Multiplexed detection by inkjet-printing assisted colorimetry [119]
			Cu / Cd	0.02 ppm	
			Pb / Cr	0.14 ppm	
			Ni	0.23 ppm	
Microfluidics					
Microwell	*E. coli*	Fluorescence	Hg	100 nM	Improved sensitivity by separating the *E. coli* individually [112]
Compact Disk	*E. coli*	Fluorescence	Arsenite	1 μM ~ 5 mM	Reducing the consumtion of resource by miniaturized platform [113]
			Antimonite		
PDMS chip (magnetic)	*S. cerevisiae*	Fluorescence	MMS	0.28 μM ~ 450 μM	Improved sensitivity by regulating the position of yeast [116]
PDMS chip (magnetic)	*M. gryphiswaldense*	Luminescence	DMSO	2% ~ 50%	Improved sensitivity by regulating the position of *E. coli* [117]
			Taurochenodeoxycholic acid (TCDCA)	0.001 mM ~ 10 mM	
PDMS chip	*E. coli*	Fluorescence	Cd	2 nM ~ 20 μM	Improved sensitivity by accumulating *E. coli* and multiplexed design [10]
			Hg	2 nM ~ 20 μM	
Microfluidic	*G. sulfurreducens*	Amperometric	Anthraquinone disulfide (AQDS)		Live monitoring, quantitative analysis [127]
Bioreactor					
Miniaturized bioreactor	*E .coli*	Luminescence	Ethanol	3.4%	Reducing time and the consumption of resources by miniaturized bioreactor [121]
Miniaturized bioreactor	*E. coli*	Luminescence	Tributyltin	0.02 μM	Improved sensitivity by regulating the oxygen and pH [118]
Miniaturized bioreactor	*E. coli*	Luminescence	Pheonl	300 ppm	Multiplexed detection by miniaturized parallel bioreactor [122]
			Mitomycin	50 ppb	
			Cerulenin	5 ppm	
Micro-/nanofabrication					
Photolithography	*E. coli*	Voltametric	*p*-aminophenol		Miniaturization, eight testing chamber on single chip [126]
Screen printing	*E. coli*	Amperometric	Methyl parathion	2 ~ 400 μM	Miniaturization, reproducibility, stability [131]
DRIE process	*E. coli*	Amperometric	Nalidixic acid		Improved detection signal [128]
Micro-/nanomaterials					
Carbon nanotube (CNT)	*P. putida*	Amperometric	Phenol	0.5 ~ 4 mM	Prevent electric noise signal [133, 134]
Microfiber-nanoparticle	*E. coli*	Amperometric	Glucose	0.25 ~ 0.55 mM	Self-assembly of nanoparticle (microfiber), improved electric properties [129]

2.5.2 Screening platform

Up to now, it was reviewed that a broad range of micro/nanotechnlogies is suitable for microbial biosensors to better detect target chemical compounds and/or environmental factors. In this section, it should be shortly emphasize that micro/nanotechnologies have high potential for providing an unprecedented screening platform that overcomes critical technological limitations of conventional platforms including instruments and methods. In particular, it is worthy to discuss micro/nanotechnological screening platforms for microbial biosensors because they facilitate the screening process of a large number of combinatorial library in a high-throughput manner; the larger is the mutant library size, the higher the chances are expected to find desired, optimal microbial biosensors (strains). Of course, the sensory-regulative biosensors are closely correlated with various screening platforms for both the identification of synthetic biosensors and the selection of most efficient biosensors out of the combinatorial library. On the other hands, the conventional screening platform appears to be unsuitable for dealing with such a large mutant library size because of the low throughput [72].

Here, two representative micro/nanothnological screening platforms were reviewed. First, Wang *et al.* successfully integrated a microfluidic system with a sensory-regulative microbial biosensor for cellular metabolite analysis [140]. A single microorganism is encapsulated and compartmentalized in the microfluidic microdroplet platform. The platform allowed high-throughput analysis of extracellular secreted metabolites and recognition of genetic elements that were responsive to allosteric regulative effects. Using the microfluidic platform with sensory-regulative riboswitches, the xylose over-consuming strain was effectively enriched and identified as a representative result. It appears to be impossible to achieve such accomplishment using conventional experimental platforms especially due to the limited throughput. In other words, it is obvious that not only the selection of extraordinary sample but also the identification of riboswitches benefited from micro/nanotechnologies. Second, another microfluidic platform was introduced by Karns *et al*. [141], which implemented electrophoretic mobility shift assays of microbial riboswitches from Bacillus subtilis on a chip. The electrophoretic mobility shift assay by the microfluidic platform enabled more promising and quantitative analysis of riboswitches. Therefore, the microfluidic platform has demonstrated its potential or ability to provide a facile library screening means via selection and validation of novel riboswitches. Although these types of integrative approaches have just begun the very first step toward the high-throughput screening platform, it is highly believed that micro/nanotechnologies can effectively incorporate a novel screening

platform for microbial biosensor that can be further accelerated with the aid of sensory-regulative biosensors and riboswitches.

2.6 Conclusion and future perspectives

In this review, the integration of micro/nanotechnologies with microbial biosensors and their applications were discussed previously. Microbial biosensors have been under a wide range of investigations in recent decades, but they seem to be typically limited by several factors such as low sensitivity, poor selectivity, difficult sensor engineering, and stochastic heterogeneity. With the rapid expansion of interdisciplinary convergence research, microbial biosensors have been integrated with many recent micro/nanotechnologies to overcome such limitations. Also, sensory-regulative biosensors are emerging as a novel sensing mechanism. These innovative regulative microbial biosensors, including riboswitches, require efficient screening methods to select extraordinary samples from numerous possible combinations. Hence, micro/nanotechnological screening platforms such as microfluidics platforms have been introduced with an effective integration strategy. Far more practical platforms than presented here can be developed and used to provide wider insight into how the microbial pathway dynamically controls the overall microbial status, including cell viability, genetic communication processes, and up-down regulation of productivity for various targets.

First of all, micro/nanotechnologies have contributed to improving the performance of optical microbial biosensors by considerably ameliorating the problems posed by conventional optical detection methods. In parallel, micro/nanotechnologies have revolutionized the electrochemical detection sensitivity and selectivity of microbial biosensors. To date, many attempts made to combine micro/nanotechnologies with microbial biosensors were proven successful because they fulfilled various demands from the industrial and environmental fields through miniaturization and high-throughput assay on a run. In addition, automation and miniaturization of instruments and bioreactors with optical/electrochemical detection systems allowed microbial biosensors to be used in an effective, efficient, and practical manner. Development of portable detectors and supporting tools has raised the possibility of previously impractical applications. Furthermore, micro-/nanofluidics further incorporated real miniaturization of the culture environment for microbial biosensors, reducing the consumption of resources and increasing their sensitivity from the viewpoint of optical detection. Automated and miniaturized systems for multiplex detection suggested new analytical methods for the identification of real, unknown multi-samples with improved selectivity. In particular, many microbial

biosensors integrated with micro/nanomaterials showed many unique advantages including high sensitivity, high selectivity and rapid response time with high resolution and accuracy.

Nevertheless, many hurdles in micro/nanotechnology-assisted microbial biosensors still remain before they will successfully substitute for other types of artifactual biosensors. Although microbial biosensors with high portability and high multiplexity have been widely studied and even demonstrated, several challenging issues should be taken into serious consideration. To address these issues, further investigation on immobilization techniques, long-term cultivation and rapid response time of microorganisms, the intrinsic toxicity of chemicals, solvents, and micro/nanomaterials, bio-compatible fabrication processes and materials, and reusability, contamination, and shelf-life of microbial biosensors. For instance, unless a long shelf-life without unwanted contamination is guaranteed, microbial biosensors cannot substitute for other similar biosensors because any contamination of culture media or other sources may nullify the function of the microbial biosensors. Lastly, integration with advanced micro/nanotechnologies heralds the beginning of a new era for microbial biosensors. Many interesting possibilities and promising opportunities within the field of microbial biosensors still remain. Proper integration between microbiological sciences and micro/nanotechnologies will thus unlock the full potential of microbial biosensor technology in the near future.

Chapter 3. Quantitative Analysis of Microbial Biosensors for Heavy Metal Ion Detection

3.1 Importance of heavy metal ion detection

Heavy metals are naturally found in many industrial wastes, and those heavy metal ions such as cadmium, mercury, and lead are relatively denser. Since heavy metals are toxic to living organisms, detection of toxic compounds and heavy metal ions in environments is important. Because the heavy metal ions cause oxidative stress to the cells and the accumulation over time in animal bodies, causing many critical diseases. Detection methods of heavy metal ions (HMIs) using conventional approaches inevitably includes trained labors and expensive instruments such as atomic absorption, plasma-atomic emission/mass spectroscopy, and complex configuration of electrochemical instruments [1].

3.2 Integration of microbial biosensor with microfluidic device

In order to overcome such bottleneck of the conventional methods, microbial biosensors have been artificially engineered through the significant progress of synthetic biology. The microbial biosensors provide considerable advantages: they offer low-cost, easier detection not requiring complex equipment, and facile flexibility for various post-analyses. More recently, the miniaturized analytical system such as microfluidic systems have utilized microbial biosensors to enhance the performance of the detection method and reduce labor and sample consumption. For example, Rothert *et al*. introduced the whole-cell-fluorescence-based biosensing on a centrifugal microfluidic platform to detect HMIs [31]. The device showed limited detection threshold because of the conventional batch-type chemical processing during cell culture and genetic induction.

In this chapter, a microfluidic microbial biosensor device was developed that not only concentrates motile microbes in a compartmentalized microchamber array using microfabricated ratchet structures but also grows the concentrated microbes in a continuous-feed mode. This novel device enabled the feeding of nutrients and various concentrations of HMIs (e.g., Pb^{2+} and Cd^{2+}) in the compartmentalized microchambers in a continuous manner, thereby introducing a simple and convenient chemostat-like culture environment. Using the combination of the chemostat-like culture environment and

synthetically engineered microbial biosensors, both the sensitivity and selectivity of the microbial biosensors were characterized for detecting HMIs and then compared the result with that obtained using conventional batch-type methods [10].

3.3 Experimental methods

3.3.1 Reagents and materials

For visualization and quantification of the microfluidic channels, green, red, and yellow dyes and 50 mM fluorescein isothiocyanate (FITC) were mixed with deionized water, respectively. As the target HMI, Pb^{2+} and Cd^{2+} were prepared in a cell culture solution (tryptone broth (TB), 1% tryptone, and 0.5% NaCl) with ampicillin (75 μg/mL). A Luria broth (LB) agar plate was prepared by mixing agar (1% w/v) for colony formation. For detection of HMIs, analyte solutions of $PbCl_2$ (Cat. No. 203572) and $CdCl_2$ (Cat. No. 439800) were purchased from Sigma-Aldrich and diluted into autoclaved distilled water to the desired concentrations when necessary.

3.3.2 Preparation of bacterial cells

Two *Escherichia coli* K-12 strains (MG1655 and DH5α) were used as platform cells to develop microbial sensors. The MG1655 strain harboring pTKU4-2 plasmid that constitutively expresses green fluorescent protein (GFP) was used for testing cell growth in the chemostat-like microfluidic device. DH5α cells harboring plasmids pHK194 and pHK200 were used for detecting Pb^{2+} and Cd^{2+} and named as the HK621 and HK622 strains, respectively [142]. For continuous induction testing in the microfluidic device, a single colony of the *E. coli* on an LB agar plate was grown in 5 mL in LB broth in a test tube that was rigorously agitated in a rotary shaking incubator (37°C and 200 rpm) overnight. The cells were then introduced into the microfluidic device. For batch-type detection in test tubes, the cells were grown to mid-log phase in 5 mL of LB broth until the optical density at a wavelength of 600 nm reached OD_{600} = 0.5 and various concentrations of the HMI were added for induction of fluorescent reporter gene expression followed by incubation at 37°C and 200 rpm overnight. For a fair, reasonable comparison of the batch-type biosensing method with the chemostat-like biosensing method, the cell density of the batch-type method was intentionally enhanced by centrifugation (Combi 514R, Han-Il Instrument, Incheon, Republic of Korea) at 3000 rpm for 10 min at 25°C.

3.3.3 Design and fabrication of the microfluidic device

The microfluidic device was fabricated and its channel feature was 200 μm wide and 10 μm deep. The microfluidic device consisted of a mixing channel network and a microchamber array for compartmentalized cell culture on a chip as used in our previous study [143]. The microchamber array was integrated with ratchet structures to physically isolate the microbes from the main channel but chemically allow the transport of nutrients and small molecules to and from the main channel [143-145]. The microfluidic device was fabricated using standard soft lithography as used in our previous work. Briefly, an SU-8 (Microchem 2025, Newton, MA, USA) master (approximately 10 μm thick) was fabricated using standard photolithographic procedures. The surface was silanized using trichloro(3,3,3-trifluoropropyl)silane (Sigma Aldrich, Korea) in a vacuum jar for 1 h. Polydimethylsiloxane (PDMS) was then cast, cured, and peeled off to prepare the microfluidic devices. The PDMS devices were treated with oxygen plasma under 50 sccm of O_2 and 50 W for 30 s (Cute-MP, Femto Science, Korea) prior to the experiments. This treatment was performed to make the surfaces of the PDMS channel hydrophilic so that the solutions flowed along the channel easily and no bubbles were trapped.

3.3.4 Experimental setup and data analysis

An inverted fluorescence microscope (Ti-U, Nikon, Tokyo, Japan) equipped with a CCD camera (ORCA R2, Hamamatsu Photonics, Hamamatsu, Japan) and a 10× lens was used to measure the fluorescence from the FITC and E. coli. For data analysis and image processing, Image J (NIH, Bethesda, MD, USA) and OriginPro 8 (OriginLab, Northampton, MA, USA) were used when necessary.

3.4 Ratchet microstructure-based microfluidic device

3.4.1 Generation of concentration gradients and culture chambers with ratchet structures

Figure 7 shows the microfluidic device consisting of a mixing channel network [143] and a test microchamber array. The device has 6 sets of control and test channels and each set has five cell-culture chambers in a column to minimize uncertainty in measuring fluorescent and optical signals from microbial biosensors. *Figure 7b* shows a scanning electron microscope (SEM) image from Ch. 6. Each

microchamber is connected to the main channel through ratchet structures that not only guide and accumulate motile microbes from the main channel but also prevent the trapped microbes from escaping to the main channel.

In addition, the ratchet structures offer a chemostat-like culture environment for the microbes to grow in a continuous-feed mode that continuously supplies fresh nutrients and inducer molecules (HMI) from the main channel to the chambers and, at the same time, washes away secreted metabolites from the chamber to the main channel. These aspects were well characterized in our previous work [144]. To test the mixing channels, a solution with green food dye was loaded in the top-left reservoir (c1) whereas a solution with red food dye was applied in the top-right reservoir (c2). The solutions flowed along the mixing channels and mixed together, resulting in the generation of concentration gradients from Ch. 1 to Ch. 6. The control channels (Ch. 7) were positioned in parallel with each test channel for direct comparison. *Figure 7c* shows that each set of test and control chambers exhibited different colors.

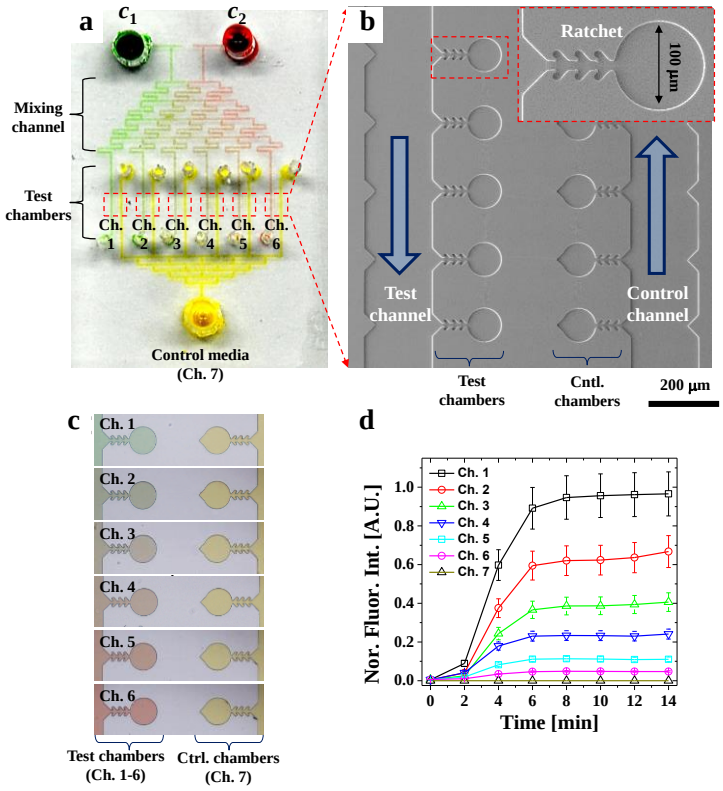

Figure 7. A microfluidic device for microbial biosensors for detecting HMIs (Pb^{2+} and Cd^{2+}). (a) Microscopic image shows the microfluidic channels consisting of a concentration gradient generator and a microbe culture chamber array. (b) SEM image shows one set of test channels and control channels. Chambers are connected to the main channel with ratchet structures that enable chemicals and molecules to be transported but prevent motile cells in the chamber from escaping to the main channel. (c) Microscopic images to visualize concentration gradients in the test chambers and the control chambers. (d) Quantification of concentration gradients by using fluorescence intensity (50 μM FITC solution).

Therefore, the mixing channels successfully generate concentration gradients suggesting utility for high-throughput assays. The concentration gradients of HMI were indirectly characterized by application of a buffer solution with fluorescein (50 μM FITC) and then quantified as shown in *Figure 7d*. As designed and expected, each test channel showed different fluorescence intensities, corresponding to the following concentrations: 100% (50 μM), 63 (31.5 μM), 39 (19.5 μM), 23 (11.5 μM), 10 (5 μM), 5 (2.5 μM), and 0% (buffer only) from Ch. 1 through Ch. 7. Because HMIs are much smaller than FITC and thus have higher diffusivity than FITC, the concentrations of HMIs in the microfluidic device are likely the same as the quantified concentration of FITC.

3.4.2 Bacterial cell growth in a chemostat-like culture environment

E. coli cell growth was tested by using fresh and spent TB medium as shown in *Figure 8a* to determine whether cellular growth was affected by continuous feeding generated using ratcheting structure. Because the microfluidic device can generate various concentration gradients as designed, a single experiment provided six different culture conditions plus a control on a chip. To determine whether cellular growth properly increases in microchambers as nutrients are supplied, the growth of *E. coli* cells as shown in *Figure 8b* were monitored that constitutively express green fluorescent protein (GFP) using a fluorescent microscope. *Figure 8c* shows the quantified fluorescence intensities corresponding to the cell growth results presented in the growth of *E. coli* cells as shown in *Figure 8b*. At t = 0 h, the number of fluorescent *E. coli* cells in each microchamber appeared to be unbiased. However, the fluorescence intensities, although they only indirectly represent the growth rate of the cells in each chamber, significantly changed over time in every chamber. For Ch. 1, in which 100% fresh medium was added (continuous feed mode), the fluorescent intensities showed an exponential increase between 3 h and 7 h, which is likely to be proportional to the increase in the number of fluorescent cells. In contrast, for Ch. 7, in which 100% spent TB medium was added (similar to the batch-type mode), the fluorescent intensities did not increase and remained almost constant over time. For other various intermediate conditions, the growth rates appeared to be precisely proportional to the nutrient gradients.

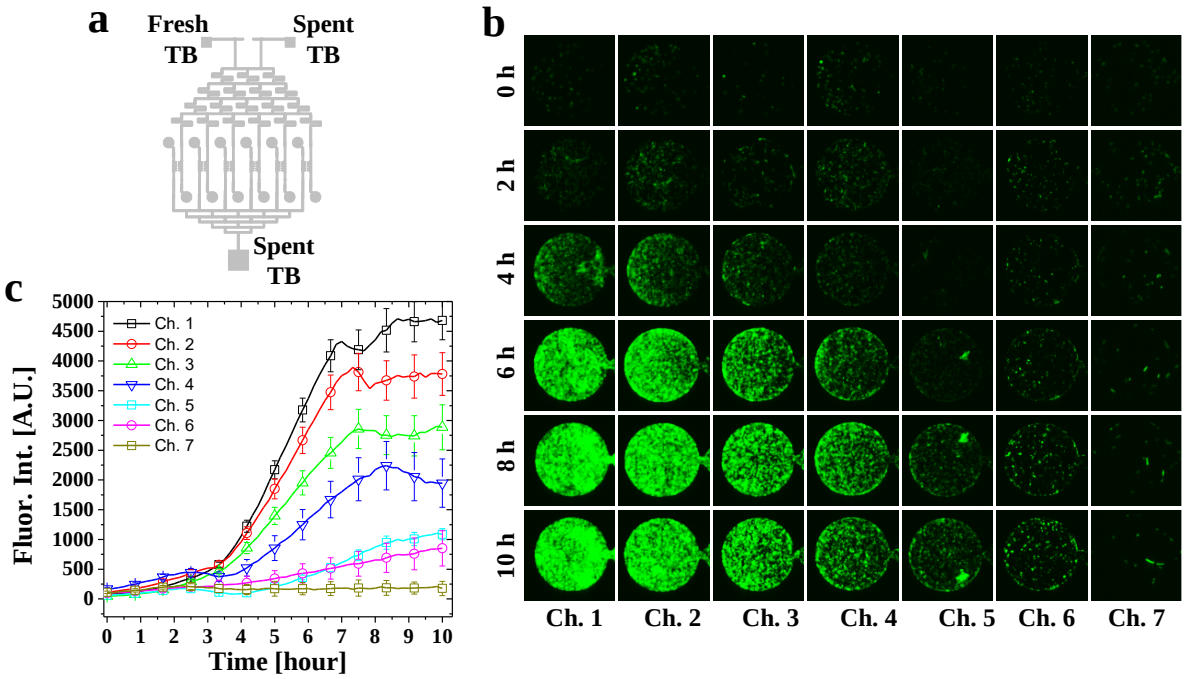

Figure 8. Bacterial cell growth (*E. coli*) in continuous-feed and batch modes. (a) A microimage showing experimental conditions in which concentration gradients of fresh TB media and spent TB media are produced at the same time from left to right and vice versa. (b) Fluorescent time-lapse images show cell growth in various nutrient-feeding conditions. Ch. 1 represents a continuous-feed mode (100% fresh TB), whereas Ch. 7 (control) represents a batch-type mode (100% spent TB). (c) Quantification of GFP signals of the cells in the chambers reveal various growth rates determined by the mixing ratios (concentrations) of the fresh and used TB.

Even though fully grown fluorescent cells, after overnight incubation in a test tube, were injected into the device, the cell growth in the microchambers was observed further as nutrients were supplied. Additionally, the fluorescent cells were not able to escape from the microchambers with the ratchet structures, but nutrients and metabolites could freely diffuse into and out of the microchambers. The chemostat-like cell culture environment dramatically increased the cell density on the chip, which in turn was helpful to improve the performance of microbial HMI detection compared to conventional cell culture environments such as test tubes and microplate instruments that only allow a batch-type culture environment. This remarkable rise of cell growth may play a key role in increasing the biosensing sensitivity because intense fluorescence signals were measured in response to target HMIs continuously delivered in the microchambers.

3.5 Detection of heavy metal ion by microbial biosensors in microfluidic device

3.5.1 Characterization of gene expression level to detect HMIs

Two types of microbial whole-cell biosensors were employed by harboring artificially engineered plasmids for detection of Pb^{2+} or Cd^{2+} in solution. The detection mechanism was based on the negative control of the GFP reporter gene mediated by CadC-type transcriptional repressors, which bind to Pb^{2+} or Cd^{2+} divalent ions and derepress the GFP reporter promoters. Two *cadC* transcriptional modules were cloned from the genome of *Bacillus oceanisediminis* 2691 [142]. These microbial biosensors were integrated into the ratchet structure-integrated microfluidic device to provide a chemostat-like environment for improving the sensitivity of the sensors. The microbial biosensors HK621 for Pb^{2+} ions and HK622 for Cd^{2+} ions using the microfluidic device was characterized. The HMIs dissolved in TB medium (20 μM) was introduced to the left-top reservoirs and only TB media was introduced to the right-top and right-bottom control reservoirs.

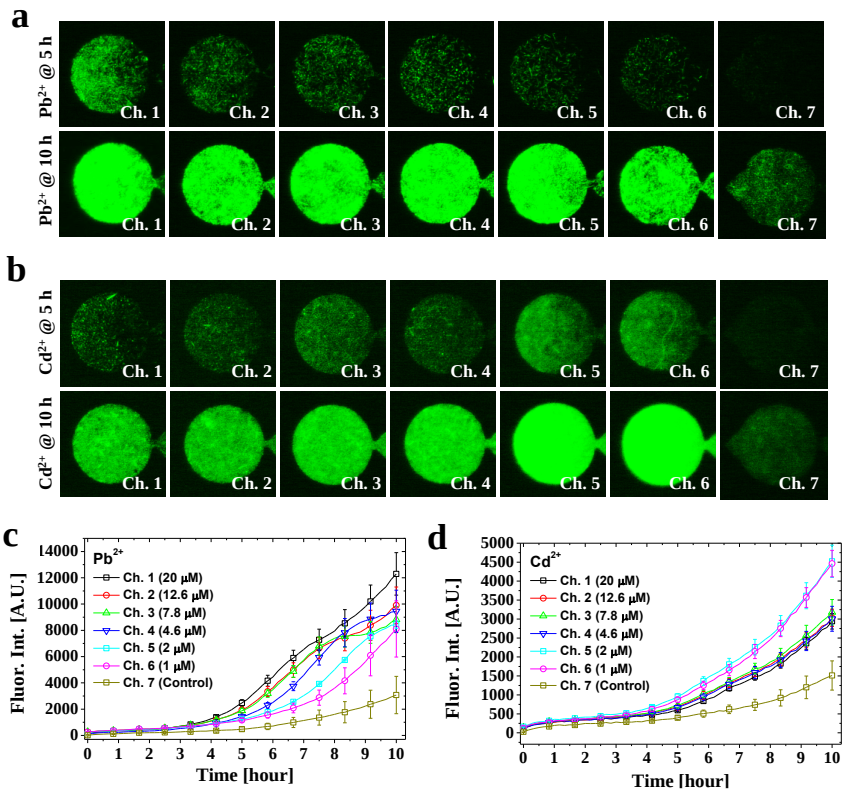

Figure 9. Detection of HMIs by the microfluidic device and the microbial biosensors. (a) and (c) Detection of Pb^{2+} ions using *E. coli* HK621 cells at various concentrations ranging from 20 μM to 0 μM (control). (b) and (d) Detection of Cd^{2+} ions using *E. coli* HK622 cells at various concentrations ranging from 20 μM to 0 μM (control). The fluorescent intensities depended on the concentrations of HMIs over time.

As shown in *Figure 9a* and *Figure 9c*, each microfluidic device was used for seven different detection experiments on a chip with various concentrations of Pb^{2+}. After five hours of cell culture, the fluorescent intensities showed a linear dependency on the concentration of the Pb^{2+} ion; a higher concentration was associated with stronger fluorescence intensity. After 10 h, the differences among the normalized fluorescence intensities from Ch. 1 to Ch. 6 appeared to decrease. This effect was attributed to the continuous supplementation with Pb^{2+} ions, which activated microbial transcription to over-express the biosensor construct and trigger the accumulation of GFP within the cells. For Cd^{2+} ion detection, the fluorescence intensities showed a nonlinear dependency on the concentration of Cd^{2+} as shown in *Figure 9b* and *Figure 9d*. The plasmid activity and cell growth appeared to be affected by high concentrations of Cd^{2+} in the solution. However, the continuous-feed culture enabled by the microfluidic device showed increased fluorescence intensity, especially with low concentrations of metal ions. It could therefore be speculated that Cd^{2+} ions gradually accumulate in cells up to a concentration sufficient to turn on the reporter gene without interfering with cellular growth. Therefore, the combination of the microfluidic device and the microbial biosensors improved the sensitivity and the dynamic range for HMI detection.

3.5.2 Comparison of continuous induction and batch-type induction for HMI detection

The detection performance for HMIs using the microfluidic device was compared to that of the conventional detection method using batch culture under the same microscopic image acquisition conditions. First, the fluorescent intensities were obtained from the microbial biosensors for different concentrations of Pb^{2+} ions (20 μM, 200 nM, and 2 nM; none as a negative control) after 10 h of incubation in the chemostat-like environment as shown in *Figure 9a* and *Figure 9b*. Because the device enabled continuous supplementation of nutrients and maintained Pb^{2+} ions in their initial state in the detection chamber, a signal increase of approximately 4–5 fold was obtained when compared with the control experiment (without HMI) even at low concentrations such as 200 nM and 2 nM. However, the batch-type induction did not produce sufficient fluorescence signal to enable differentiation from the control signal because of the lower cell density and limited supplementation of Pb2+ ions. An alternative method of increasing the signal difference in the batch-type induction method was demonstrated by increasing the cell density by a factor of 15 using an external centrifuge as described in *3.2.2 experimental methods section.* However, the fluorescence signals in the 15x batch-type induction were still much lower than those in continuous induction. Moreover, this method required an additional cell-concentrating step with increasing sample consumption and labor. Similar to the findings

during Pb^{2+} detection, Cd^{2+} ions showed a higher signal-to-noise ratio in the continuous induction method than in the batch-induction method, as shown in *Figure 10c-d*. Therefore, the microbial biosensors with a continuous chemostat-like environment improved the sensitivity and dynamic range of the microbial biosensors by approximately three orders of magnitude compared to the conventional batch-induction method for detecting HMIs [86]. The enhanced performance can be attributed to the continuous expression of the engineered genes and the larger number of cells in the detection chamber. Even with a low concentration of HMI (e.g., 2 nM), the genes appeared to continuously activated over time by continuous supplementation and/or intracellular accumulation of the target HMI, resulting in over-expression of GFP in the cells [19].

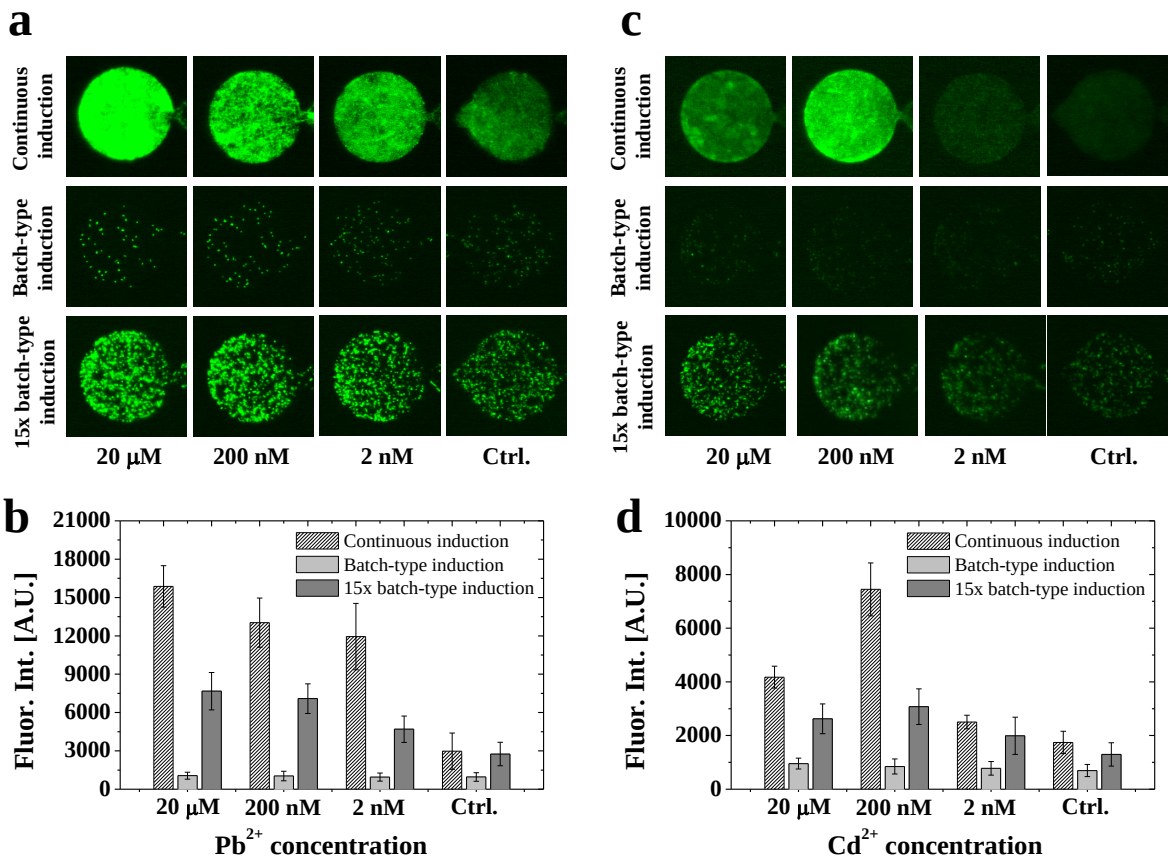

Figure 10. Comparison between continuous and batch-type induction of microbial biosensors. (a) and (b) Continuous and batch-type induction of *E. coli* HK621cells in various concentrations of Pb^{2+} ions such as 20 μM, 200 nM, 2 nM, and 0 nM as a control. In continuous induction, the microbial cells were grown and treated with inducer molecules (Pb2+ ions) in the chemostat-like microfluidic device for 10 h. The batch-type induction and 15x accumulated batch-type induction were performed in conventional batch-type culture tubes for 10 h, and then the induced microbial cells were loaded into the microfluidic device for immediate fluorescent measurements. The 15x concentration enhancement was achieved by using a centrifuge immediately before loading into the microfluidic device. (c) and (d) Induction of *E. coli* HK622 cells in various concentrations of Cd^{2+} ions. All fluorescence images were obtained under the same microscopic configurations.

3.5.3 Characterization of the selectivity of the microbial biosensors

The microfluidic device enables diverse characterizations of microbial biosensors in various HMI conditions. For example, to confirm the selectivity of the microbial biosensor, each type of microbial cells was tested with a non-target HMI; the microbial sensor cells that were designed for Pb^{2+} detection were exposed to a solution containing both 20 μM Pb^{2+} and 20 μM Cd^{2+} and vice versa. As described in *Figure 11*, the microbial biosensors showed the maximum fluorescent intensity in the target HMI conditions, indicating heavy metal selectivity. Although the results with the non-target HMI showed a low amount of fluorescence intensity caused by leaky expression or non-specific removal of the repressor on the *cad*C gene in the engineered microbes, the microfluidic device provides a quantitative platform with remarkable potential to characterize the whole-cell-based biosensing system in various HMI conditions with a considerably decreased response time and reduced sample consumption. The microfluidic device is also simple and operated by only using static hydraulic heads, thus showing high potential as a portable biosensor.

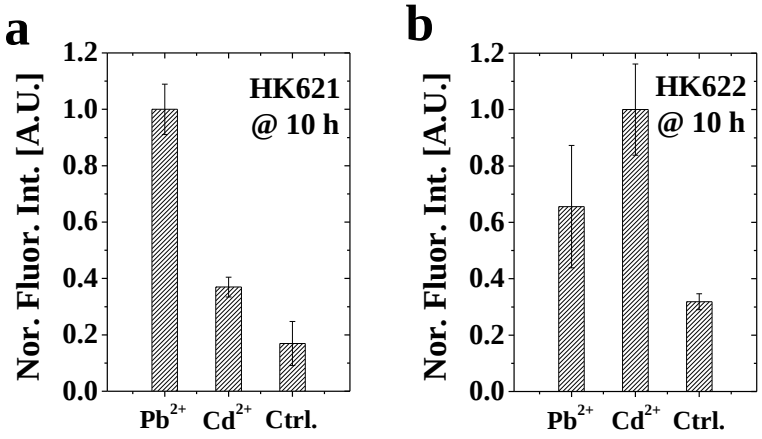

Figure 11. High-throughput characterization of the selectivity and cross-talk of the two microbial biosensor cells, HK621 and HK622, respectively, using the microfluidic device. (a) Induction of the HK621 biosensor in a solution containing both 20 μM Pb^{2+} and 20 μM Cd^{2+} ions after 10 h. (b) Induction of the HK622 biosensor in the same solution after 10 h. The fluorescence intensities measured under the same microscopic conditions were normalized by the maximum fluorescence intensity value.

3.5.4 Characterization of T7 signal amplification module assembled biosensor

In the previous sections, pCadC1945 and pCadC640 in DH5α platform strain were characterized using the chemostat-like microfluidic platform (*e.g.* HK621 for lead detection harboring pCadC1945 and HK622 for cadmium detection harboring pCadC640). Then T7 transcription modules were

harnessed in the biosensing system to address the wide variations and low fluorescence signals in cadC–gfp prototype constructs in the *E. coli* system (*Figure 12*). In the presence of heavy metal ions in cells, T7 RNA polymerase (T7 RNAP) was expressed, and the T7 promoter was activated and amplified expression level of its fluorescence protein.

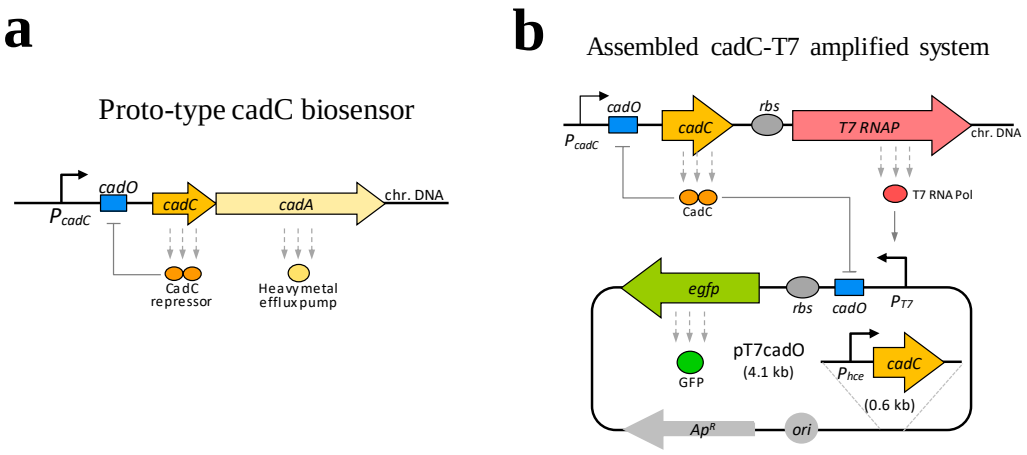

Figure 12. Improved heavy metal microbial biosensors carrying CadC-T7 circuits.

The ratchet microfluidic structure isolated microbe into individual chambers physically, but allowed the nutrient solution to the chambers chemically. Using this chemostat-like microfluidic platform, two sets of microbial biosensors were used for HMIs detection by a transformation of the plasmid pCadC1945, pCadC640 in DH5α strain and newly developed plasmid pT7cadO1945 and pT7cadO640-H in BL21(DE3) strain. After the injection of cell mixtures and nutrient medium containing target HMIs, the microfluidic chambers were incubated for 5 hours at 60% humid incubator on top of the microscope stage. The fluorescence intensities were measured from the microbial biosensors with four different concentrations of Pb^{2+} and Cd^{2+} ions (20 μM, 200 nM, 2 nM and a negative control). Compared to the previously constructed biosensor pCadC1945 and pCadC640, newly developed plasmid pT7cadO1945 and pT7cadO640-H showed higher fluorescence intensities for all concentrations at the same time point. These increased intensities may have been affected by mainly two factors that were 1) the development of the T7-based amplified genetic biosensor circuit as well as 2) the intrinsic difference of growth rate between bacterial strain DH5α and BL21(DE3).

For lead detection, the fluorescence intensity of pT7cadO1945 was increased approximately 7.8 times than pCadC1945 at the optimal detection concentration of 20 μM $PbCl_2$ as shown in *Figure 13*. Especially for the concentration of 20 μM of $PbCl_2$, pT7cadO1945 showed significantly higher intensities than other concentrations (200 nM, 2 nM and negative control). This remarkable increase may be caused by continuous chemical expose from the ratchet microfluidic structure. For cadmium

detection, the noteworthy improvement of microbial biosensor was speculated with a linear correlation between HMI concentration and fluorescence intensity (*Figure 13c* and *Figure 13d*). For effective and efficient microbial biosensor, sensitivity and selectivity are most important features. Previously constructed biosensor plasmid pCadC640 showed non-linear fluorescence intensity compare to HMI concentration [10]. As cadmium concentrations in nutrient medium increased, the fluorescence intensity of pT7cadO640-H relatively increased. For optimal cadmium detection concentration of 20 μM of $CdCl_2$, fluorescence intensity of pCadC640 showed 5.6 times higher than pT7cadO640-H [146].

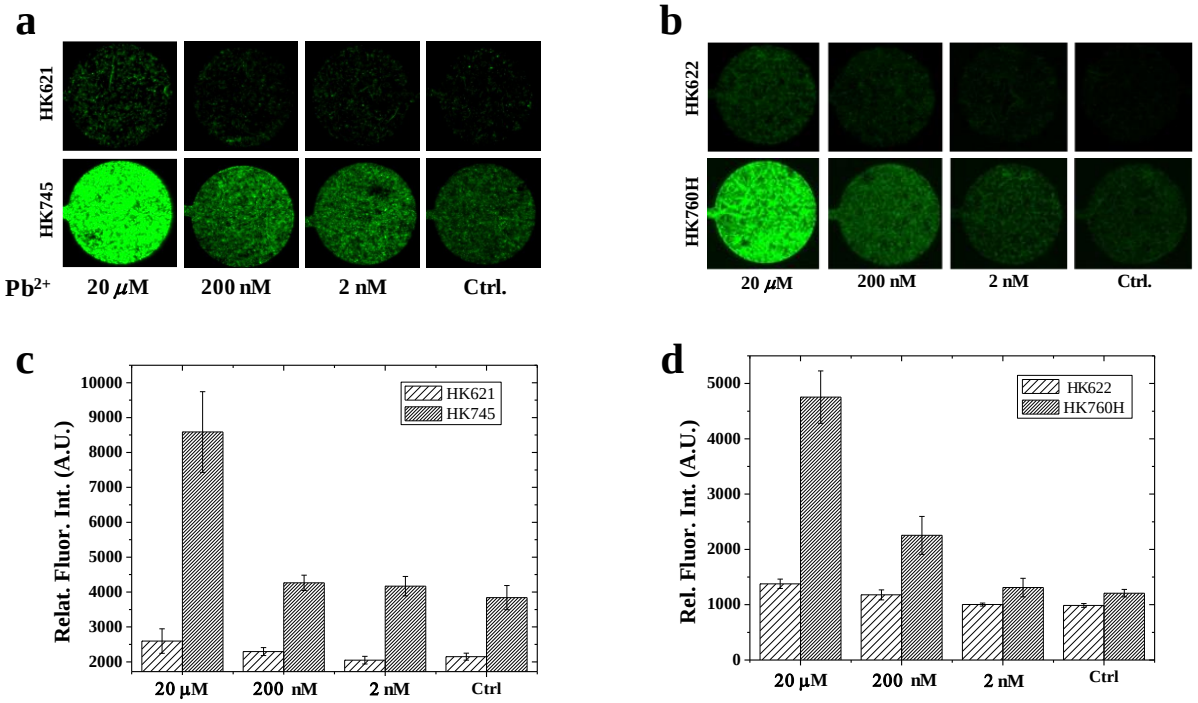

Figure 13. Detection of heavy metal ions by the microfluidic biosensor device. Time-course quantification of fluorescence intensities generated by *E. coli* cells grown in microfluidic chambers. Fresh nutrients with (a,c) lead and (b,d) cadmium ions were continuously supplied with various concentrations ranging from 0 to 20 μM. Prototypes and CadC-T7 biosensors are indicated by different symbols, respectively.

3.6 Conclusion

A microfluidic platform was developed that consisted of a micromixer to generate concentration gradients of HMIs and a microchamber array with ratchet structures to concentrate and compartmentalize motile microbial whole-cell biosensors. The microfluidic platform provided a chemostat-like culture environment with the microbial biosensors such that an extremely high cell population (density) in each microchamber was achieved because the microbes grew well in a continuous feed mode. In addition, the culture environment enabled higher reporter gene expression in the microbes, enhancing the sensitivity and dynamic range by three to four orders of magnitude for

detection of Pb^{2+} and Cd^{2+} when compared to conventional batch-type feeding and induction methods. This increase was achieved because the microfluidic platform not only provided fresh solutions containing nutrients and HMIs to the compartmentalized microbial biosensors but also simultaneously removed secreted metabolites.

Additionally, newly developed HMI biosensor plasmids pT7cadO1945 and pT7cadO640-H were also tested in the same chemostat-like microfluidic platform. Overall, the fluorescence intensities of T7-based amplified biosensors (*e.g.* HK744 and HK756) were increased compare to the previously constructed microbial biosensors for all HMI concentrations. These results can be a straightforward proof of the improvement of microbial biosensors caused from mainly two factors 1) T7 promotor amplification and 2) the intrinsic growth rate. Although the fluorescence intensities obtained from microscopic images showed the relative HMI detection sensitivity depending on the experimental condition of microscope, the microfluidic platform dramatically amplified the detection range and signal using its original features that are the continuous supply of nutrient and HMI expose. These results from microfluidic platform can strongly support the improvement of molecular level of biosensor circuits.

Notably, the total amount of the solutions used was much lower than that with other conventional methods (*e.g.* only 200 μL was required for 6 experiments on a chip basis, compared to one sample in a 5 mL tube in conventional experiment). Moreover, the combination of the chemostat-like microfluidic platform and synthetic microbial biosensors offered remarkable advantages compared to conventional biosensors for detecting HMIs: 1) cost-effective and time-reduced detection without complex equipment, 2) flexibility for multiplex detection in a high-throughput manner, and 3) direct and convenient measurement without pre- or post-treatment of sample solutions.

Chapter 4. Development of Fluid Array for Screening of Small Mutant Microbial Library

4.1 Microfluidic approaches for high-throughput microbial applications

Microfluidic-based microdroplet devices, that were described in the previous chapter, were widely used as a great and latent tool for many biological fields including microorganism symbiosis [57], MIC (Minimal Inhibition Concentration) research [58], heterogeneous enzymatic assays [60] as well as molecular works such as high-throughput PCR reactions [59]. However, one of the important issues on the microdroplet in the practical field is a possibility to monitor and identify each microdroplet during long-term and complex experimental process. Owing to the micro-scale small size, random movement of the droplets and complex liquidity [147], it was considered as a challenge to trap the droplets with incubation or chemical reaction to detect and monitor the experimental processes.

In order to handle the issue, many research groups have tried to develop an effective method to immobilize the microdroplet with various trapping device. Edd *et al*. trapped microdroplets in a way of sequential manner using orifice structures which are exactly fitted with the target droplet diameter [148]. Huebner *et al.* have reported a two dimensional trapping structure successfully captured droplets, however, caused a serious shrinkage of droplet [61]. Although the trapping devices developed from both Huebner *et al.* [61] and Tan *et al*. [149] showed an excellent droplet trapping efficiency, those devices had disadvantages in device design dependent and not suitable for high-throughput assay.

4.2 High-throughput screening methods for a microbial library

Conventional HTS technologies for mutant libraries can be categorized into two types according to the screening mechanism: reporter-gene-based screening (*e.g.* fluorescence) and growth-based screening (*e.g.* auxotrophic growth factors) [8]. The reporter-gene-based screening method is widely used for microbial mutant libraries that show variation in fluorescent [150] or colorimetric intensities [151, 152]. In particular, for the fluorescence-based HTS, a fluorescence activated cell sorting (FACS) system is the state-of-the art instrument because it can sort $>10^4$ cells per second [8, 153]. Despite the advantages, including rapid process time, high resolution, and high-throughput, such FACS systems are

generally expensive, sometimes unavailable, or unsuitable due to the need of a fluorescent signal for detection. The growth-based screening method is based on the growth rate differences of the mutant libraries [8]. For another mechanism, the growth rate differences in a mutagenic library frequently occur because a mutation affects genes related to metabolic pathways. The growth-based screening of a mutant library is important for the identification of the auxotrophy associated with the loss of enzymatic function [8, 154]. However, the throughput of microplate readers is limited to 96 or 384 individual wells. Thus, they can only be useful for very small mutation libraries [150]. Moreover, cells are prepared for the HTS in bulk and batch type of culture conditions; hence, the fluorescence or growth rate of each cell can be affected by its neighboring cells. For this reason, compartmentalized cell culture environments are required for the practical microbial screening application.

4.3 Microfluidic HTS methods

To advance the conventional HTS technologies, many microfluidic HTS approaches have been introduced and applied to the screening of mutant libraries. For example, droplets are one of the representative approaches because they can produce numerous, homogeneous, and discrete cell-encapsulated samples [63, 155, 156]. Static droplets in an array format particularly showed a synergetic advantage at a high-throughput by enabling metabolic assays at the single cell level [156-158]. Additionally, a stationary fluid array was utilized to culture bacterial or mammalian cells, in which a fluid-sample-partitioning method was essential and played a key role in high-throughput biological assays [55]. These microfluidic devices and methods showed remarkable potential for high-throughput biological assays. However, they also exhibited several drawbacks. Numerous droplets on a microfluidic device should be fixed and/or tagged in a certain confined location for sequential analyses. Additionally, complex fluid control systems are required for handling numerous droplets. In fact, all the aforementioned microfluidic approaches showed a common point that less attraction has been drawn to extraction than culturing and screening of mutant libraries. Therefore, a more concrete sample extraction technique needs to be developed and integrated with a high-throughput cell culture technique to successfully demonstrate a microfluidic HTS application on a chip.

In this chapter, microfluidic HTS platform was described in detail that enables not only the generation of a fluid array for the compartmentalization and culture of microorganisms, but also the extraction of target cells based on both phenotypical differences (*e.g.* reporter gene system and growth difference) of mutated libraries. A novel device was fabricated with a microwell array in a matrix format using the immiscible feature and the difference of specific gravity between oil and water. In addition,

an automated fluorescence imaging system with a custom-made image processing software was employed for high-throughput identification of target cells. Unlike other microfluidic approaches, our platform allows us to extract target cells in a simple manner. For reporter gene based screening, a spike recovery test was demonstrated the feasibility of the HTS platform. Lastly, the same platform was utilized to growth-based screening to sort a random mutation library according to cellobiose consumption rates.

4.4 Experimental methods

4.4.1 Reagents and materials

Two types of oils with different specific gravity (SG) were used for compartmentalization of aqueous solutions: hydrocarbon oil (Hexadecane, SG = 0.76, Sigma-Aldrich, Korea) and fluorinated oil (FC-40, SG = 1.61, Sigma-Aldrich, Korea). Red food dye and 50 μM of fluorescein isothiocyanate (FITC) solutions were used for the visualization and characterization of the fluid array. For cell culture, Luria Bertani broth (LB, Sigma-Aldrich, Korea) was prepared with proper antibiotics such as ampicillin (Amp, 75 μg/mL), chloramphenicol (Cm, 50 μg/mL) and kanamycin (Km, 50 μg/mL) (all purchased from Bioshop Canada Inc.). M9 minimal medium (Minimal salt 5×, Becton Dickinson, Franklin Lakes, NJ, USA) supplemented with 2 mM $MgSO_4$, 0.1 mM $CaCl_2$, and 0.3% (w/v) cellobiose was used for the growth-based screening of the mutant library. An LB agar plate was also prepared (1% of w/v, Agar, Becton Dickinson) for colony formation. To avoid shrinking of the produced fluid array, FC-40 oil was mixed with distilled water (0.1%, v/v) up to the limit of solubility in a rotary shaker at 60°C. Distilled water was not fully mixed with the oils so that the final concentration of water in the oils was estimated to be approximately 0.02% (v/v) according to previous report [159]. For the extraction of target cells, both fused-silica capillary tubes (CAT no. #1068150011, Polymicro Technologies, Phoenix, AZ, USA) with 25.3 μm inner diameter and 360 μm outer diameter (OD) and commercially available insulin syringes with OD = 200 μm were used.

4.4.2 Preparation of bacterial cells

All *Escherichia coli* (*E. coli*) stains and plasmid used in this study are listed in *Table 2*. *E. coli* K-12 strain MG1655 was used as a platform cell. The MG1655 strains, MG-GFP and MG-RFP, which

constitutively expresses either green or red fluorescent protein (GFP or RFP) were used for testing cell growth in the fluid array device. For the spike and recovery test used to demonstrate the fluorescence-reporter-gene-based screening, two different recombinant strains were employed: MG1655 harboring pFAS and MG1655 Δ*fad*E harboring pFAS and pET28a-Km. Additionally, for the growth-based screening, the CP12chbasc strain was chosen because it utilizes β-glucoside sugars such as cellobiose. The strain was then randomly mutated by using the EZ-Tn5^{TM} transposon mutagenic kits (Epicentre, Madison, WI, USA) and an approximately 4,000 mutant library was generated. For cell culture, a single colony grown on an LB agar plate was picked up and a culture tube filled with 5 mL of LB medium and proper antibiotics was inoculated with it. The culture tube was vigorously agitated in a rotary shaking incubator (37ºC and 200 rpm) overnight. The cells were then diluted into fresh LB medium with the proper ratio in order to achieve a pre-designed number of cells per microwell and then introduced into the oxygen plasma treated fluid array platform. For the visualization of the individual cells in the CP12chbasc small mutant library, the BglBrick vector pBbE4c-rfp was transformed to the CP12chbasc strain to express RFP during the microscope speculation [160].

Table 3. Plasmids and *E. coli* strains used and newly constructed in this study.

Plasmid or *E. coli* strain	**Featured characteristics**
Plasmid	
pTKU4-2	GFP constitutive expression
pTKU4-65	RFP constitutive expression
pBbB4c-RFP	*p*Prp-rfp, Propionate inducible RFP expression
pFAS	Fatty acid biosensor / RFP inducible expression
pET28a-Km	Kanamycin antibiotic resistance
pEZ-TN5	from Epicentre Transposon mutagenesis kit
***E. coli* strain**	
MG1655	MG1655 Wild Type (WT)
MG-GFP	MG1655 harboring pTKU4-2
MG-RFP	MG1655 harboring pTKU4-65
MG-Ctrl	MG1655 harboring pFAS
MG-ΔfadE	MG1655 ΔfadE harboring pFAS and pET28a-Km
CP12chbasc	AscG::pCP12 harboring pBbB4c-RFP
CP12chbasc Library	CP12chbasc random mutation library by pEZ-Tn5
CP30chbasc	Optimized cellobiose metabolism

4.4.3 Experimental setup and data analysis

An inverted fluorescence microscope (IX-71, Olympus, Tokyo, Japan), equipped with a CCD camera (Clara, Andor, Belfast, Northern Ireland) and 1.5×, 10×, and 20× objective lenses, was used to acquire fluorescence images from the fluid array device. The images were automatically acquired by using a microscope stage controller (MAC5000/Bioprecision2, Ludl Electronic Products, Hawthorne, NY, USA). The fluorescence intensities of the images were then analyzed using a custom-made m-file in MATLAB R2014a (Mathworks, Natick, MA, USA). For additional data analysis and necessary image processing, Image J (NIH, Bethesda, MD, USA) and OriginPro 8 (OriginLab, Northampton, MA, USA) were used. A manually controlled probe positioner (PB50, MS Tech, Hwaseong, Korea) was used to fix either syringe needles or capillary tubes for the extraction of target cells.

4.4.4 Fabrication of the fluid array device

The microfluidic device was fabricated and the dimension of the microwells was 100 μm in diameter and 50, 100, and 150 μm in depth. As described previously [145], an SU-8 (Microchem 2075, Newton, MA, USA) master was fabricated using the standard photolithography technology [161]. The processed surface of a Si-wafer was silanized using trichloro(3,3,3-trifluoropropyl) silane (Sigma Aldrich, Korea) in a vacuum jar for 1 h. Polydimethylsiloxane (PDMS, Sylgard 184 Silicone Elastomer Kit, Dow Corning, Mid-land, MI, USA) was then casted, cured, and peeled off to prepare the microfluidic devices. The PDMS devices were dipped into distilled water for several hours, resulting in a fully moisturized state (i.e., the highest solubility of water into PDMS) so that the fluid in the microwell remained stable without apparent volume shrinkage over 24 h.

4.4.5 Generation of a fluid array

Figure 14 illustrates the generation and compartmentalization of a fluid array on a chip. The demolded PDMS devices were treated with oxygen plasma under 15 *sccm* of O_2 and 70 W for 30 s (Cute-MP, Femto Science, Hwaseong, Korea) prior to the experiments [162]. This treatment was carried out to render the surfaces of the PDMS hydrophilic, which helped aqueous solutions to completely fill the microwell without air bubbles. An aqueous solution containing target cells was deposited on the PDMS surface, thereby filling all the microwells. Because of the capillary effect and the highly gas-permeable property of PDMS, gas bubbles were naturally removed in a few minutes from the

microwells. The surface of the device was gently swept away using another PDMS slab to ensure complete formation of a fluid array and to remove the residual solution left on the surface (*Figure 14A*).

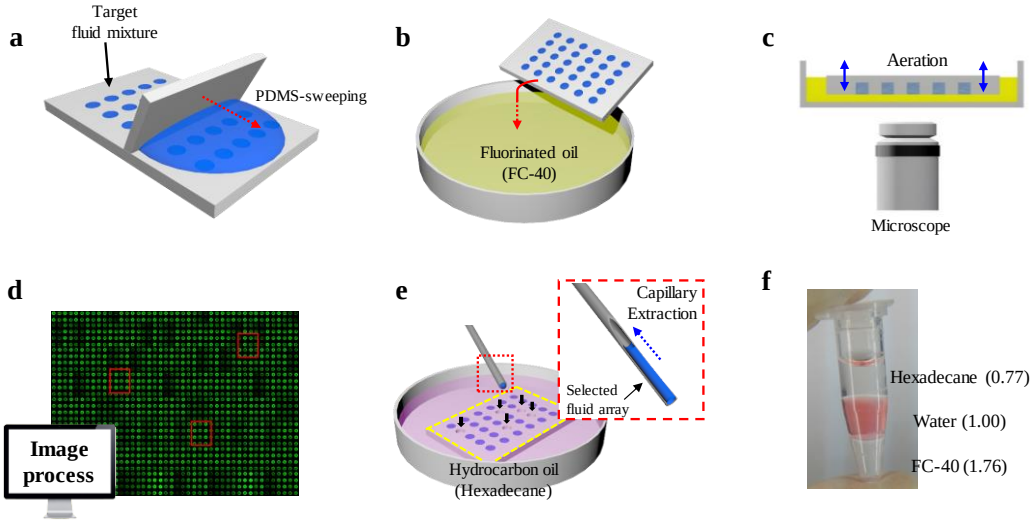

Figure 14. Schematic of fluid array generation and capillary-based extraction process. (a) Thousands of microwells were fabricated on a PDMS surface on which a cell suspension solution was deposited. (b) A PDMS slab was used to gently sweep the PDMS surface, resulting in the formation of a fluid array. (c) The device was inverted and placed into a Petri dish filled with fluorinated oil for long-term culture and observation. (d) Microscopic images were automatically acquired by using a motorized microscope stage and a controller system for a quantitative analysis. (e) The device was inverted again and immersed into hydrocarbon oil because the lighter hexadecane retains the heavier aqueous fluid array at the bottom, thereby preventing dehydration when capillary tubes or needles were used for the extraction of target samples. (f) Visualization of specific gravity differences of hexadecane (0.77), water (1.00), and FC-40 (1.76).

Notably, the fluid array device was immediately turned upside down and placed into the transparent Petri dish that was filled with fluorinated oil (FC-40) to completely compartmentalize the microwells (*Figure 14B*). It should be noted that the process was very important to prevent fast evaporation of the fluid array into the atmosphere since the volume of the microwell was about 1.3 nL. *Figure 14C* shows that the fluid array retained its shape due to the specific gravity difference and the immiscible feature between the aqueous solution (*e.g.* water) and the oil. Notably, oxygen transport through the fluid array can be either allowed or inhibited by simply manipulating the immersion level of the PDMS in the oil, implying that aerobic or anaerobic environments can be created.

4.4.6 Image processing method

The fluorescence intensities of all microscopic images were analyzed by using a custom-made m-file in MATLAB R2014a (Mathworks, Natick, MA, USA). A control image with eight microwells in a

four by two matrix format with the FITC solution was acquired and the eight fluorescence areas were defined as the quantification regions that are designed to be measured for the rest of the image process. Each fluorescence image containing eight microwells was then compared with the control image to reconstruct the fluorescence intensities of all original images. The background signals were subtracted accordingly from all fluorescence images to minimize unwanted noises. Additionally, it was necessary to relocate the center of the images to align them with the control image in order to homogenize the quantification regions. The fluorescence intensities of the quantification regions were automatically pixelated, binary-encoded, and then measured using the 'convolution matching function' provided in MATLAB. Using the aforementioned procedure, the fluorescence intensities of all the microwells in a fluid array were obtained automatically and then determined target microwells that contained target cells. For the extraction and re-culture processes, the net fluorescence intensities were numerated in a descending order and the top 5–10% of the microwells was selected and then extracted.

4.5 Fluid array device characterization

4.5.1 Characterization of a fluid array

Various aspects of the fluid array were characterized for possible HTS applications as shown in *Figure 15* and *Figure 16*. First, aqueous drops in contact with oils need to be maintained for long-term purposes. The small amount of aqueous fluid in the PDMS microwell was compartmentalized by oil with different interfacial energies so that the aqueous fluid may diffuse into the immiscible oils, resulting in the dehydration of the aqueous fluid over time [147]. The solubility of water molecules to the oil was previously reported to be in the range of about 10^{-5} mol/mm^3, which is very low, but can be significant for small sample volumes [159]. In this study, the dehydration problem of the fluid array was simply avoidable by fully hydrating the oils, remaining stable for more than 24 h without apparent distortion and volume shrinkage (*Figure 15a,b*).

Figure 16c shows a large number of microwells that were successfully filled with a fluorescent dye (FITC) solution. Fluorescence intensities of each patterned fluid were measured and quantified by the image processing method explained in the below section of Image processing method in *4.4.6 section* for *imaging processing method*. The quantitative analysis result shows the linear correlation with the volume of each patterned fluid in the statistical histogram as shown in *Figure 15d*. The histogram represents the fluorescence intensities normalized by the average intensities obtained from a 150 μm deep fluid array. The patterned fluids in the microwells with different depths show a remarkable

uniformity and microwells with higher aspect ratios tended to present a better uniformity than microwells with lower aspect ratios. For example, deeper microwells (*e.g.* 150 μm in depth) show smaller standard deviation (± 0.031) than shallower ones (*e.g.* 50 μm, ± 0.053). Therefore, the fluid array device can provide stable and uniform cell culture environment for the long-term culture of microorganisms at a high-throughput.

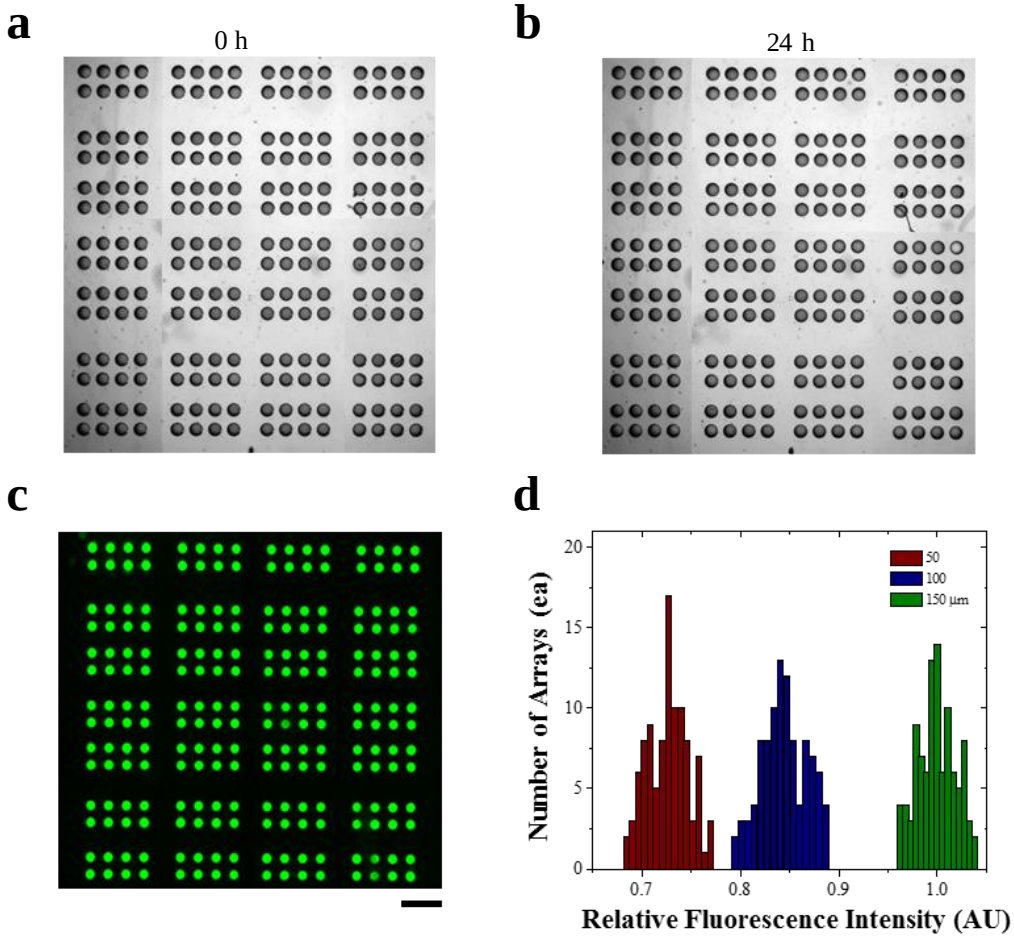

Figure 15. Stability and uniformity test of a patterned fluid array. (a, b) Microscope images of 244 microwells containing a color dye solution at 0 h (left) and 24 h (right). (c) A fluorescence microscope image of 244 microwells containing 100 μM of FITC solution. (d) Histograms of the patterned fluid array when the diameter of the microwell is 120 μm, 50 μm, and 100 μm, respectively. The depth of all microwells was fixed at 150 μm. Scale bar is 500 μm.

The produced fluid array was also characterized in uniformity of arrays, stability for a long-term purpose, and prevention of dehydration. Using a custom-made image processing software, the fluorescence intensities was measure for all the microwells and then sorted them out in descending order to locate target microwells/cells. As shown in *Figure 14e* shows the SG differences among the water and two oils, the fluid array device was removed from the Petri dish and inverted into another Petri dish

filled with hydrocarbon oil for the next extraction process. The lighter hexadecane oil retained the aqueous fluid array at the bottom so that the dehydration of the microwells was completely prevented. A syringe needle or an empty capillary tube was used to extract the target fluid sample. The oils used in all the experiments were fully hydrated to minimize the dehydration of the fluid array. Otherwise, the fluid array would undergo dehydration and volume shrinkage during the long-term culture [147]. Additionally, *Figure 16* shows the effect of PDMS hydration on the dehydration of the fluid array.

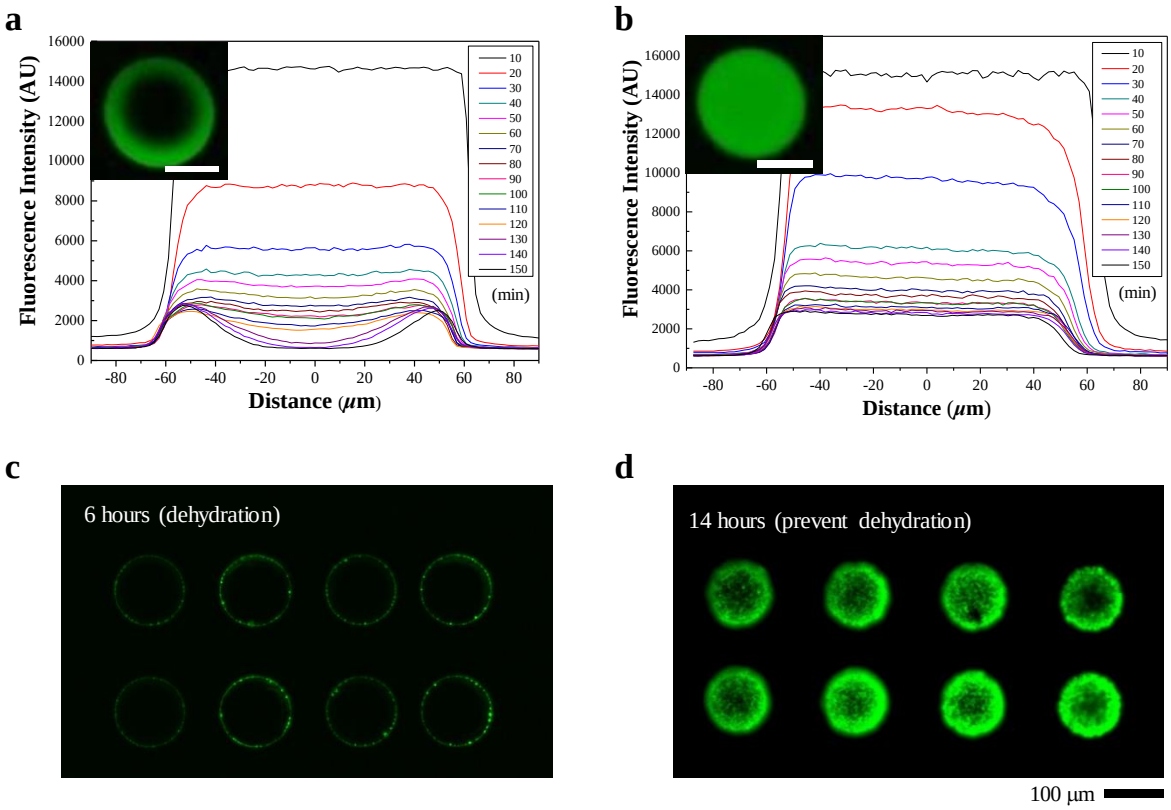

Figure 16. Effect of PDMS hydration on the long-term stability of a fluid array. A fluorescent dye solution (FITC) was used for generating a fluid array on two different PDMS devices. (a), (c) A regular PDMS device shows the dehydration of the fluid array over time. (b), (d) A fully hydrated PDMS device shows high stability of the fluid array, providing an even better cell culture environment. Scale bars in the insets of (a) and (b) are 50 μm.

4.5.2 Bacterial cell growth in the fluid array device

The growth of *E. coli* cells constitutively expressing GFP was demonstrated that the fluid array device provided a compartmentalized microenvironment for the cells for 14 h as shown in *Figure 17a*.

The increase of fluorescence intensities over time can be attributed to both the cellular growth and continuous production of GFP. Three different PDMS thicknesses were also tested to investigate the effect of oxygen transport to the microwell on cell growth. A thick PDMS can transport less oxygen from the outside air to the microwell than a thin one, resulting in lower fluorescence intensities. The result indicates that the fluid array device enables the cells to grow better than conventional culture tubes and microplates. In particular, for the thinnest PDMS, the cell density was over OD_{600} = 3, which is rarely achieved when using conventional culture conditions as shown in *Figure 17*.

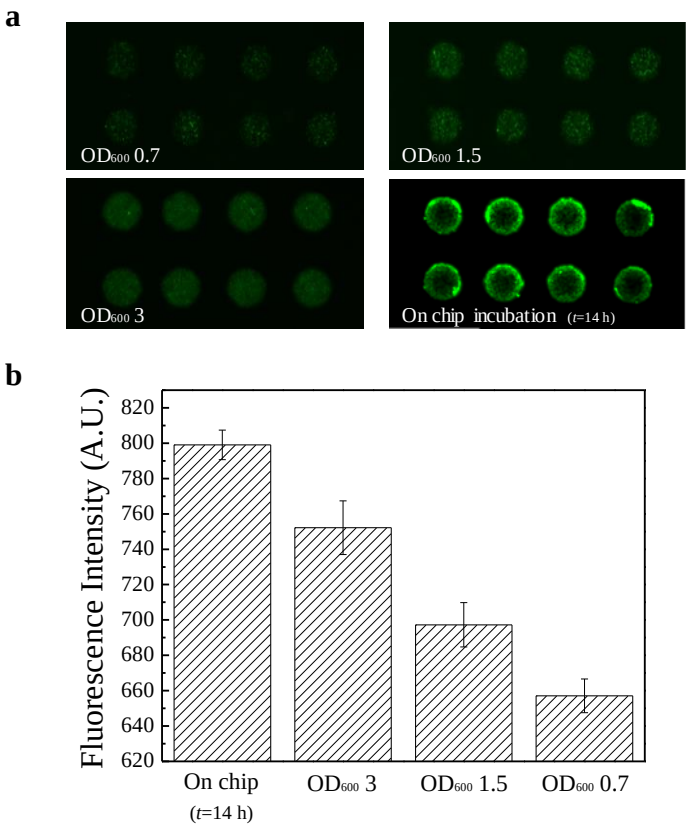

Figure 17. Calibration result of the fluorescence intensities of *E. coli* cells harboring pTKU4-1that constitutively express GFP. (a) Fluorescence images were acquired after generating a fluid array with fully grown cells of which optical densities were OD_{600} = 0.7, 1.5, and 3, respectively. The fluorescence intensities were compared to those of the cells grown in the fluid array device for 14 h. (b) Quantitative results of the fluorescence images. Scale bar is 100 μm.

Additionally, it was tested whether the fluid array device can be used to culture bacterial cells in anaerobic conditions. Since the gas permeability of oils is nearly zero for standard temperature and pressure, when the fluid array device was fully immersed into and covered with oil, no further oxygen transport from the air to the microwells was allowed. *Figure 18C* shows that cells fully grew for 14 h in aerobic and anaerobic conditions. The fluorescence intensities obtained in aerobic conditions were

much stronger than those obtained in anaerobic conditions. This can be attributed to the sufficient oxygen supply from the air to the cells through the PDMS for better cell growth and GFP expression; the more oxygen is supplied, the more GFP is produced [163].

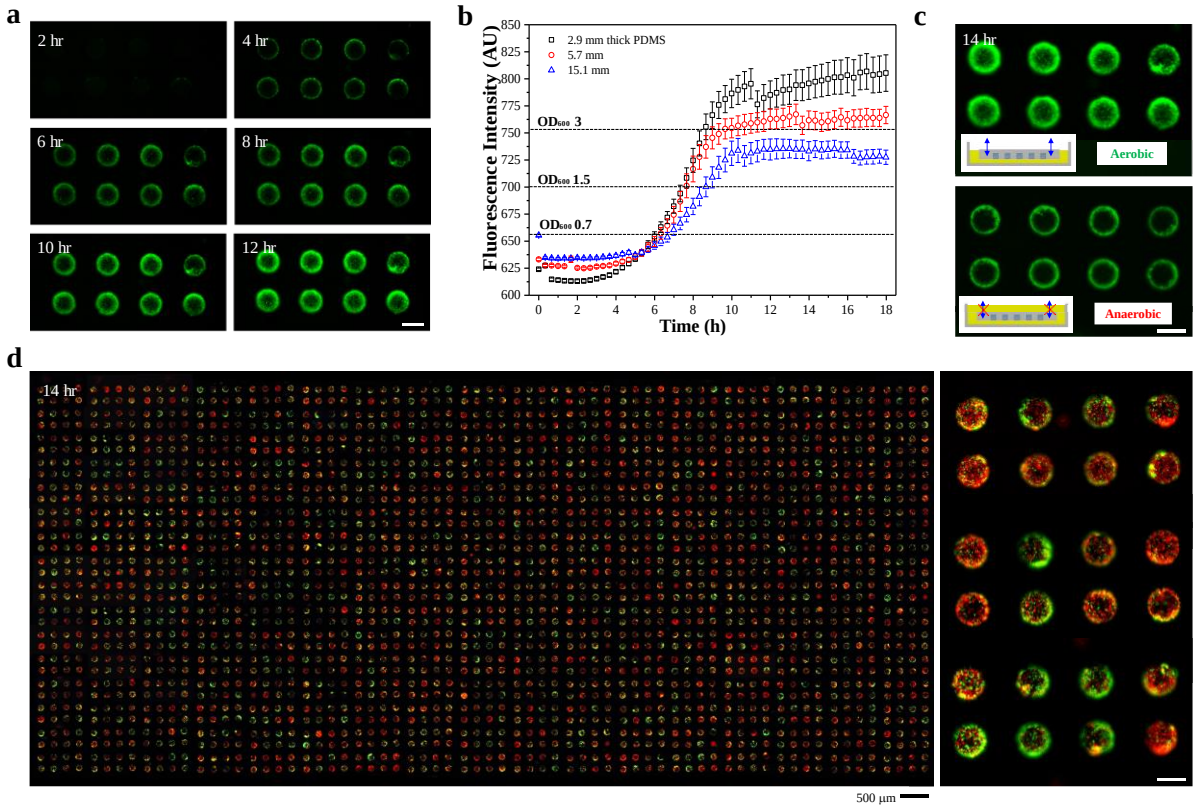

Figure 18. Various cell cultures using the fluid array device. (a) Time-lapse fluorescence images of GFP-expressing bacterial cells for 14 h. (b) Quantification of fluorescence intensities showing the effect of three PDMS thicknesses (*e.g.* 2.9 mm, 5.7 mm, and 15.1 mm) on cell growth (GFP expression levels) over time. (c) Fluorescence images of the GFP-expressing cells over time in aerobic and anaerobic culture conditions. (d) A mixture of GFP- and RFP-expressing cells was compartmentalized in the 2,172 microwells and the fluorescence images were acquired and stitched. All scales bars are 100 μm, unless otherwise indicated.

Another modality of the cell growth is that the distribution of the cells is obviously different. In aerobic conditions, cells appear to swim around the microwells, resulting in a uniform distribution. On the other hand, when the fluid array device was immersed into oil for providing anaerobic conditions to the PDMS device, cells appeared to be concentrated near the perimeter of the microwell. This seems related to the oxygen transport because *E. coli* cells tend to move toward oxygen [164]. In fact, more oxygen exists in PDMS surface because both the solubility and diffusivity of oxygen in PDMS are much higher than those in the medium. Therefore, it was hypothesized that the cells migrate to the PDMS walls after consuming the oxygen in the medium due to the aerotaxis. *Figure 18D* demonstrates that the fluid array device allows high-throughput cell cultures on a chip with 2,176 microwells, thereby

showing high potential for HTS of a small mutant library. Two different strains, MG-GFP and MG-RFP, were mixed, patterned and then cultivated together for 14 h. The cells were successfully cultured in 2,167 microwells out of the total microwells (*e.g.* 99.6%). Only five failures were observed because of SU-8 delamination during the microfabrication.

4.5.3 Extraction and re-culture of selected target cells from the fluid array device

Unlike most biological assays in microfluidic platforms, the screening requires the extraction or retrieval of target cells, followed by culture. Thus, an easy and simple extraction/retrieval method needs to be integrated in the previous cell culture process. The experimental setup for the extraction of the target cells simply consisted of the microscope stage controller and the probe positioner as shown in *Figure 19*.

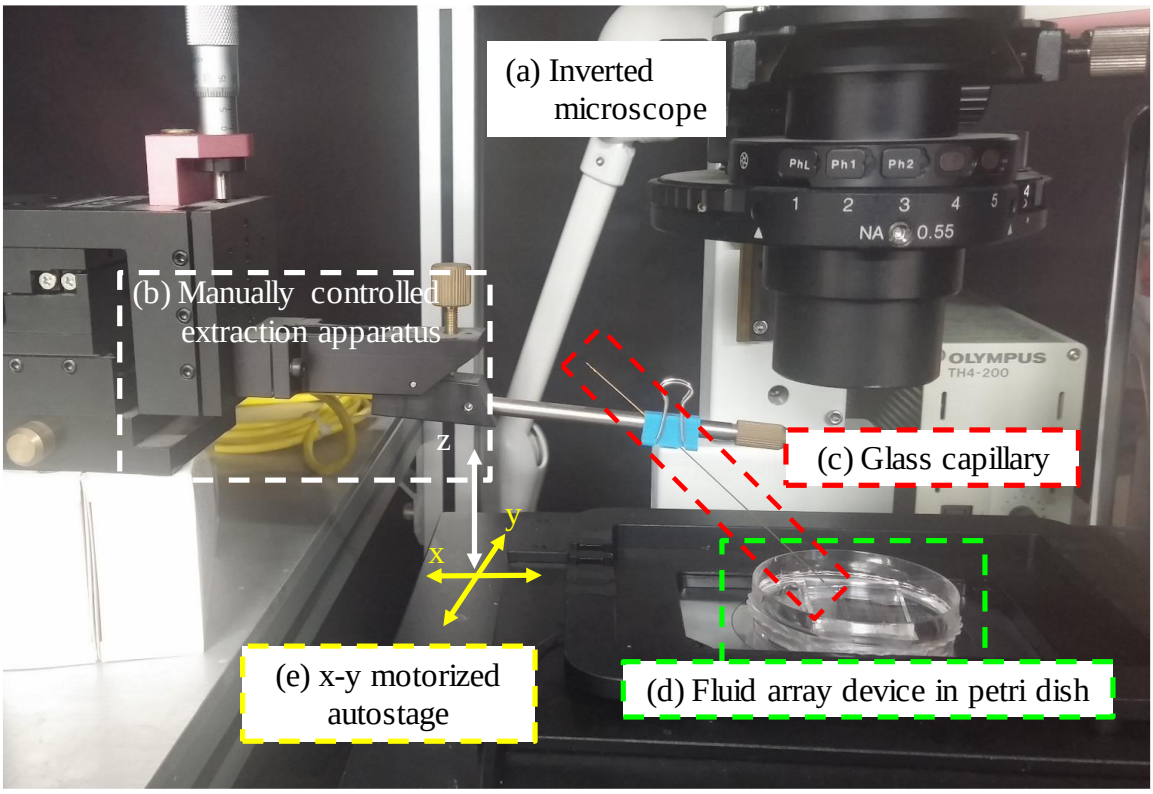

Figure 19 Snapshot of the custom-made extraction system. (a) An inverted fluorescence microscope. (b) An extraction manipulator that can be controlled along the z-axis using a manually controllable probe positioner. (c) A silica capillary tube (or syringe needle) for selective extraction. (d) A fluid array device is placed in a Petri dish (400 mm in diameter) filled with FC-40. (e) A motorized microscope stage of which position is controlled in a synchronous manner with a CCD camera.

The possibility of the extraction of target cells was also investigated by using a commercially available capillary tube or an insulin syringe needle. First, the polyimide coating of the capillary tube was removed by burning it to render the tube transparent and both optical and fluorescence images were acquired (*Figure 20*). The capillary tip was then placed on the target microwell to absorb the fluid, including target cells one by one. *Figure 20b* shows one example of microwells after the extraction process. The absorbed fluid in the capillary was visualized both optically and fluorescently in *Figure 20c* and *Figure 20d*. It turned out that the estimated volume from the images was approximately 30% of the total volume of the microwell. This low value can be attributed to the surface tension caused by the PDMS microwell that may prohibit the complete absorption of the fluid through the capillary tube.

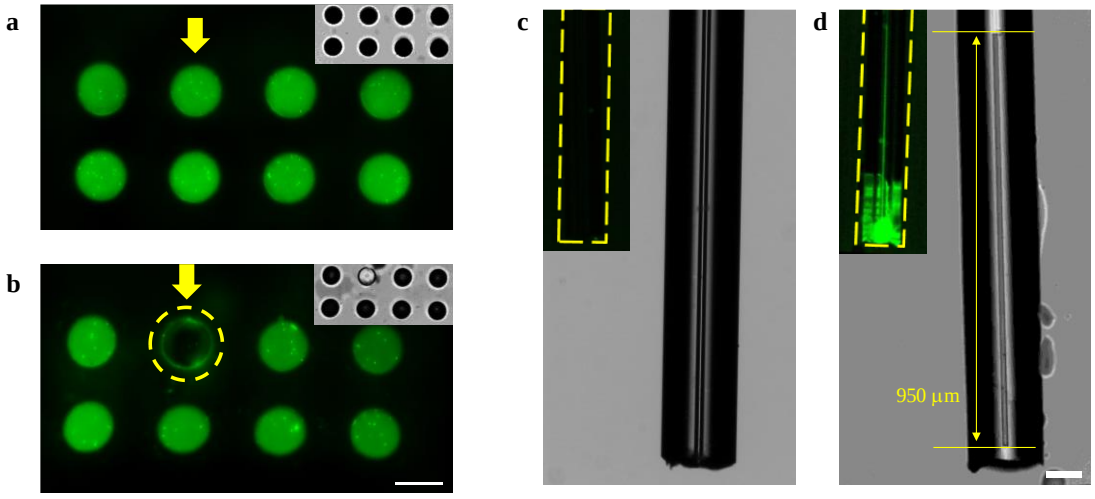

Figure 20. Target cell extraction process. (a)–(b) Comparison of fluorescence images of a fluid array containing GFP-expressing cells before and after the capillary-based extraction process, respectively. (c)–(d) Optical (bright field) and fluorescence images of a capillary tube before and after the extraction process. An initially empty capillary tube absorbed the cell suspension solution in the microwell so that fluorescence signals were measured from the surface and inside of the channel. All scale bars are 100 µm.

Next, the extracted cells were re-cultured. Five fluid array devices/sets were prepared and, from each device, 30 syringe needle tips were used for the separate extraction and culture by inoculating 30 culture tubes individually. The recovery ratio of the 30 culture tubes were quantified and the average recovery ratio was calculated to be about 84.6% as summarized in *Table 4*. This indicates that 126 inoculations were successfully recovered out of 150 extractions. In addition, each set showed considerably smaller variation. Only two failures were observed out of 30 extractions. Therefore, 30% of the total volume of the microwell was more than enough to re-culture the cells in the microwell and the successful recovery ratio allowed the fluid array device in conjunction with the extraction and culture processes to HTS and high-throughput post-analysis of microorganisms in other bioassays. We

note that the silica capillary tubes (hydrophilic) showed a similar recovery ratio to the syringe needles when polyimide coatings were removed whereas a relatively low recovery ratio was obtained when the hydrophobic polyimide coatings remained unremoved as delivered; this is why the syringe needles were chosen for the rest of extraction experiments.

Table 4. Recovery ratio of the extraction method using syringe needles.

	Set 1	**Set 2**	**Set 3**	**Set 4**	**Set 5**	**Avg.**
Recovery/ Extraction	27/30	24/30	25/29	27/30	23/30	25.4 (± 1.5)
Success ratio	90.0%	80.0%	86.2%	90.0%	76.6%	84.6%

4.6 Demonstration of high-throughput screening application

4.6.1 Spike and recovery test for reporter gene-based screening

A spike and recovery test was applied to demonstrate that our microfluidic platform can be applied to the HTS of a small mutant library ($<10^4$) [165]. As shown in *Figure 21a*(i), two different strains were prepared: wild-type MG1655 and its FadE-deficient derivative MG1655 Δ*fad*E. The first strain was transformed with a fatty acid biosensor (pFAS), named MG-Ctrl, and used as a control group. The second strain was transformed with not only the same fatty acid biosensor plasmid, but also another plasmid (pET28a) for Km resistance, and was named MG-Δ*fad*E, and used as an experimental group. It should be noted that the experimental strain exhibited stronger fluorescence signals (RFP) than the control group because the former produces more intracellular fatty acids than the latter. Next, the fluid arrays was produced with 2,832 microwells containing the spiked samples (approximately 10 cells per microwell) and cultured the cells for 14 h (iii). For the entire period of culture, fluorescence images were automatically acquired and their fluorescence intensities were analyzed to identify the target cells. From the analyzed results, about top 5% of all the microwells were chosen for every screening cycle and their cells were extracted (iv) using syringe needles as described previously. All extracted cells were re-cultured in a culture tube overnight (v) and the screening processes were repeated from (iii) to (v). Right before the next screening, the enrichment factors were quantified by counting the number of target cells that grew on a LB agar plate with Km. This was possible because only the target cells

possess a Km antibiotic resistance gene. To almost completely screen out the target cells, the screenings were repeated until the target cells were sufficiently enriched.

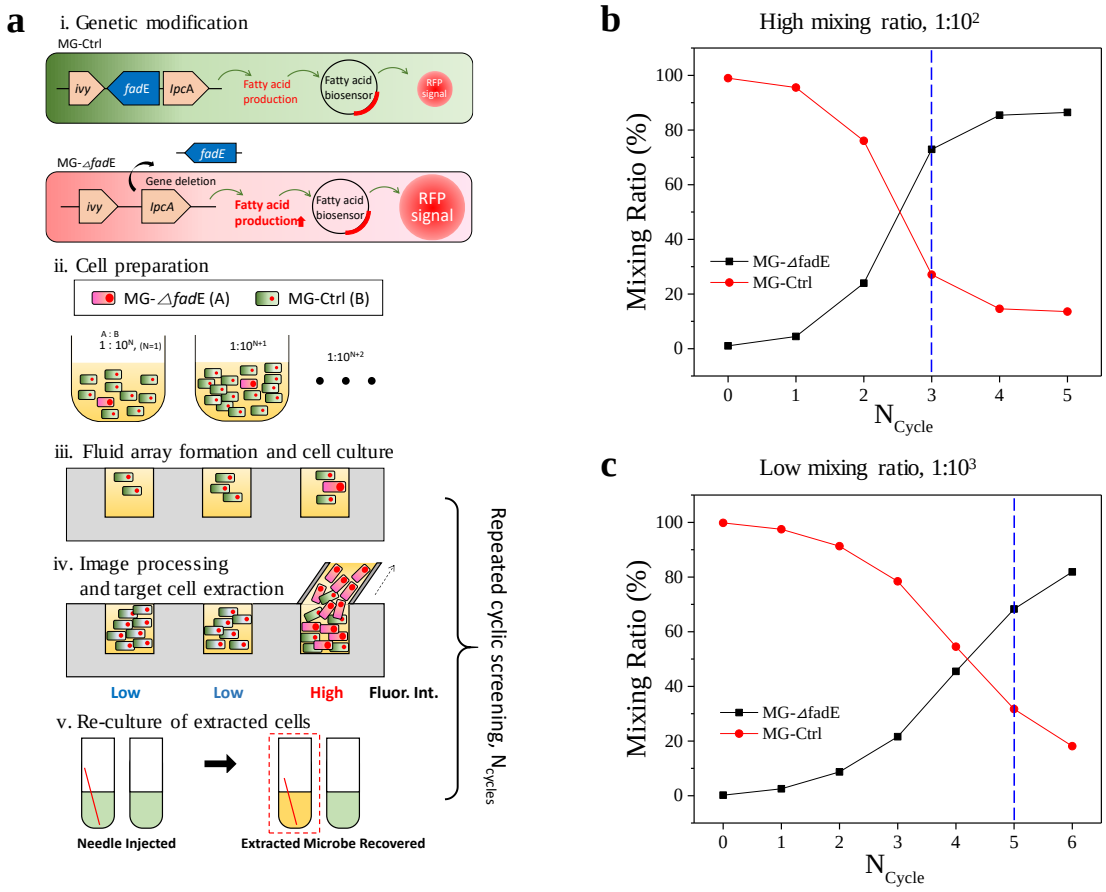

Figure 21. The reporter gene-based screening process. (a) A schematic illustration shows the screening processes. i) Genetic modification of MG-Δ*fad*E. ii) A mutant library is prepared. MG-Δ*fad*E strain was spiked in MG-Ctrl strain at the ratios of S_T:S_N = 1:10^2 and S_T:S_N = 1:10^3, respectively. iii) A fluid array containing the spiked samples was generated and cultured over time. iv) Fluorescence intensities of all the microwells were analyzed and then target cells were chosen and extracted. v) The extracted cells were re-cultured in a culture tube and the screening processes were repeated. (b)–(c) The enrichment of the target cells for the S_T:S_N = 1:10^2 and S_T:S_N = 1:10^3 mixing ratios, respectively. The blue dotted lines represent the screening cycle when the ratio of target cells (MG-Δ*fad*E) to the non-target cells (MG-Ctrl) reverses.

As illustrated in *Figure 21a*, the MG-Δ*fad*E (target strain, S_T) was spiked into the MG-Ctrl (non-target strain, S_N) at the mixing ratios of S_T:S_N = 1:10^2 and S_T:S_N = 1:10^3, respectively. In order to confirm both the mixing ratios at the initial stage, two different streaking and confirmation methods were used. For the high mixing ratio sample (1:10^2), we streaked 10 μL of the cell mixture solution on an agar plate (no antibiotics) and incubated it overnight. Then randomly chosen 96 colonies were inoculated to a 96-well microplate with the colonies one by one in a kanamycin environment. Since only the target strain possessed kanamycin resistance conferred by the pET28a-Km plasmid (refer to *Table 3*), which was intentionally engineered for easy streaking and selection on the agar plate, the surviving samples were

expected to be the target strains. As a result, only one well out of the 96 wells presented a fluorescence signal, confirming that the cell mixture sample was well prepared. For statistical and rational confirmation, 96-well microplates were used for 1% spiked samples ($1:10^2$). However, the same method could not be used for 0.1% spiked samples ($1:10^3$) for the same verification.

For the low mixing ratio sample ($1:10^3$), an agar plate with Km resistance and then spread 100 μL of 1,000 cells by adjusting the population of the cell mixture sample based on the OD_{600} measurement. Subsequently, it was possible to confirm the screening result for the low mixing ratio (e.g., for the mixing ratio of $S_T:S_N = 18:10^3$, about 18 target cell colonies formed out of 10^3 spread cells including both target cells and non-target cells). In parallel, a fluid array device consisting of 2,832 microwells was prepared and the cell mixture sample was compartmentalized on the device. After the re-culture, target cells were enriched and the screening process was repeated. The mixing ratios of each screening process were confirmed as illustrated in *Figure 21b* and *Figure 21c* in the main manuscript. After several repeated cyclic screening rounds, more target cells were obtained than non-target cells. Consequently, the final mixing ratios reached $S_T:S_N = 83:13$ and $S_T:S_N = 819:181$ from the high ($1:10^2$) and low ($1:10^3$) mixing ratios, respectively.

Figure 21b shows the gradual enrichment steps for the high mixing ratio of the target cells (MG-Δ*fad*E) to the non-target cells (MG-Ctrl) as the screening repeats. After four screening rounds, we obtained more target cells than the non-target cells and after six rounds, more than 80% of target cells were screened and dominant over the non-target cells. *Figure 21c* shows the enrichment steps for the low mixing ratio as the screening repeats. As expected, the target cells were gradually enriched, while the non-target cells were sufficiently diluted out in the enrichment conditions. After the first screening process, the initial mixing ratio of $S_T:S_N = 1:10^3$ reached $S_T:S_N = 25:975$, which is almost the same as the high initial mixing ratio of $S_T:S_N = 1:10^2$ (*Figure 21b*). Therefore, it is theoretically estimated that, after five additional screening processes, the resulting ratio should be close to $S_T:S_N = 80:20$. Not unexpectedly, in five additional screening processes, the final mixing ratio turned out to be $S_T:S_N = 819:181$, which is close to the final result of the high mixing ratio experiment. It is noted that the quantification method for the number of cells used in this work may cause some systematic errors. The gradual escalations were possible because the extracted cells showing stronger fluorescence signals contained more 'MG-Δ*fad*E' cells than 'MG-Ctrl' via the repeated cyclic screening.

4.6.2 Screening of a small mutant library based on cell growth

The same microfluidic platform was applied to the screening of fast growing mutants that were fed cellobiose as a nutrient. The higher cellobiose consumption rate implies the faster cellular growth rate. For such cell growth-based screening, a CP12chbasc strain was used as a basal strain that expresses cryptic operons *asc* and *chb* under the synthetic CP12 constitutive promoter to confer efficient cellobiose metabolism [166-168]. The strain CP12chbasc was used to construct a random transposition mutant library (*e.g.* 4,000) (*Figure 22a*).

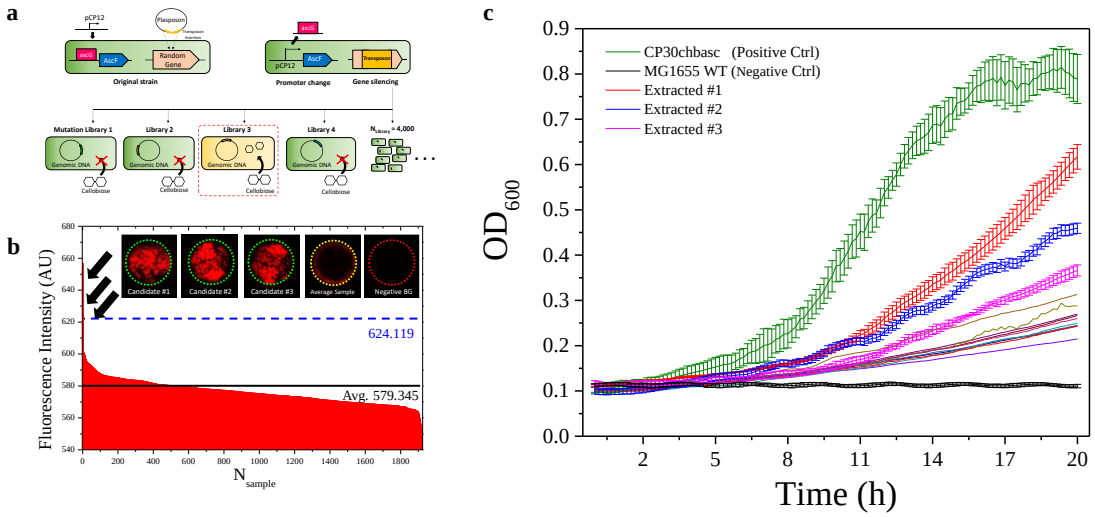

Figure 22. Growth rate-based screening process. (a) A schematic representation of the mutagenic library construction. (b) Quantified results of a fluid array incubated in cellobiose environments for 20 h. Three black arrows indicated three candidate strains consuming cellobiose as the carbon source. (c) OD_{600} values were obtained: the CP30chbasc strain (green), the three extracted samples (red, blue, and purple) consuming cellobiose, and other ten randomly extracted samples obtained by using a conventional microplate reader.

Presumably, some mutants may have positive mutations in genes involved in cellobiose metabolism. Thus, the fluid array platform would allow us to sort and screen out the target cells with fast growth on cellobiose (0.2% in M9 minimal medium). a fluid array was precisely produced with approximately 20 cells per microwell (total 2,832 microwells). And then the cells were cultured for 20 h, which was longer than the previous cell culture because the M9 minimal medium contains less nutrients than the LB medium. RFP fluorescence intensities from the cells were measured. The stronger fluorescence intensities indicate that the target mutant cells grow better by feeding on cellobiose and produce more RFP. From the analyzed fluorescence signals in *Figure 22b*, three potential candidates presenting superior cellobiose consumption rates were identified, followed by their extractions and re-culture (see insets in *Figure 22b*). Non-target cells in 10 microwells showing relatively weaker fluorescence signals were randomly extracted for comparison with the target cells. *Figure 22c* shows the OD_{600} values of the target and non-target cells measured by using a microplate reader in the presence

of cellobiose nutrients as a sole carbon source for 20 hours. It is obvious that three extracted candidates showed much higher growth rates than the non-target cells while they showed slightly lower growth rates than the positive control strain CP30chbasc with optimized cellobiose metabolic pathways [166].

4.7 Discussion

One may think that our platform uses similar analytical approaches as the commercialized OpenArray system™ (Applied Biosystems, Foster City, CA, USA) that was developed for quantitative or real-time PCR in a high-throughput manner [169]. However, the fluid array and cell extraction platform described in this study was particularly developed for HTS of small mutant libraries, showing several and unique differences. First of all, the fluid array device can be easily fabricated by using the standard photolithography and repeatedly replicated by using a master mold *via* soft-lithography. In addition, the platform does not need any microfluidic accessories such as syringe pumps, pneumatic valves, and other fluid controller systems. As demonstrated, aerobic and anaerobic cultures of microorganisms can be easily chosen and even switched in the middle of the experiments. Additionally, for complete anaerobic culture, once the fluid array device is encapsulated within a small container into which nitrogen gas is continuously flown, the oxygen dissolved in the PDMS can be completely eliminated. The extraction process was performed manually in our experiments, but it should be easy to fully automate the process with the help of robotic arms equipped with needles. As shown in this study, the fluorescence images of the entire fluid array can also be automatically acquired by using a motorized stage with a z-axis auto-focusing function and then processed by using our in-house code to determine target cells for future HTS applications.

Typically screening hinges on phenotypic features of target cells. For example, target cells can be engineered to exhibit stronger fluorescent signals as used in this work. In addition to the fluorescence signal method, several other methods can be used for screening target cells such as colorimetric methods, enzymatic reaction with appropriate metabolites, and two component system in which one cell secretes biomolecules to which the other responds. Notably, it seems straightforward that the fluid array platform can be combined with all of the aforesaid methods. For the growth-based screening, the target cells were successfully extracted, which fed on and digested cellobiose as a carbon source, by using a positive selection approach. In the case of screening target cells with poor growth rate, the fluid array platform allows us to sort target cells in the same manner as those with the high growth rate. Therefore, it is needless to say that the fluid array platform shows many advantages for various screening conditions and experimental demands that are not easily achieved in conventional culture environments. Lastly,

the platform can be further utilized for practical applications in many phenotypic screenings partially demonstrated in this study, isolations of extraordinary microorganisms under controlled environments, microbial resistance tests to various antibiotics, directed evolutions, optimization of metabolic pathways, discoveries of new metabolic factors, etc. Of course, the platform in its current version possesses several weaknesses: manual extraction method, low extraction volume, and screening performance. However, it does not seem to be challenging to overcome these weaknesses in the near future [36].

4.8 Conclusion

A novel microfluidic HTS technique was developed in this study for a small mutant library by combining the fluid array device with the capillary-tube-based extraction and re-culture processes. The fluid array device consisted of microwells to culture microbial cells and a fluorinated oil container for high-throughput compartmentalization of the cells. Since each microwell of the fluid array device provided separate, but identical cell culture environments, the cell population in each microwell was extremely high, showing much higher values of OD_{600} than those obtained by using conventional culture methods. In addition, the extraction and re-culture of target cells out of the fluid array device enabled repeated cyclic screening. Using the spike and recovery test, the platform could be used for the HTS of a small mutant library based on reporter gene differences. Not only did the reporter gene based screening was performed, but it was demonstrated the feasibility of the growth based screening using the same platform, making it possible to screen and sort target cells in a certain ascending or descending order. Therefore, the combination of the fluid array device and the target cell extraction method developed in this study offers remarkable advantages over the conventional HTS techniques. Indeed, a relatively small number of microwells was used (<3,000 wells in 2 cm by 3 cm), but the expansion of the device up to a wafer scale (6” or higher) may increase the total number of microwells up to 10^6 to 10^7, showing high potential for the HTS and the enrichment of target cells. This proposed platform can be an alternative for HTS applications. However, the entire processes could be fully automated, including the generation of a fluid array, culture, image acquisition, processing, selective extraction, and re-culture, in the near future [36].

Chapter 5. Advanced High-throughput Screening Applications by Fluid Array

5.1 Microbial platform for fatty acid production

Fatty acids have been used as the precursor substrate of various type of fuels and chemicals in the last few decades. Free fatty acids (FFAs) have attracted public interest due to its potential to meet the demand for controllable and renewable energy. Also the FFAs are considered to have many industrial uses including bio-fuels, cosmetics, lubricants/solvents and pharmaceutical drugs. Microorganisms show a considerable potential in terms of an efficient platform for FFAs production [170-172]. While the corn-based production methods for FFAs resulted in a competition with food, increased refinery costs, land-use efficiency and environmental concerns, FFAs production using microorganism *E. coli* is a more ideal approach for production purposes in terms of its economic costs, rapid growth, and comparably spatial-efficient method [173].

5.2 Rationally designed engineering of TesA for improved microbial fatty acid production

Since *E. coli* is a well-studied industrial organism, there are many studies regarding the improved production of FFAs using various approaches. Through many related metabolic pathways, microbial FFAs have been mostly synthesized from acyl-ACP (acyl carrier protein) by the key enzyme, thiosesterase I (TesA) [174, 175]. With the well-studied enzymatic characteristics of TesA, catalytic enzyme reaction of TesA have often been utilized to increase cellular FFAs in several alternative studies. However, a genetic overexpression for enzymatic component of the fatty acid synthase (FAS) does not always guarantee for maximization of the FFAs production in *E. coli* as reported by Jiang *et al* [176]. It is required to have the optimal ratio of enzymes and FAS components in the fatty acid synthetic pathway for the improvement of production yield. According to previous findings, Shin *et al*. reported a high-throughput screening approach of a TesA mutant library to screen out the extraordinary TesA mutant which produces a twofold greater amount of FFAs than the WT enzyme [175]. The constructed mutation library size reached 10^6 which is an impossible number to handle by using conventional

experimental tools. A two-step selection pressure system was therefore sequentially applied: (1) FFA-dependent tetracycline resistance for growth-based antibiotic enrichment of the expected mutants and then (2) FFA-dependent RFP expression for FACS machine screening. However, in the process of such mass culture for growth enrichment, few extraordinary samples can only dominate the whole mutant library due to antibiotic competitive growth. Still, the individual growth of mutants that possibly have suboptimal production performances of FFAs can be negatively affected by competitive crosstalk of the bulky populated condition. Therefore, compartmentalization is required to apply in this screening application for avoiding such crosstalk.

5.3 C2C communication screening for extracellular fatty acid production

In addition to such modification of thioesterase enzymes to achieve the improvement of total biosynthesis for fatty acids, a secretion of fatty acid from inside of the microbial membrane is an important issue for optimization of FFAs production, due to an intracellular pH changes and a feedback inhibition of intracellular fatty acid. There are also innovative approaches including the precise control of enzyme activities/expression levels and optimizing/redesigning of metabolic pathways for the secretion purpose [38, 177, 178]. However, an understanding of a precise metabolic pathway still stayed in poor level due to too many cellular properties related with the metabolism. In contrary, random approaches such as transposon mutagenesis do not require preliminary knowledge of relevant metabolic pathways. For example, Shin *et al.* reported microbial secretion pathways of fatty acids on genomic DNA (gDNA) of *E. coli* by the identification for locations of transposon insertions.

However, the previous research suggested FFA-Tet fusion genetic circuit which are vulnerable for an unknown crosstalk from in/-outside of the microbe, since the FFAs sensing system and the growth-coupled genetic circuit were embedded together. Therefore, separation of the sensing part and the production part of microbe would convey new opportunity to perform the screening of extracellular FFAs secretion mutant from the transposon mutation library. In order to achieve such purpose, it is necessary to design a cell-to-cell communication system consists of donor cells and recipient cells whereas the donor cells (DC) produce/secrete certain biomolecules that precisely stimulate recipient cells (RC) with gene expression of the designed reporter gene including fluorescence and colorimetric way.

Although there are some studies regarding a cell-to-cell communication on a microorganism level [179, 180], only few reported research publications have considered the possible effect of a cell-to-cell communication (C2C) based screening approach in a practical way [181-183]. Having a C2C

communication system for a screening purpose, apart from the functions of producing/sensing the secreted biomolecule in different cellular platforms, reduces cell-to-cell variation, stochastic heterogeneity of metabolic pathways and crosstalk from other intracellular bioactivities [184]. Conventionally, such C2C screening systems are performed by using a microplate with a lot of effort to seed two different cells in a single microplate array or spraying the recipient cells on an agar plate that has a colony of donor cells. However, such conventional approaches have critical limitations on the throughput of a sample, procedure reliability, and accuracy of colony locations. Therefore, more designated experimental methods to encapsulate such C2C donor/recipient cells in isolated arrays had more attention, for instance microdroplets in a microfluidic platform. The use of microdroplets in microfluidic platforms is usually suggested as an alternative for such C2C application [182]. However, since there is a technical tradeoff between compartmentalized arrays/throughput and selective extraction systems for many microfluidic approaches, up to date, no specialized microfluidic devices were introduced which have satisfied the requirement for both a high-throughput performance and a compartmentalization.

5.4 Fluid array applied to two screening applications

In this research, two different screening approaches were introduced to complement the two conventional microbial screening approaches mentioned earlier. First, the microfluidic fluid array platform [36] was applied for the screening of 10^6 TesA mutant library. The screening based on the fluid array platform has several advantages over our previous two-step screening pressure approach. For example, a hybrid type screening procedure with both reporter gene-based and growth-based screening was applied for randomly mutated cells in isolated culture conditions to avoid crosstalk from the bulk culture condition. Second, the C2C based high-throughput screening was designed, and we obtained the mutants showing outstanding secretion performance of fatty acid molecules. After the completion of two screening processes, the improved thioesterase I enzyme mutants were integrated with another screened mutant showing over-secretion performance of extracellular fatty acids. The combination of different fatty acid biosynthetic systems screened by the fluid array was synthesized and tested with fatty acid production by GC analysis.

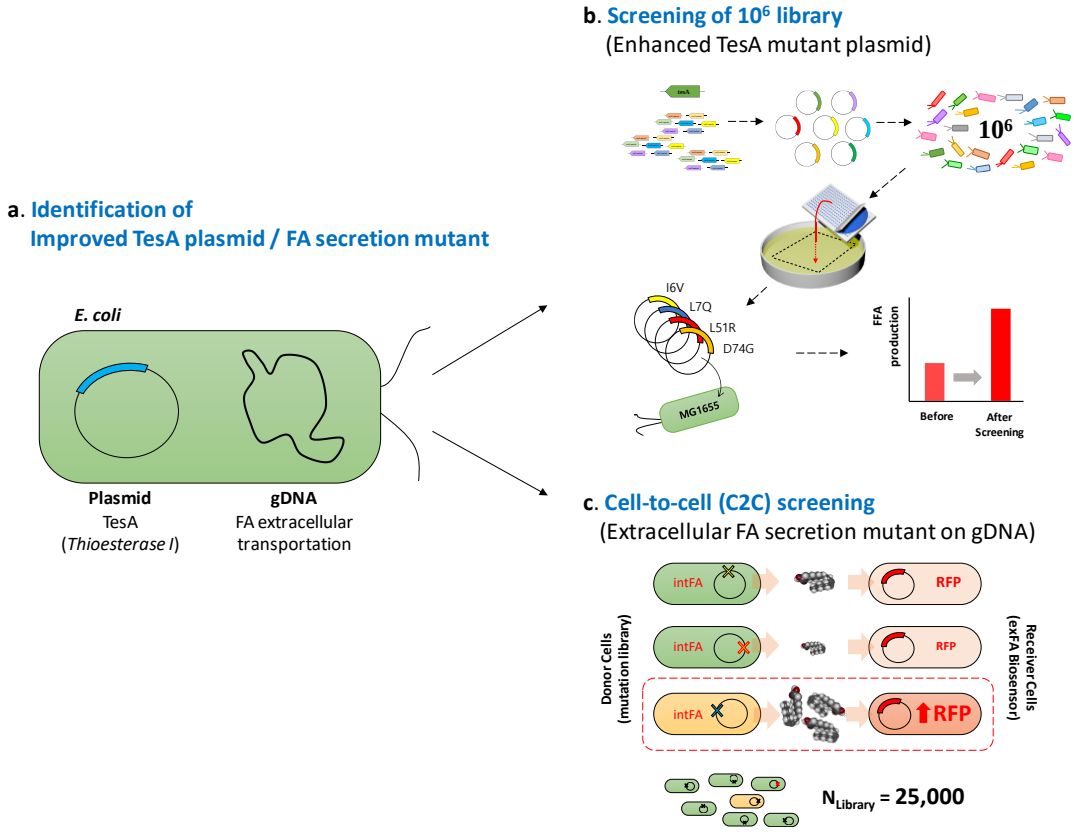

Figure 23. A schematic diagram of two different screening strategies. (a) Engineering of TesA on plasmid and random gene deletion on gDNA for FA extracellular secretion. (b) A schematic of screening for TesA 10^6 library by the fluid array device. (c) Cell-to-cell communication based screening with DC and RC in compartmentalized environments.

5.5 Experimental methods

5.5.1 Material and reagents

Two types of oils with different specific gravity (SG) were used for compartmentalization of aqueous solutions: hydrocarbon oil (Hexadecane, SG = 0.76, Sigma-Aldrich, Korea) and fluorinated oil (FC-40, SG = 1.61, Sigma-Aldrich, Korea). Red food dye and 50 μM of fluorescein isothiocyanate (FITC) solutions were used for the visualization and characterization of the fluid array. For cell culture, Luria Bertani broth (LB, Sigma-Aldrich, Korea) was prepared with proper antibiotics such as ampicillin (Amp, 75 μg/mL), chloramphenicol (Cm, 50 μg/mL), kanamycin (Km, 50 μg/mL) and tetracycline (Tet, 50 μg/mL) (all purchased from Bioshop Canada Inc.). An LB agar plate was also prepared (1% of w/v, Agar, Becton Dickinson) for colony formation. To avoid shrinking of the produced fluid array, FC-40 oil was mixed with distilled water (0.1%, v/v) up to the limit of solubility in a rotary shaker at 60 °C. Distilled water was not fully mixed with the oils so that the final concentration of water in the oils was

estimated to be approximately 0.02% (v/v) according to previous report. For the extraction of target cells, both fused-silica capillary tubes (CAT no. #1068150011, Polymicro Technologies, Phoenix, AZ, USA) with 25.3 μm inner diameter and 360 μm outer diameter (OD) and commercially available insulin syringes with OD = 200 μm were used.

For the analysis of the FFAs production, M9 minimal medium (Minimal salt 5×, Becton Dickinson, Franklin Lakes, NJ, USA) supplemented with 2 mM MgSO4, 0.1 mM CaCl2, and 0.5% (w/v) glucose was used for the growth-based screening of the mutant library. Yeast extract 1 g/L (w/v) and trace elements were additionally added. The trace elements consist of 2.4 g of $FeCl_3 \cdot 6H_2O$, 0.3 g of $CoCl_2 \cdot 6H_2O$, 0.15 g of $CuCl_2 \cdot 2H_2O$, 0.3 g of $ZnCl_2$, 0.3 g of $Na_2MO_4 \cdot 2H_2O$, 0.075 g of H_3BO_3, and 0.495 g of $MnCl_2 \cdot 4H_2O$ per liter. The pH was maintained at 7.0 with 2 N NaOH buffer solution by rigorous mixing of 57.7% Na_2HPO_4 and 42.3% NaH_2PO_4. For induction of the expression of thioesterase, 0.3 mM of Isopropyl β-D-1-thiogalactopyranoside (IPTG) was added at OD_{600} of 1 [175].

5.5.2 Preparation of bacteria cells and GC analysis of FFAs microbial production

E. coli K-12 strain MG1655 was used as a platform cell. For the high-throughput screening of TesA mutant library, fatty acid biosensor (FAB) cells were prepared with harboring biosensor plasmid pFAB as described in previous studies [175]. For production of FFAs, the essential enzyme TesA in a leaderless form (‘TesA) has been used in several studies. Before the construction of random mutation library, *tetA-rfp* fusion protein on the BioBrick plasmid pBbE8a-*rfp* was transformed for the tetracycline antibiotic resistance. Then, error-prone PCR mutagenesis of TesA was conducted and the PCR products were cloned into EcoRI and XhoI with substituted sites of pBbB6c-*gfp* by Mutagenex (Suwanee, GA, USA) resulted in 10^6 independent colonies as total library size without hot spots of certain mutation sites.

Second screening based on cell-to-cell communication used the extracellular fatty acid biosensor (exFAB) which was engineered with PLR promoter as reported previously [177]. To construct donor cell library, *E. coli* strain MFDpir, which was used as the plasposon donor strain, was purchased from the Pasteur Institute (Paris, France). MFDpir cells were transformed with pTNMod-R6KKm^R, and this plasposon was transferred to *E. coli* MG1655 by bacterial conjugation, as previously described [185]. After transformation of the plasposon, the cells were collected and plated on LB medium containing kanamycin. In total, approximately 25,000 clones containing the desired transposon insertion were obtained [186].

GC analysis was conducted to analysis microbial FFAs production yield in a precise quantitative manner. Selectively extracted cells were cultivated in LB medium and diluted 1/100 in M9 minimal medium with 2% (w/v) glucose, phosphate buffer to maintain pH 7.0. When OD_{600} is reached approximately 1, IPTG was added to the final concentration of 0.3mM for genetic induction of thioesterase, TesA. After 48 hours of incubation with FFAs microbial production, each of 500 μL cultures were stored in -20 degree refrigerator for an hour. Then, 50μL of pure HCl and 500 μL Ethyl Acetate were added in sequence. 30 sec of mixing by Vortex was conducted and centrifuged for 2 minutes. 500 μL of top supernatants were collected in GC vials for further GC analysis of microbial FFAs, respectively.

5.5.3 Statistical modeling of the library coverage and the optimal seeding condition

The two-different type of genetic screening tools, that are similar to a duel selection system, were simultaneously employed in this microfluidic screening process to obtain overproducing mutants from the 'TesA mutant library. In our previous paper [175], the first screening tool was the modified genetic circuit for FFA-dependent tetracycline resistance, which differentiates the cellular doubling time to perform an antibiotic enrichment. The second tool was the FFA-sensing plasmid, which shows a dose response of fluorescence intensity, equivalent to the presence of intracellular fatty acids. The experimental calibrations of the RFP biosensor of FFA-sensing and the genetic circuit of FFA-dependent tetracycline resistance were already investigated, previously [175].

For the appropriate screening coverage of the mutation library that we constructed, a simple statistical formula below was used and the equation was derived from *Poisson's Law*. According to the equation, P is defined as the probability to cover the whole mutation library, *f* is the number of the mutation library represented by collected colonies whereas *N* is defined as the amount of coverage required to get *P*.

$$N = \frac{\ln(1-P)}{\ln\left(1-\frac{1}{f}\right)} \quad (eq.\ 1)$$

For the 10^6-random mutation library of 'TesA, the experiment which had initial seeding number of 30 cells per chamber with 20 fluid array devices, was delicately designed after considering the library

coverage. Therefore, the experiment accomplished the screening of approximately 1.8×10^6 samples on the fluid array devices which statistically covered over 95% of the 10^6-whole mutation library by following the above equation (*eq. 1*). After seeding 30 cells at the initial state, we performed microbial incubation for 20 hours to provide more than enough time to differentiate the enrichment process of the FFA-dependent tetracycline resistance as well as the fluorescence signal from FAB biosensor plasmid. In terms of the throughput perspective, therefore, the 20 fluid array chips in parallel preparation were used, and covered more than 95% of 10^6 of the 'TesA mutant library. Although it was difficult to quantify the enrichment of dominant cells that was happened again in the recovery process (*e.g.* test tubes with modified M9 medium with tetracycline antibiotic environment), it was assumed that 30 different initially seeded library cells resulted in only few mutants because of the enrichment growth from the FFA-dependent tetracycline resistance. Among those chambers in the fluid array device, we measured the fluorescent intensity from RFP corresponding to the intracellular FFAs concentration in a quantitative manner as second screening criteria. By sorting the quantified fluorescence intensities, top <1% fluorescence samples were selected, extracted and recovered in the modified M9 medium. The fatty acid production yield by GC were analyzed from at least 5 individual colonies per one chamber extracted by a glass capillary.

For C2C communication based screening, there are some experimental factors to be considered such as optimal ratio between the extracellular amount of fatty acids from DC and sensitivity of RC harboring exFAB biosensor prior to the actual microfluidic screening process. Various ratio of DC/RC were tested by a microplate reader to find the optimized mixing condition of two strains (*Figure 24*). The optimal seeding ratio of DC/RC at the initial state was determined to be 3:1 according to the previous result showing the highest fluorescence intensities from 4:1 and 2:1 cases. Considering a screening coverage for mutant library and compartmentalization efficiency, initial mixing ratio of DC/RC was 9:3. The mutation library of donor cells were prepared by the TN5 transposon insertion, as previously explained, which mutation library size reached approximately 25,000 mutants [186]. To cover all the mutant library, it was prepared to have three fluid array devices that had 3,000 individual arrays for 9 mutant DCs in each chambers, resulting in more than 90,000 cells were seeded. According to the equation (*eq*. 1), more than 99% of mutant library was statistically covered by three fluid array devices. After 20 hours of incubation in the modified M9 medium, top 1% of arrays showing the highest fluorescence signal of RCs were extracted and recovered on agar plates to make individual colonies. Individual 5 colonies from each agar plates were picked, re-incubated and analyzed the fatty acid production yield by GC analysis.

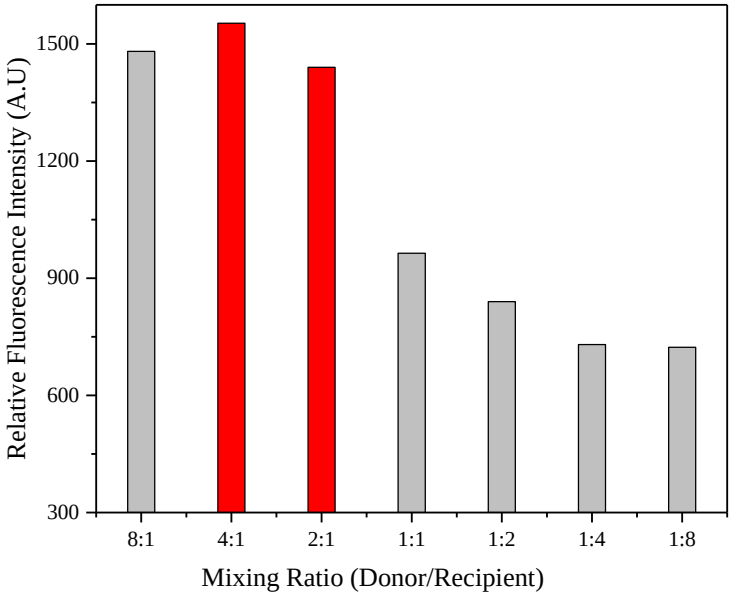

Figure 24. Optimized mixing ratio for DC/RC using a microplate reader. While the MG1655-envR were chosen as the positive control of donor cells showing higher extracellular fatty acid production, recipient cells MG1655 harbouring exFAB biosensor plasmid were calibrated using a microplate reader. Red filled bars indicate the optimized detection range for exogenous fatty acid detection by exFAB biosensor.

5.5.4 Fabrication of the fluid array device

The microfluidic device was fabricated and the dimension of the microwells was 100 μm in diameter and 150 μm in depth having 3,000 arrays in a single device (3 × 3 cm). Spacing between individual arrays on a device were delicately redesigned from 4 × 2 to 3 × 2 matrix with considering the recovery efficiency of the glass capillary extraction process [36]. As described previously, an SU-8 (Microchem 2075, Newton, MA, USA) master was fabricated using the standard photolithography technology. The processed surface of a Si-wafer was silanized using trichloro(3,3,3-trifluoropropyl) silane (Sigma Aldrich, Korea) in a vacuum jar for 1 hour. Polydimethylsiloxane (PDMS, Sylgard 184 Silicone Elastomer Kit, Dow Corning, Mid-land, MI, USA) was then casted, cured, and peeled off to prepare the microfluidic devices. The PDMS devices were dipped into distilled water for several hours, resulting in a fully moisturized state (*e.g.* the highest solubility of water into PDMS) so that the fluid in the microwell remained stable without apparent volume shrinkage over 24 h. During long-term incubation (> 12 h), fluid array device was half dipped oil and half dipped water to minimize drying of array chambers.

5.5.5 Experimental setup and data analysis

An inverted fluorescence microscope (IX-71, Olympus, Tokyo, Japan), equipped with a CCD camera (Clara, Andor, Belfast, Northern Ireland) and 1.5×, 10×, and 20× objective lenses, was used to acquire fluorescence images from the fluid array device. The images were automatically acquired by using a microscope stage controller (MAC5000/Bioprecision2, Ludl Electronic Products, Hawthorne, NY, USA) using the multi-dimensional acquisition (MDA) function from the image software Metamorph 7.1 (Molecular Devices, Sunnyvale, CA, USA). The fluorescence intensities of the images were then analyzed using a custom-made m-file in MATLAB R2014a (Mathworks, Natick, MA, USA). For additional data analysis and necessary image processing, Image J (NIH, Bethesda, MD, USA) and OriginPro 8 (OriginLab, Northampton, MA, USA) were used. A manually controlled probe positioner (PB50, MS Tech, Hwaseong, Korea) was used to fix either syringe needles or capillary tubes for the extraction of target cells.

5.6 Screening of larger mutant library : Increased throughput of 10^6 TesA mutants

5.6.1 GC analysis of FFAs and genetic identification of extracted mutants

The hybrid type screening suggested in this study integrated two such screening genetic tools into the one hybrid screening approach with several advantages. The fluid array brought the advantages over conventional experiments, for example, high-throughput compartmentalization, data sorting in a sequential manner, and avoiding competitive crosstalk caused by the FFA-tetracycline fusion genetic circuit. As discussed in *Section 5.5.3* by considering the coverage of the mutant library and the throughput of the device, we determined that 30 individual mutant library cells per single chamber are more than enough to distinguish and meet the first screening criteria, the FFA-dependent tetracycline resistance. After incubation process in the fluid array platform and data analysis, capillary extractions were conducted by a descending order of the fluorescence signals from each chamber. Finally, the 17 samples based on the hybrid type of screening criteria were chosen, and their FFA production yields were analyzed by GC analysis (*Figure 25*). The extracted samples were incubated repeatedly to compare the fluorescence signal of the negative control MG1655 in visualized images (*Figure 26a*) and the quantitative analysis (*Figure 26b*). The mutants showing higher fluorescent signals also showed increased FFA production yield as the results of the GC analysis (*Figure 25*).

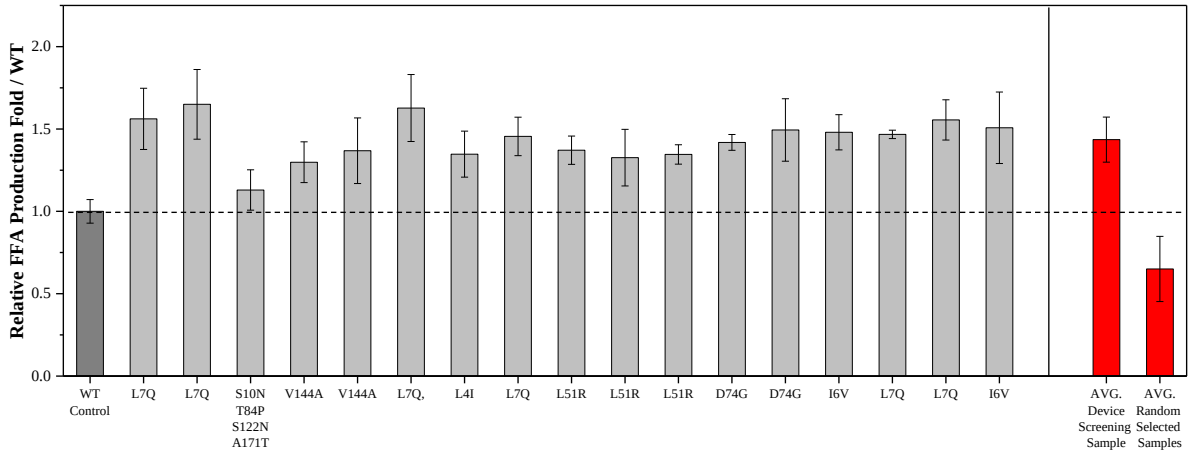

Figure 25. Fatty acid GC analysis. (Left) All screened 17 mutants were identified each of mutation residues (Right) Average FFA production from the mutants that were selectively extracted by the order of fluorescence intensity. To see the difference of efficiency of the fluid array device, arbitrarily selected 20 extractions were also analyzed their FFA production by GC analysis.

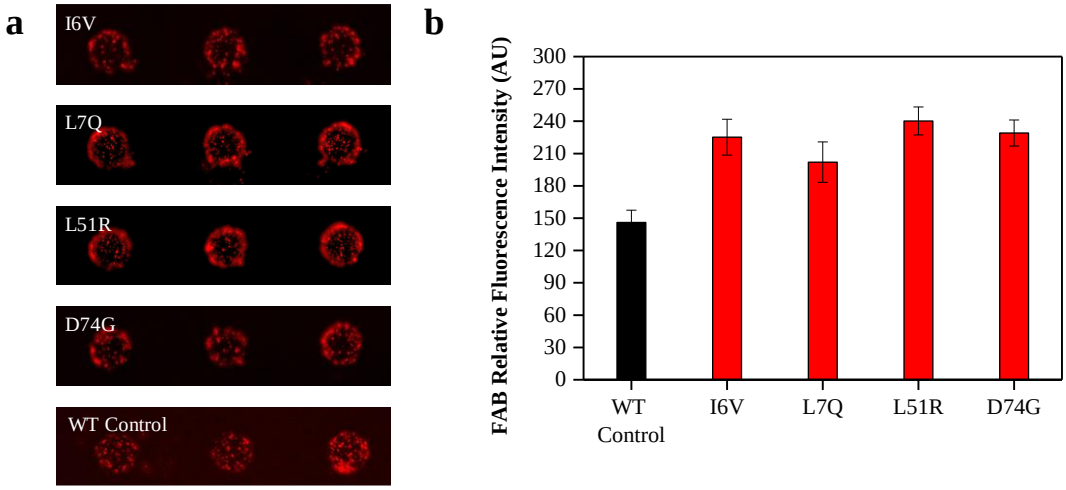

Figure 26. Images of screened mutants on fluid array devices and quantification. (a) Fluorescence microscopic images of re-cultivated selected mutants and WT control. (b) Quantified fluorescence intensities of selected four mutants.

We then identified the 17 mutated sequences of 'TesA, as shown in *Figure 25* and *Table 5*. The GC analysis data in *Figure 26* was plotted against the relative FFAs production yields compared to the WT TesA strain. The identified mutation sequence of 'TesA showed some meaningful genetic results. We not only found some mutation points that overlapped with our previous results, we also obtained newly discovered 'TesA mutants that increases FFAs production by almost two fold. The substitution of aspartic acid to glycine at the 74th position in 'TesA increased FFA production (*Figure 27*). This

result was consistent with previous work that the mutation at the 74th substitution (D74G) produced 1.5-fold higher FFA [187]. As an N-terminus of the loop (residues 75–80) that significantly moves when 'TesA interacts with its substrates, the Asp 74 regulates the movements of the loop during catalysis [188]. Therefore, it was hypothesized that the change in the 74th residue might influence interaction between substrates and 'TesA, resulting in higher FFA production. Research on the 171st residue has not been reported, however, it might be involved in increased FFA production as previously reported [187]. The change in the 122nd residue might influence the movement of F121 that surrounds the substrate-binding crevice, resulting in substrate affinity [188, 189]. The mutants harboring L7Q, L4I, and I6V exhibited approximately a 1.4 fold increase in FFA production. The role of the residues has not been reported previously, however, the mutation in N-terminal in 'TesA might affect the properties of protein as mutation in the N-terminal of the protein affect activity [190]. It is difficult to explain how two mutations (V144A and L51R) improve the FFA production because there are no studies on the residues. Previously, mutations in noncatalytic residue altered substrate specificity and ligand binding, driven by structural changes of the protein [191]. The mutations (V144A and L51R) might act in a similar manner to that seen in the other studies.

Table 5. Identification of mutations for screened mutants

Mutations	Number of colonies in total selected colonies (% percentage)	Fold increase in FFA production	Remarks
L7Q	6/16 (37%)	1.3	
L51R	3/16 (18%)	1.3	
D74G	2/16 (~11%)	1.7	Same mutation (D74) from Shin *et al*. [175]
V144A	2/16 (~11%)	1.4	
L4I	1/16 (~6%)	1.2	
I6V	1/16 (~6%)	1.3	
S10N, T84P, S122N, A171T	1/16 (~6%)	1.2	Same mutation (A171) from Shin *et al*. [175]

To see a relativeness between the screening performance of the fluid array and the FFAs production yields, the extracted mutant samples were categorized into two distinguished groups. The first group consists of 17 chosen mutants based on top <1% chambers showing the highest fluorescence intensities from the fluid array device and another group was arbitrarily selected 20 samples as comparison. In the first group, the average of production yield from the 17 mutants showed the improved production yields

of FFAs (*Figure 25, right*), compared to that of randomly selected 20 mutants, the second group. This result shows the hybrid type of screening method worked very well with a significantly different FFAs production yields between two categorized groups.

5.6.2 Effect of mutations on TesA changes FFA production yield

Throughout the hybrid screening process, several genetic mutants of 'TesA were revealed and analyzed by DNA sequencing of the extracted cells. To confirm that the increase in FFA production originated from the replacement of revealed mutated 'TesA, it is necessary to verify that the mutation sequences are also genuine to the WT MG1655 whether the replacement of 'TesA plasmid is resulted in an improvement of FFA production. The WT TesA was replaced with top 4 isolated mutations showing the highest FFA microbial production (*Figure 25*) which mutated residues were I6V, L7Q, L51R, and D74G. After the replacement of mutation thioesterase, GC analysis of those mutation showed increased FFA production with ranging from 1.3 to 1.7 fold larger than the WT TesA (*Figure 27*). These results indicate that the isolated 'TesA mutant replacements directly accelerate fatty acid biosynthesis compared with the WT TesA.

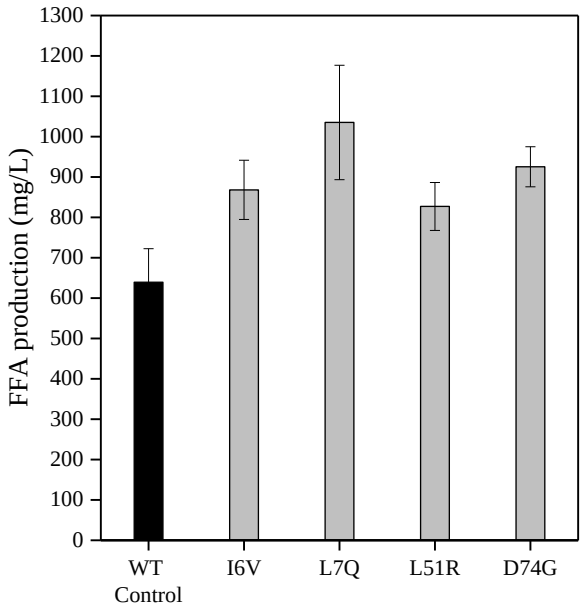

Figure 27. Free fatty acid production analysis. This analysis was obtained from selected TesA mutations which are artificially engineered TesA on a plasmid. The expression of mutated TesA enzymes were induced with 0.3mM IPTG. The black bar in the left column indicates FFA production of WT MG1655 control.

5.7 C2C communication based screening : New type of screening application

5.7.1 Calibration of extracellular fatty acid biosensor

For C2C communication based screening system, it is required to have appropriate donor cells (DC) and recipient cells (RC). We prepared the DCs as random mutation library constructed by transposon insertion method which are expected to show different secretion performances because of the disrupted transport system for fatty acids. On the other hands, we engineered RC for extracellular fatty acid biosensor having replacement of promoter P_{LR} instead of previous promoter P_{tet} [192]. This newly engineered extracellular fatty acid biosensors (exFAB plasmid) was induced by the presence of exogeneous fatty acids in a liquid state from DCs, presumably. We then evaluated the responses of exFAB with the different concentrations of exogenous fatty acids (*Figure 28*). The dynamic sensing range of the exFAB biosensor is defined from 0.05 to 0.4 g/L which considerably matches to the expected production yield of DCs.

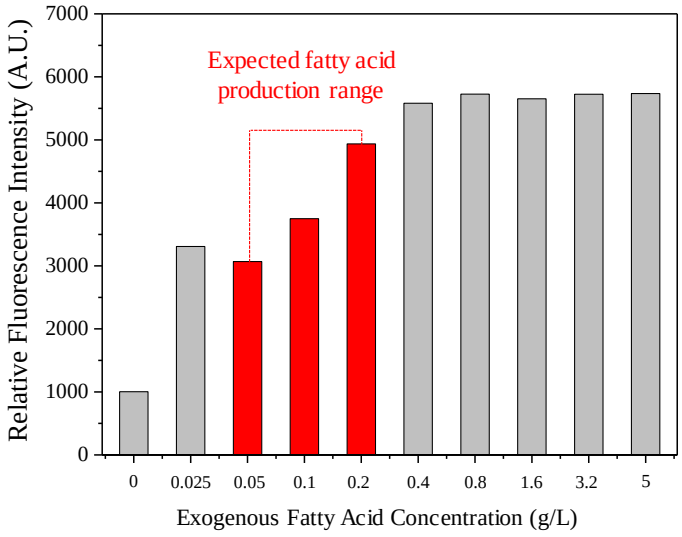

Figure 28. Optimal sensitivity test for exFAB biosensor plasmid. Different exogenous fatty acid concentrations were prepared ranging from 0.025 to 5 g/L. The extracellular fatty acid biosensor (exFAB) plasmid was engineered and tested its detection performance in the microplate reader with different concentrations of exogenous fatty acids in a liquid medium. Red bars indicate the expected fatty acid production yields from donor library cells.

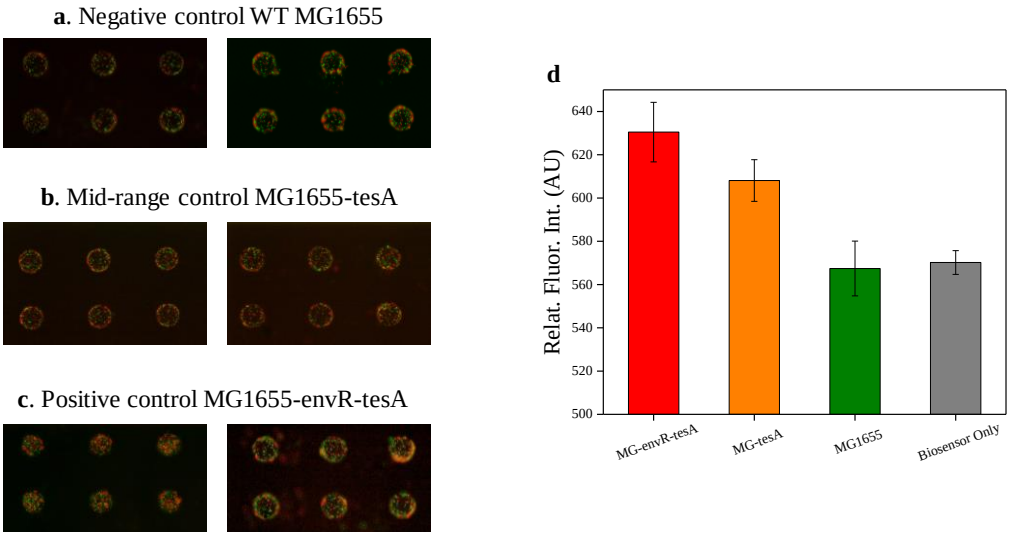

Figure 29. Fluorescence microscopic images and quantification results of C2C communication based screening system. (a-c) Overlapped fluorescence images (GFP-RFP) of exFAB with control group as negative, mid-range, and positive fatty acid production yield. (d) Quantification data of fluorescence intensity from red fluorescence protein in the exFAB biosensor recipient cells (RCs).

We next tested the response of the exFAB biosensors to the extracellular produced fatty acids from three different control microbial groups within the fluid array platform (*Figure 29*). The microbial control groups include WT MG1655 as negative, MG1655 with the WT TesA and MG1655-envR harboring the WT TesA as a positive control producing more fatty acid than others. For this experiment, it is confirmed that the exFAB biosensors with positive control group showed brighter fluorescence signal compared to the case of the wild type MG1655. Not only the WT MG1655 case, but also the exFAB biosensor itself showed similar fluorescence intensity that indicates almost no exogenous fatty acids in the liquid medium.

5.7.2 Screening of mutant library using C2C communication system

The fluid array device was used again for effective C2C communication based on interaction between DC and RC in a chamber array environment. After 20 hours of incubation in a fluid array device, all the fluorescence intensities of individual arrays were quantified. Approximately 30 arrays per a fluid array device (top <1%) were selectively extracted, recovered and analyzed their production yield of fatty acids by GC analysis. We then chose outstanding 10 mutants showing higher secretion performance of fatty acids and identified sequences of the transposon insertion regions from each of selected samples. According to the GC analysis results (*Figure 30*), the average of total fatty acid production yields are varied ranging in mostly similar to that of WT. Whereas the WT MG1655 with

WT TesA showed intra/extracellular fatty acids ratio as 7:3, the isolated 10 mutants increased almost two fold extracellular fatty acids compared to the WT MG1655. It is noted that insertion transposon may have disrupted a transport system of fatty acid in FAS pathways. The transposon insertion sequences were not identified yet.

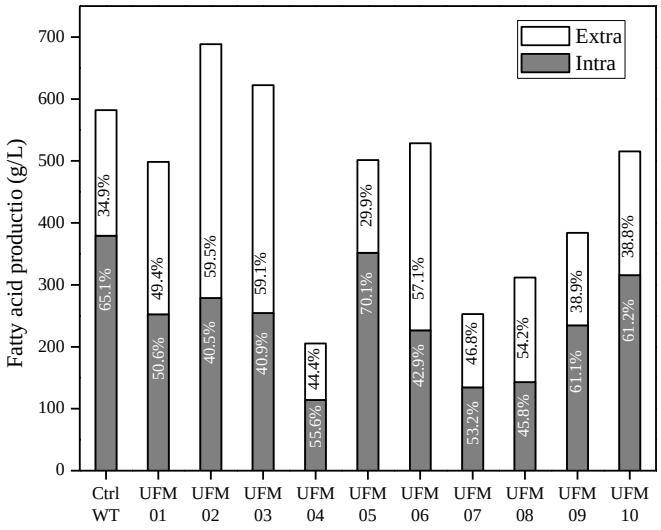

Figure 30. Fatty acid prodcution by transposon mutants. The concentration of intra/extracellulular fatty acids were measured from ten mutants screened by C2C communication based screeening of the fluid array platform. Identification of such mutations are not sequenced yet.

5.8 Conclusion

A screening of more than 10^3 of the microbial mutant library has not been realized yet in the microfluidic platform, due to a tradeoff relation between high-throughput compartmentalized environment and difficulties in selective extraction. Using the fluid array platform developed previously, we were able to screen the fatty acids overproducing mutants from random mutant library of 10^6 with satisfying high-throughput arrays and the selective extraction. This platform can deal with the growth-based screening as well as the reporter gene-based screening approach simultaneously. The screened microbial mutants showed that not only this platform can reveal extraordinary mutants, but also screening of suboptimal mutants producing more fatty acid than the wild type. There outstanding mutants showing almost a two fold increase in fatty acid production were isolated, compared to the wild type. Additionally, the platform can perform the experimental concept of C2C communication screening (*e.g.* donor/recipient cells) which was limited by conventional approaches and tools. The isolated mutants showed enhanced extracellular fatty acid production compared to that of WT control production yield. In the near future, identification of those screened mutants will be performed as well as further advanced genetic analysis of the mutations.

Chapter 6. Summary and Future Outlook

6.1 Summary of findings

In this dissertation, different type of microfluidic devices were developed for various collaborative purposes for the bottleneck of conventional microbiology [21, 33, 60, 63]. As described in previous chapters, the high-throughput screening of bacterial mutant library is still merely one of successful integration examples to demonstrate practical cases showing advantages of using the microfluidic device. Not only high-throughput screening application, but also microfluidic device integrated with microbial biosensors showed a promising research perspective as well as an industrial need for the better detector than current heavy instruments in a quantitative manner.

First, microbial biosensors were investigated with a reviewing previous studies from other groups. There, micro/nanotechnologies for microbial biosensors were reviewed carefully (*Chapter 2*). With that background knowledge regarding microbial biosensors, various microbial biosensor applications were introduced and performed on ratchet structured microfluidic devices to improve sensitivity of the biosensors. With having the novel ratchet structures at the orifice of the microfluidic chamber, the motile cells were physically concentrated. While the cells are concentrated in the microfluidic chambers, the chemicals are diffused without any obstacles providing the continuous feeding of nutrients. Therefore, a simple and convenient chemostat-like culture environment met with the application of microbial biosensors that express a fluorescence signal in the presence of target heavy metal ions (*Chapter 3*). Concentration and accumulation of chemical nutrients in a continuous mode to the chamber enabled outstanding increase in a sensitivity of the microbial biosensors.

Second, the fluid array device was developed (*Chapter 4*) by applying two common knowledges, such as immiscible character between water and oil, and specific gravity difference of all substrates. Since the concept of the fluid array device is a passive and open type instruments, it satisfies all the requirements for high-throughput screening research field including high-throughput microbial incubation, a simple and selective extraction method, and a good recovery efficiency for post analysis. Not only this fluid array device has shown a successful demonstration of high-throughput screening for small microbial mutant library, it was also successfully performed that a larger size of mutant library ($> 10^6$) based on the hybrid type of screening strategies. In addition, cell-to-cell communication based screening was applied to implement the concept of donor/recipient cells (*Chapter 5*).

Overall, the microfluidic approaches introduced in this dissertation were successfully used for the quantitative analysis and the high-throughput screening of synthetically engineered microbes. It is strongly believed that the bioMEMS technologies including such microfluidic approaches would be a practical step to realize fully integrated total analysis system for various biological applications which were limited by conventional approaches.

6.2 Future outlooks and perspectives

Although the fluid array has knocked the new door for high-throughput screening application for synthetically engineered microorganisms, most of achievements in this dissertation are still in the sub-level of single cells. Therefore, the future research for screening of synthetic microbes should aim for an actual single cell analysis (not the single cell level). Yet there is no such device reported that achieves the actual single cell analysis with high-throughput more than $10^{5\sim6}$. The reason why the actual single cell analysis is considered to be almost impossible and difficult task to achieve, is because of the technical tradeoff relation aforementioned in previous chapters. According to the fundamental statistic theory, in an example of free food ticket distribution to the random crowd, distribution with less number of tickets must have higher standard deviation (%) than the larger number ticket case. Therefore, the actual single cell analysis always requires highly sophisticated flow regulation system that can even control a single cell.

However, solving this tradeoff issue can be alternatively suggested in this dissertation by the complementary experimental condition. For example, C2C communication based screening experiment in this dissertation (*Chapter 5*) defined the initial cell seeding number for donor cells as approximately 9. The experiment would have been more sophisticated and accurate, if the initial cell seeding number was exactly encapsulated in number 1. There we can find a point of compromise by having a post colony analysis process that complements the disadvantages of sub-single cell level analysis. Because picking up the 10 individual colonies after the fluid array C2C screening may reduce significantly the possibility of missing samples during the whole screening process.

Another future perspective issue for the fluid array would be the disadvantages from the passive and open type device structure. Since the fluid array device implies a simple but effective high-throughput screening tool, the fluid device is still vulnerable in terms of stability. Compared to the conventional channel type microfluidic device, the fluid array has a significantly unstable status for example when the device is inverted for capillary extraction, and is exposed dehydration of aqueous phase. Therefore, future high-throughput microfluidic tools should aim for more solid platform and

procedures.

The field of BioMEMS, more specifically, microfluidics still has tremendous potential to various biological applications. A variety of research demonstrated a highly synergetic and practical applications between microbiology and micro/-nanotechnology with the ability to control their physical and chemical characteristics within the active scale of micro/nanometer.

References

1. Lim, J.W., *et al*., *Review of micro/nanotechnologies for microbial biosensors.* Front Bioeng Biotechnol, 2015. **3**: p. 61.
2. Beg, Q.K., *et al*., *Microbial xylanases and their industrial applications: a review.* Applied Microbiology and Biotechnology, 2001. **56**(3-4): p. 326-338.
3. Shallom, D. and Y. Shoham, *Microbial hemicellulases.* Current Opinion in Microbiology, 2003. **6**(3): p. 219-228.
4. Clardy, J., M.A. Fischbach, and C.T. Walsh, *New antibiotics from bacterial natural products.* Nature Biotechnology, 2006. **24**(12): p. 1541-1550.
5. Demain, A.L. and S. Sanchez, *Microbial drug discovery: 80 years of progress.* Journal of Antibiotics, 2009. **62**(1): p. 5-16.
6. Ladygina, N., E.G. Dedyukhina, and M.B. Vainshtein, *A review on microbial synthesis of hydrocarbons.* Process Biochemistry, 2006. **41**(5): p. 1001-1014.
7. Schirmer, A., et al., *Microbial Biosynthesis of Alkanes.* Science, 2010. **329**(5991): p. 559-562.
8. Dietrich, J.A., A.E. McKee, and J.D. Keasling, *High-Throughput Metabolic Engineering: Advances in Small-Molecule Screening and Selection.* Annual Review of Biochemistry, Vol 79, 2010. **79**: p. 563-590.
9. Ratner, B.D. and S.J. Bryant, *Biomaterials: Where we have been and where we are going.* Annual Review of Biomedical Engineering, 2004. **6**: p. 41-75.
10. Kim, M., *et al.*, *Chemostat-like microfluidic platform for highly sensitive detection of heavy metal ions using microbial biosensors.* Biosens Bioelectron, 2014. **65C**: p. 257-264.
11. Cuypers, A., *et al.*, *Cadmium stress: an oxidative challenge.* Biometals, 2010. **23**(5): p. 927-940.
12. Ercal, N., H. Gurer-Orhan, and N. Aykin-Burns, *Toxic metals and oxidative stress part I: mechanisms involved in metal-induced oxidative damage.* Curr Top Med Chem, 2001. **1**(6): p. 529-39.
13. Coen, N., *et al.*, *Heavy metals of relevance to human health induce genomic instability.* Journal of Pathology, 2001. **195**(3): p. 293-299.
14. Karri, S.K., R.B. Saper, and S.N. Kales, *Lead encephalopathy due to traditional medicines.* Curr Drug Saf, 2008. **3**(1): p. 54-9.
15. Duruibe, J.O., M.O.C. Ogwuegbu, and J.N. Egwurugwu, *Heavy metal pollution and human biotoxic effects.* International Journal of Physical Sciences, 2007. **2**(5): p. 112-118.
16. Roels, H.A., *et al.*, *Health Significance of Cadmium Induced Renal Dysfunction - a 5 Year Follow Up.* British Journal of Industrial Medicine, 1989. **46**(11): p. 755-764.
17. Jackson, K.W. and G.R. Chen, *Atomic absorption, atomic emission, and flame emission spectrometry.* Analytical Chemistry, 1996. **68**(12): p. R231-R256.
18. Burlingame, A.L., R.K. Boyd, and S.J. Gaskell, *Mass spectrometry.* Analytical Chemistry, 1996. **68**(12): p. R599-R651.
19. Anderson, J.L., E.F. Bowden, and P.G. Pickup, *Dynamic electrochemistry: Methodology and application.* Analytical Chemistry, 1996. **68**(12): p. R379-R444.
20. Hynninen, A. and M. Virta, *Whole-Cell Bioreporters for the Detection of Bioavailable Metals.* Whole Cell Sensing Systems Ii, 2010. **118**: p. 31-63.
21. Shimomura-Shimizu, M. and I. Karube, *Applications of Microbial Cell Sensors.* Whole Cell Sensing Systems Ii, 2010. **118**: p. 1-30.
22. Charrier, T., *et al.*, *A multi-channel bioluminescent bacterial biosensor for the on-line detection of metals and toxicity. Part II: technical development and proof of concept of the biosensor.* Analytical and Bioanalytical Chemistry, 2011. **400**(4): p. 1061-1070.
23. Chiou, C.H., *et al.*, *Rapid whole-cell sensing chip for low-level arsenite detection.* Biosensors & Bioelectronics, 2011. **26**(5): p. 2484-2488.
24. Lei, Y., W. Chen, and A. Mulchandani, *Microbial biosensors.* Analytica Chimica Acta, 2006. **568**(1-2): p. 200-210.
25. Su, L.A., *et al.*, *Microbial biosensors: A review.* Biosensors & Bioelectronics, 2011. **26**(5): p. 1788-1799.
26. D'Souza, S.F., *Microbial biosensors.* Biosensors & Bioelectronics, 2001. **16**(6): p. 337-353.
27. Castillo, J., *et al.*, *Biosensors for life quality - Design, development and applications.* Sensors and Actuators B-Chemical, 2004. **102**(2): p. 179-194.
28. Leth, S., et al., *Engineered bacteria based biosensors for monitoring bioavailable heavy metals.* Electroanalysis, 2002. **14**(1): p. 35-42.
29. Shetty, R.S., *et al.*, *Luminescence-based whole-cell-sensing systems for cadmium and lead using genetically engineered bacteria.* Analytical and Bioanalytical Chemistry, 2003. **376**(1): p. 11-17.

30. Gu, M.B., *et al.*, *A miniature bioreactor for sensing toxicity using recombinant bioluminescent Escherichia coli cells.* Biotechnology Progress, 1996. **12**(3): p. 393-397.
31. Rothert, A., *et al.*, *Whole-cell-reporter-gene-based biosensing systems on a compact disk microfluidics platform.* Analytical Biochemistry, 2005. **342**(1): p. 11-19.
32. Garcia-Alonso, J., *et al.*, *Microscreening toxicity system based on living magnetic yeast and gradient chips.* Analytical and Bioanalytical Chemistry, 2011. **400**(4): p. 1009-1013.
33. Garcia-Alonso, J., *et al.*, *A prototype microfluidic chip using fluorescent yeast for detection of toxic compounds.* Biosensors & Bioelectronics, 2009. **24**(5): p. 1508-1511.
34. Groisman, A., *et al.*, *A microfluidic chemostat for experiments with bacterial and yeast cells.* Nature Methods, 2005. **2**(9): p. 685-689.
35. Agresti, J.J., *et al.*, *Ultrahigh-throughput screening in drop-based microfluidics for directed evolution.* Proc Natl Acad Sci U S A, 2010. **107**(9): p. 4004-9.
36. Lim, J.W., *et al.*, *A Microfluidic Platform for High-Throughput Screening of Small Mutant Libraries.* Analytical Chemistry, 2016. **88**(10): p. 5234-5242.
37. Keasling, J.D., *Manufacturing Molecules Through Metabolic Engineering.* Science, 2010. **330**(6009): p. 1355-1358.
38. Lee, S.Y., *Metabolic Engineering and Synthetic Biology in Strain Development.* Acs Synthetic Biology, 2012. **1**(11): p. 491-492.
39. Sathesh-Prabu, C. and S.K. Lee, *Production of Long-Chain alpha,omega-Dicarboxylic Acids by Engineered Escherichia coli from Renewable Fatty Acids and Plant Oils.* J Agric Food Chem, 2015. **63**(37): p. 8199-208.
40. Yang, H.Q., *et al.*, *Molecular engineering of industrial enzymes: recent advances and future prospects.* Applied Microbiology and Biotechnology, 2014. **98**(1): p. 23-29.
41. Buettner, K., T.C. Hertel, and M. Pietzsch, *Increased thermostability of microbial transglutaminase by combination of several hot spots evolved by random and saturation mutagenesis.* Amino Acids, 2012. **42**(2-3): p. 987-996.
42. Molloy, S., *et al.*, *Engineering of a bacterial tyrosinase for improved catalytic efficiency towards D-tyrosine using random and site directed mutagenesis approaches.* Biotechnology and Bioengineering, 2013. **110**(7): p. 1849-1857.
43. Yokoyama, K., *et al.*, *Screening for improved activity of a transglutaminase from Streptomyces mobaraensis created by a novel rational mutagenesis and random mutagenesis.* Applied Microbiology and Biotechnology, 2010. **87**(6): p. 2087-2096.
44. Tran, T.M., *et al.*, *From tubes to drops: droplet-based microfluidics for ultrahigh-throughput biology.* Journal of Physics D-Applied Physics, 2013. **46**(11).
45. Lagus, T.P. and J.F. Edd, *A review of the theory, methods and recent applications of high-throughput single-cell droplet microfluidics.* Journal of Physics D-Applied Physics, 2013. **46**(11).
46. Olsen, M., B. Iverson, and G. Georgiou, *High-throughput screening of enzyme libraries.* Current Opinion in Biotechnology, 2000. **11**(4): p. 331-337.
47. Anna, S.L., N. Bontoux, and H.A. Stone, *Formation of dispersions using "flow focusing" in microchannels.* Applied Physics Letters, 2003. **82**(3): p. 364-366.
48. Thorsen, T., *et al.*, *Dynamic pattern formation in a vesicle-generating microfluidic device.* Phys Rev Lett, 2001. **86**(18): p. 4163-6.
49. Leung, K., et al., *A programmable droplet-based microfluidic device applied to multiparameter analysis of single microbes and microbial communities.* Proceedings of the National Academy of Sciences of the United States of America, 2012. **109**(20): p. 7665-7670.
50. Baret, J.C., et al., *Fluorescence-activated droplet sorting (FADS): efficient microfluidic cell sorting based on enzymatic activity.* Lab on a Chip, 2009. **9**(13): p. 1850-1858.
51. Balagadde, F.K., et al., *Long-term monitoring of bacteria undergoing programmed population control in a microchemostat.* Science, 2005. **309**(5731): p. 137-40.
52. Zhu, Q., et al., *Self-priming compartmentalization digital LAMP for point-of-care.* Lab Chip, 2012. **12**(22): p. 4755-63.
53. Cohen, D.E., et al., *Self-digitization of sample volumes.* Anal Chem, 2010. **82**(13): p. 5707-17.
54. Gansen, A., et al., *Digital LAMP in a sample self-digitization (SD) chip.* Lab on a Chip, 2012. **12**(12): p. 2247-2254.
55. Cohen, D.E., et al., *Self-Digitization of Sample Volumes.* Analytical Chemistry, 2010. **82**(13): p. 5707-5717.
56. Zhu, Q.Y., et al., *Digital PCR on an integrated self-priming compartmentalization chip.* Lab on a Chip, 2014. **14**(6): p. 1176-1185.
57. Park, J., et al., *Microdroplet-enabled highly parallel co-cultivation of microbial communities.* PLoS One, 2011. **6**(2): p. e17019.
58. Churski, K., et al., *Rapid screening of antibiotic toxicity in an automated microdroplet system.* Lab Chip, 2012.

12(9): p. 1629-37.
59. Mary, P., et al., *Analysis of gene expression at the single-cell level using microdroplet-based microfluidic technology.* Biomicrofluidics, 2011. **5**(2): p. 24109.
60. Chang, C., et al., *Droplet-based microfluidic platform for heterogeneous enzymatic assays.* Lab Chip, 2013. **13**(9): p. 1817-22.
61. Huebner, A., et al., *Static microdroplet arrays: a microfluidic device for droplet trapping, incubation and release for enzymatic and cell-based assays.* Lab Chip, 2009. **9**(5): p. 692-8.
62. Nisisako, T., T. Torii, and T. Higuchi, *Droplet formation in a microchannel network.* Lab Chip, 2002. **2**(1): p. 24-6.
63. Theberge, A.B., et al., *Microdroplets in Microfluidics: An Evolving Platform for Discoveries in Chemistry and Biology.* Angewandte Chemie-International Edition, 2010. **49**(34): p. 5846-5868.
64. Clark, L.C. and C. Lyons, *Electrode Systems for Continuous Monitoring in Cardiovascular Surgery.* Annals of the New York Academy of Sciences, 1963. **102**(1): p. 29-&.
65. Kusterbeck, A.W., G.A. Wemhoff, and F.S. Ligler, *Antibody-Based Biosensor for Continuous Monitoring.* Biosensor Technology, 1990: p. 345-347.
66. Kricka, L.J., et al., *Current perspectives in protein array technology.* Annals of Clinical Biochemistry, 2006. **43**: p. 457-467.
67. Wilson, G.S. and Y.B. Hu, *Enzyme based biosensors for in vivo measurements.* Chemical Reviews, 2000. **100**(7): p. 2693-2704.
68. Ispas, C.R., G. Crivat, and S. Andreescu, *Review: Recent Developments in Enzyme-Based Biosensors for Biomedical Analysis.* Analytical Letters, 2012. **45**(2-3): p. 168-186.
69. Mello, L.D. and L.T. Kubota, *Review of the use of biosensors as analytical tools in the food and drink industries.* Food Chemistry, 2002. **77**(2): p. 237-256.
70. Ehrenreich, A., *DNA microarray technology for the microbiologist: an overview.* Applied Microbiology and Biotechnology, 2006. **73**(2): p. 255-273.
71. Miller, M.B. and Y.W. Tang, *Basic Concepts of Microarrays and Potential Applications in Clinical Microbiology.* Clinical Microbiology Reviews, 2009. **22**(4): p. 611-+.
72. Zhang, F.Z. and J. Keasling, *Biosensors and their applications in microbial metabolic engineering.* Trends in Microbiology, 2011. **19**(7): p. 323-329.
73. Winkler, W.C. and R.R. Breaker, *Regulation of bacterial gene expression by riboswitches.* Annual Review of Microbiology, 2005. **59**: p. 487-517.
74. Arefev, K.M., M.A. Guseva, and B.M. Khomchenkov, *Determination of the Coefficient of Diffusion of Cadmium and Magnesium Vapors in Gases by the Stefan Method.* High Temperature, 1987. **25**(2): p. 174-179.
75. Mulchandani, A. and K.R. Rogers, *Enzyme and microbial biosensors : techniques and protocols*. Methods in biotechnology. 1998, Totowa, N.J.: Humana Press. xii, 264 p.
76. Casavant, N.C., et al., *Use of a site-specific recombination-based biosensor for detecting bioavailable toluene and related compounds on roots.* Environmental Microbiology, 2003. **5**(4): p. 238-249.
77. Jouanneau, S., et al., *Improvement of the Identification of Four Heavy Metals in Environmental Samples by Using Predictive Decision Tree Models Coupled with a Set of Five Bioluminescent Bacteria.* Environmental Science & Technology, 2011. **45**(7): p. 2925-2931.
78. Brehm-Stecher, B.F. and E.A. Johnson, *Single-cell microbiology: Tools, technologies, and applications.* Microbiology and Molecular Biology Reviews, 2004. **68**(3): p. 538-+.
79. Swain, P.S., M.B. Elowitz, and E.D. Siggia, *Intrinsic and extrinsic contributions to stochasticity in gene expression.* Proceedings of the National Academy of Sciences of the United States of America, 2002. **99**(20): p. 12795-12800.
80. Shaw, J.J. and C.I. Kado, *Development of a Vibrio Bioluminescence Gene Set to Monitor Phytopathogenic Bacteria during the Ongoing Disease Process in a Nondisruptive Manner.* Bio-Technology, 1986. **4**(6): p. 560-564.
81. Joyner, D.C. and S.E. Lindow, *Heterogeneity of iron bioavailability on plants assessed with a whole-cell GFP-based bacterial biosensor.* Microbiology-Uk, 2000. **146**: p. 2435-2445.
82. Fujimoto, H., et al., *Whole-cell arsenite biosensor using photosynthetic bacterium Rhodovulum sulfidophilum. Rhodovulum sulfidophilum as an arsenite biosensor.* Appl Microbiol Biotechnol, 2006. **73**(2): p. 332-8.
83. Santos, C.N. and G. Stephanopoulos, *Melanin-based high-throughput screen for L-tyrosine production in Escherichia coli.* Appl Environ Microbiol, 2008. **74**(4): p. 1190-7.
84. Di Gennaro, P., et al., *Development of microbial engineered whole-cell systems for environmental benzene determination.* Ecotoxicol Environ Saf, 2011. **74**(3): p. 542-9.
85. Rocaboy-Faquet, E., et al., *Novel bacterial bioassay for a high-throughput screening of 4-hydroxyphenylpyruvate dioxygenase inhibitors.* Applied Microbiology and Biotechnology, 2014. **98**(16): p. 7243-7252.
86. Corbisier, P., et al., *Whole cell- and protein-based biosensors for the detection of bioavailable heavy metals in*

environmental samples. Analytica Chimica Acta, 1999. **387**(3): p. 235-244.
87. Petanen, U. and M. Romantschuk, *Use of bioluminescent bacterial sensors as an alternative method for measuring heavy metals in soil extracts.* Analytica Chimica Acta, 2002. **456**(1): p. 55-61.
88. Kim, B.C. and M.B. Gu, *A bioluminescent sensor for high throughput toxicity classification.* Biosensors and Bioelectronics, 2003. **18**(8): p. 1015-1021.
89. Taylor, C.J., et al., *Construction of a whole-cell gene reporter for the fluorescent bioassay of nitrate.* Anal Biochem, 2004. **328**(1): p. 60-6.
90. Wells, M., et al., *Ultrasensitive reporter protein detection in genetically engineered bacteria.* Analytical Chemistry, 2005. **77**(9): p. 2683-2689.
91. Keenan, P.O., et al., *Clear and present danger? The use of a yeast biosensor to monitor changes in the toxicity of industrial effluents subjected to oxidative colour removal treatments.* Journal of Environmental Monitoring, 2007. **9**(12): p. 1394-1401.
92. DeBusschere, B.D. and G.T. Kovacs, *Portable cell-based biosensor system using integrated CMOS cell-cartridges.* Biosensors and Bioelectronics, 2001. **16**(7): p. 543-556.
93. Odaci, D., et al., *Use of a thiophene-based conducting polymer in microbial biosensing.* Electrochimica Acta, 2008. **53**(12): p. 4104-4108.
94. Kohlmeier, S., et al., *Comparison of naphthalene bioavailability determined by whole-cell biosensing and availability determined by extraction with Tenax.* Environmental pollution, 2008. **156**(3): p. 803-808.
95. Chouteau, C., et al., *A bi-enzymatic whole cell conductometric biosensor for heavy metal ions and pesticides detection in water samples.* Biosensors and Bioelectronics, 2005. **21**(2): p. 273-281.
96. Guedri, H. and C. Durrieu, *A self-assembled monolayers based conductometric algal whole cell biosensor for water monitoring.* Microchimica Acta, 2008. **163**(3-4): p. 179-184.
97. Neufeld, T., et al., *Genetically Engineered p fabA p fabR Bacteria: an Electrochemical Whole Cell Biosensor for Detection of Water Toxicity.* Analytical chemistry, 2006. **78**(14): p. 4952-4956.
98. Kırgöz, Ü.A., et al., *Graphite epoxy composite electrodes modified with bacterial cells.* Bioelectrochemistry, 2006. **69**(1): p. 128-131.
99. Tag, K., et al., *Amperometric detection of Cu< sup> 2+</sup> by yeast biosensors using flow injection analysis (FIA).* Sensors and Actuators B: Chemical, 2007. **122**(2): p. 403-409.
100. Tkac, J., et al., *Improved selectivity of microbial biosensor using membrane coating. Application to the analysis of ethanol during fermentation.* Biosensors and Bioelectronics, 2003. **18**(9): p. 1125-1134.
101. Mulchandani, P., et al., *Amperometric microbial biosensor for direct determination of organophosphate pesticides using recombinant microorganism with surface expressed organophosphorus hydrolase.* Biosensors and Bioelectronics, 2001. **16**(7): p. 433-437.
102. Shul'ga, A., et al., *Thin-film conductometric biosensors for glucose and urea determination.* Biosensors and Bioelectronics, 1994. **9**(3): p. 217-223.
103. Mikkelsen, S.R. and G.A. Rechnitz, *Conductometric tranducers for enzyme-based biosensors.* Analytical chemistry, 1989. **61**(15): p. 1737-1742.
104. Ding, L., et al., *Trends in cell-based electrochemical biosensors.* Current medicinal chemistry, 2008. **15**(30): p. 3160-3170.
105. Wang, J. and J. Wang, *Stripping analysis: Principles, instrumentation, and applications*. 1985: Vch Deerfield Beach, FL.
106. Gokhale, A.A., J. Lu, and I. Lee, *Recent Progress in the Development of Novel Nanostructured Biosensors for Detection of Waterborne Contaminants*, in *Nanoscale Sensors*. 2013, Springer. p. 1-34.
107. Durrieu, C., F. Lagarde, and N. Jaffrezic-Renault, *Nanotechnology assets in biosensors design for environmental monitoring*, in *Nanomaterials: A Danger or a Promise?* 2013, Springer. p. 189-229.
108. Scognamiglio, V., *Nanotechnology in glucose monitoring: Advances and challenges in the last 10 years.* Biosensors and Bioelectronics, 2013. **47**: p. 12-25.
109. Park, S., et al., *Microfabricated ratchet structure integrated concentrator arrays for synthetic bacterial cell-to-cell communication assays.* Lab on a Chip, 2012. **12**(20): p. 3914-3922.
110. Si, G., et al., *A parallel diffusion-based microfluidic device for bacterial chemotaxis analysis.* Lab Chip, 2012. **12**(7): p. 1389-94.
111. Park, S., et al., *A microfluidic concentrator array for quantitative predation assays of predatory microbes.* Lab on a Chip, 2011. **11**(17): p. 2916-2923.
112. Biran, I., et al., *Optical imaging fiber-based live bacterial cell array biosensor.* Analytical Biochemistry, 2003. **315**(1): p. 106-113.
113. Rothert, A., et al., *Whole-cell-reporter-gene-based biosensing systems on a compact disk microfluidics platform.* Anal Biochem, 2005. **342**(1): p. 11-9.
114. Xia, Y.N. and G.M. Whitesides, *Soft lithography.* Angew. Chem. Int. Edit., 1998. **37**(5): p. 551-575.
115. Garcia-Alonso, J., et al., *A prototype microfluidic chip using fluorescent yeast for detection of toxic compounds.*

Biosens Bioelectron, 2009. **24**(5): p. 1508-11.
116. Garcia-Alonso, J., et al., *Microscreening toxicity system based on living magnetic yeast and gradient chips.* Anal Bioanal Chem, 2011. **400**(4): p. 1009-13.
117. Roda, A., et al., *Bioengineered bioluminescent magnetotactic bacteria as a powerful tool for chip-based whole-cell biosensors.* Lab Chip, 2013. **13**(24): p. 4881-9.
118. Thouand, G., et al., *Development of a biosensor for on-line detection of tributyltin with a recombinant bioluminescent Escherichia coli strain.* Appl Microbiol Biotechnol, 2003. **62**(2-3): p. 218-25.
119. Hossain, S.M. and J.D. Brennan, *beta-Galactosidase-based colorimetric paper sensor for determination of heavy metals.* Anal Chem, 2011. **83**(22): p. 8772-8.
120. Kumar, S., C. Wittmann, and E. Heinzle, *Minibioreactors.* Biotechnol Lett, 2004. **26**(1): p. 1-10.
121. Gu, M.B., et al., *A Miniature Bioreactor for Sensing Toxicity Using Recombinant Bioluminescent Escherichia coli Cells.* Biotechnology Progress, 1996. **12**(3): p. 393-397.
122. Gu, M.B. and G.C. Gil, *A multi-channel continuous toxicity monitoring system using recombinant bioluminescent bacteria for classification of toxicity.* Biosensors & Bioelectronics, 2001. **16**(9-12): p. 661-666.
123. Chen, Y. and A. Pepin, *Nanofabrication: Conventional and nonconventional methods.* Electrophoresis, 2001. **22**(2): p. 187-207.
124. Scognamiglio, V., *Nanotechnology in glucose monitoring: Advances and challenges in the last 10 years.* Biosensors & Bioelectronics, 2013. **47**: p. 12-25.
125. Claussen, J.C., et al., *Electrochemical biosensor of nanocube-augmented carbon nanotube networks.* Acs Nano, 2009. **3**(1): p. 37-44.
126. Popovtzer, R., et al., *Novel integrated electrochemical nano-biochip for toxicity detection in water.* Nano letters, 2005. **5**(6): p. 1023-1027.
127. Li, Z., et al., *A Laminar-Flow Microfluidic Device for Quantitative Analysis of Microbial Electrochemical Activity.* ChemSusChem, 2012. **5**(6): p. 1119-1123.
128. Ben-Yoav, H., et al., *Modified working electrodes for electrochemical whole-cell microchips.* Electrochimica Acta, 2012. **82**: p. 109-114.
129. Deng, L., et al., *A silk derived carbon fiber mat modified with Au@ Pt urchilike nanoparticles: A new platform as electrochemical microbial biosensor.* Biosensors and Bioelectronics, 2010. **25**(10): p. 2189-2193.
130. Alonso-Lomillo, M., O. Domínguez-Renedo, and M. Arcos-Martínez, *Screen-printed biosensors in microbiology; a review.* Talanta, 2010. **82**(5): p. 1629-1636.
131. Shitanda, I., et al., *Amperometric screen-printed algal biosensor with flow injection analysis system for detection of environmental toxic compounds.* Electrochimica Acta, 2009. **54**(21): p. 4933-4936.
132. Odaci, D., S. Timur, and A. Telefoncu, *Bacterial sensors based on chitosan matrices.* Sensors and Actuators B: Chemical, 2008. **134**(1): p. 89-94.
133. Timur, S., et al., *Development of a microbial biosensor based on carbon nanotube (CNT) modified electrodes.* Electrochemistry Communications, 2007. **9**(7): p. 1810-1815.
134. Odaci, D., S. Timur, and A. Telefoncu, *A microbial biosensor based on bacterial cells immobilized on chitosan matrix.* Bioelectrochemistry, 2009. **75**(1): p. 77-82.
135. Cho, J.C., et al., *A novel continuous toxicity test system using a luminously modified freshwater bacterium.* Biosens Bioelectron, 2004. **20**(2): p. 338-44.
136. Choi, S.H. and M.B. Gu, *A portable toxicity biosensor using freeze-dried recombinant bioluminescent bacteria.* Biosensors and Bioelectronics, 2002. **17**(5): p. 433-440.
137. Charrier, T., et al., *A multi-channel bioluminescent bacterial biosensor for the on-line detection of metals and toxicity. Part II: technical development and proof of concept of the biosensor.* Anal Bioanal Chem, 2011. **400**(4): p. 1061-70.
138. Knight, A.W., et al., *Development of a flow-through detector for monitoring genotoxic compounds by quantifying the expression of green fluorescent protein in genetically modified yeast cells.* Measurement Science & Technology, 1999. **10**(3): p. 211-217.
139. Berno, E., et al., *Recombinant Escherichia coli for the biomonitoring of benzene and its derivatives in the air.* Ecotoxicol Environ Saf, 2004. **57**(2): p. 118-22.
140. Wang, B.L., et al., *Microfluidic high-throughput culturing of single cells for selection based on extracellular metabolite production or consumption.* Nature Biotechnology, 2014. **32**(5): p. 473-U194.
141. Karns, K., et al., *Microfluidic Screening of Electrophoretic Mobility Shifts Elucidates Riboswitch Binding Function.* Journal of the American Chemical Society, 2013. **135**(8): p. 3136-3143.
142. Kim, H.J., et al., *Insights into diversity and specificity of heavy metal resistance and efflux systems in Bacillus oceanisediminis 2691.* (in preparation). 2014.
143. Park, S., et al., *Microfabricated ratchet structure integrated concentrator arrays for synthetic bacterial cell-to-cell communication assays.* Lab on a Chip, 2012. **12**(20): p. 3914-3922.
144. Kim, S.Y., et al., *Microfabricated ratchet structures for concentrating and patterning motile bacterial cells.*

Journal of Micromechanics and Microengineering, 2010. **20**(9).
145. Kim, M., et al., *Microfluidic device for analyzing preferential chemotaxis and chemoreceptor sensitivity of bacterial cells toward carbon sources.* Analyst, 2011. **136**(16): p. 3238-3243.
146. Kim, H.J., et al., *Development of a highly specific and sensitive cadmium and lead microbial biosensor using synthetic CadC-T7 genetic circuitry.* Biosensors & Bioelectronics, 2016. **79**: p. 701-708.
147. Wu, T.Z., et al., *Shrunk to femtolitre: Tuning high-throughput monodisperse water-in-oil droplet arrays for ultra-small micro-reactors.* Applied Physics Letters, 2012. **101**(7).
148. Edd, J.F., et al., *Nucleation and solidification in static arrays of monodisperse drops.* Lab Chip, 2009. **9**(13): p. 1859-65.
149. Tan, W.H. and S. Takeuchi, *A trap-and-release integrated microfluidic system for dynamic microarray applications.* Proc Natl Acad Sci U S A, 2007. **104**(4): p. 1146-51.
150. Collins, L.A., M.N. Torrero, and S.G. Franzblau, *Green fluorescent protein reporter microplate assay for high-throughput screening of compounds against Mycobacterium tuberculosis.* Antimicrobial Agents and Chemotherapy, 1998. **42**(2): p. 344-347.
151. Di Mascio, P., S. Kaiser, and H. Sies, *Lycopene as the Most Efficient Biological Carotenoid Singlet Oxygen Quencher.* Archives of Biochemistry and Biophysics, 1989. **274**(2): p. 532-538.
152. Kim, S.W. and J.D. Keasling, *Metabolic engineering of the nonmevalonate isopentenyl diphosphate synthesis pathway in Escherichia coli enhances lycopene production.* Biotechnology and Bioengineering, 2001. **72**(4): p. 408-415.
153. Becker, S., et al., *Ultra-high-throughput screening based on cell-surface display and fluorescence-activated cell sorting for the identification of novel biocatalysts.* Current Opinion in Biotechnology, 2004. **15**(4): p. 323-329.
154. Connon, S.A. and S.J. Giovannoni, *High-throughput methods for culturing microorganisms in very-low-nutrient media yield diverse new marine isolates.* Applied and Environmental Microbiology, 2002. **68**(8): p. 3878-3885.
155. Um, E., et al., *Mesh-integrated microdroplet array for simultaneous merging and storage of single-cell droplets.* Lab on a Chip, 2012. **12**(9): p. 1594-1597.
156. Huebner, A., et al., *Static microdroplet arrays: a microfluidic device for droplet trapping, incubation and release for enzymatic and cell-based assays.* Lab on a Chip, 2009. **9**(5): p. 692-698.
157. Shemesh, J., et al., *Stationary nanoliter droplet array with a substrate of choice for single adherent/nonadherent cell incubation and analysis.* Proceedings of the National Academy of Sciences of the United States of America, 2014. **111**(31): p. 11293-11298.
158. Dewan, A., et al., *Growth kinetics of microalgae in microfluidic static droplet arrays.* Biotechnology and Bioengineering, 2012. **109**(12): p. 2987-2996.
159. Abraham, M.H., et al., *Thermodynamics of Solute Transfer from Water to Hexadecane.* Journal of the Chemical Society-Perkin Transactions 2, 1990(2): p. 291-300.
160. Lee, T.S., et al., *BglBrick vectors and datasheets: A synthetic biology platform for gene expression.* Journal of Biological Engineering, 2011. **5**(1).
161. Merkel, T.C., et al., *Gas sorption, diffusion, and permeation in poly(dimethylsiloxane).* Journal of Polymer Science Part B-Polymer Physics, 2000. **38**(3): p. 415-434.
162. Massi, M., et al., *Effects of plasma etching on DLC films.* Thin Solid Films, 1999. **343**: p. 381-384.
163. Byun, C.K., et al., *Productive Chemical Interaction between a Bacterial Microcolony Couple Is Enhanced by Periodic Relocation.* Journal of the American Chemical Society, 2013. **135**(6): p. 2242-2247.
164. Yu, H.S., et al., *Aerotactic responses in bacteria to photoreleased oxygen.* Fems Microbiology Letters, 2002. **217**(2): p. 237-242.
165. Xu, J., et al., *A critical view on spike recovery for accuracy evaluation of analytical method for medicinal herbs.* Journal of Pharmaceutical and Biomedical Analysis, 2012. **62**: p. 210-215.
166. Parisutham, V. and S.K. Lee, *Novel Functions and Regulation of Cryptic Cellobiose Operons in Escherichia coli.* Plos One, 2015. **10**(6).
167. Hall, B.G. and L. Xu, *Nucleotide-Sequence, Function, Activation, and Evolution of the Cryptic Asc Operon of Escherichia-Coli K12.* Molecular Biology and Evolution, 1992. **9**(4): p. 688-706.
168. Kachroo, A.H., et al., *Mutations that alter the regulation of the chb operon of Escherichia coli allow utilization of cellobiose.* Molecular Microbiology, 2007. **66**(6): p. 1382-1395.
169. Morrison, T., et al., *Nanoliter high throughput quantitative PCR.* Nucleic acids research, 2006. **34**(18): p. e123-e123.
170. Janssen, H.J. and A. Steinbuchel, *Fatty acid synthesis in Escherichia coli and its applications towards the production of fatty acid based biofuels.* Biotechnol Biofuels, 2014. **7**(1): p. 7.
171. Pfleger, B.F., M. Gossing, and J. Nielsen, *Metabolic engineering strategies for microbial synthesis of oleochemicals.* Metab Eng, 2015. **29**: p. 1-11.
172. Xu, P., et al., *Improving fatty acids production by engineering dynamic pathway regulation and metabolic control.* Proc Natl Acad Sci U S A, 2014. **111**(31): p. 11299-304.

173. Antoni, D., V.V. Zverlov, and W.H. Schwarz, *Biofuels from microbes.* Applied Microbiology and Biotechnology, 2007. **77**(1): p. 23-35.
174. Lee, L.C., et al., *Functional role of catalytic triad and oxyanion hole-forming residues on enzyme activity of Escherichia coli thioesterase I/protease I/phospholipase L1.* Biochem J, 2006. **397**(1): p. 69-76.
175. Shin, K.S., S. Kim, and S.K. Lee, *Improvement of free fatty acid production using a mutant acyl-CoA thioesterase I with high specific activity in Escherichia coli.* Biotechnology for Biofuels, 2016. **9**.
176. Jiang, P. and J.E. Cronan, Jr., *Inhibition of fatty acid synthesis in Escherichia coli in the absence of phospholipid synthesis and release of inhibition by thioesterase action.* J Bacteriol, 1994. **176**(10): p. 2814-21.
177. Hoover, S.W., et al., *Isolation of improved free fatty acid overproducing strains of Escherichia coli via nile red based high-throughput screening.* Environmental Progress & Sustainable Energy, 2012. **31**(1): p. 17-23.
178. Zhang, F., et al., *Enhancing fatty acid production by the expression of the regulatory transcription factor FadR.* Metab Eng, 2012. **14**(6): p. 653-60.
179. Waters, C.M. and B.L. Bassler, *Quorum sensing: cell-to-cell communication in bacteria.* Annu Rev Cell Dev Biol, 2005. **21**: p. 319-46.
180. Bassler, B.L., *Small talk. Cell-to-cell communication in bacteria.* Cell, 2002. **109**(4): p. 421-4.
181. Chen, M.T. and R. Weiss, *Artificial cell-cell communication in yeast Saccharomyces cerevisiae using signaling elements from Arabidopsis thaliana.* Nature Biotechnology, 2005. **23**(12): p. 1551-1555.
182. Choi, W.S., et al., *Synthetic multicellular cell-to-cell communication in inkjet printed bacterial cell systems.* Biomaterials, 2011. **32**(10): p. 2500-2507.
183. Choi, W.S., et al., *Patterning and transferring hydrogel-encapsulated bacterial cells for quantitative analysis of synthetically engineered genetic circuits.* Biomaterials, 2012. **33**(2): p. 624-33.
184. Xiao, Y., et al., *Exploiting nongenetic cell-to-cell variation for enhanced biosynthesis.* Nature Chemical Biology, 2016. **12**(5): p. 339-+.
185. Dennis, J.J. and G.J. Zylstra, *Plasposons: modular self-cloning minitransposon derivatives for rapid genetic analysis of gram-negative bacterial genomes.* Appl Environ Microbiol, 1998. **64**(7): p. 2710-5.
186. Shin, K.S. and S.K. Lee, *Increasing Extracellular Free Fatty Acid Production in Escherichia coli by Disrupting Membrane Transport Systems.* J Agric Food Chem, 2017. **65**(51): p. 11243-11250.
187. Shin, K.S., S. Kim, and S.K. Lee, *Improvement of free fatty acid production using a mutant acyl-CoA thioesterase I with high specific activity in Escherichia coli.* Biotechnol Biofuels, 2016. **9**: p. 208.
188. Lo, Y.C., et al., *Substrate specificities of Escherichia coli thioesterase I/protease I/lysophospholipase L1 are governed by its switch loop movement.* Biochemistry, 2005. **44**(6): p. 1971-9.
189. Huang, Y.T., et al., *Backbone dynamics of Escherichia coli thioesterase/protease I: evidence of a flexible active-site environment for a serine protease.* J Mol Biol, 2001. **307**(4): p. 1075-90.
190. Peelman, F., et al., *Effect of mutations of N- and C-terminal charged residues on the activity of LCAT.* J Lipid Res, 2001. **42**(4): p. 471-9.
191. Zhang, S., B.K. Barr, and D.B. Wilson, *Effects of noncatalytic residue mutations on substrate specificity and ligand binding of Thermobifida fusca endocellulase cel6A.* Eur J Biochem, 2000. **267**(1): p. 244-52.
192. Zhang, F., J.M. Carothers, and J.D. Keasling, *Design of a dynamic sensor-regulator system for production of chemicals and fuels derived from fatty acids.* Nat Biotechnol, 2012. **30**(4): p. 354-9.

Acknowledgement

First, I would like to appreciate my advisor Prof. Taesung Kim with my sincere gratitude. This work would not have been possible without his continuous support and a great insight in research. Not only as my research advisor, also Prof. Taesung Kim has been a good mentor in a personnel level with my outspoken respect for his gentle and benign character. Also, I am especially indebted to Prof. Sung Kuk Lee as my another advisor since I decided to have a research career of master degree in synthetic biology years ago. He guided me in a right direction at the very initial stage of my research career. I would like to thank the rest of my thesis committee : Prof. Cheol-Min Ghim for his great vision for my research direction, Prof. Jaesung Jang with sharing his research experience in a sensory mechanism, and Prof. Soon Ho Hong for an innovative inspiration of advanced genetic screening.

A very special gratitude goes out to all down at Microfluidics and nanomechatronics laboratory including former and present members. Dr. Minseok Kim is one of my closest colleagues and he gave me many inspirations and insightful comments regarding the research for Microfluidics, generally. For Mingjie Jia, Younkwang Nam and Hyunmoon Nam, they guided me when I had difficulties in experiments during an initial period of my PhD degree. Dogyeong Ha and Jongwan Lee, who have studied together with me during my degree mostly, three of us had many productive and in-depth discussions regarding our discussion. I will always remember those precious memories. Dr. Dong-joo Kim was postdoctoral researcher in our laboratory for a year and half. During his presence, I learned a lot from him about his progressive behavior and attitude as a good researcher. Additionally, junior students in microfluidics laboratory, Kyung Hoon Lee, Juyeol Bae, Jun Gyu Park, and Woo Yeong Lim, further gave me great inspirations with young and passionate perspectives. I also appreciate supports and helps from juniors for last few years. In my personal point of view, all the juniors have tremendous research potential than myself for sure. I can easily imagine that they will all have great research careers in near future. Also, advices and comments given by two current postdoctoral researchers, Dr. Qitao Zhou and Dr. Ashish Kumar Thockchom, have been a great help for my research. I sincerely believe that they will become one finest researchers in near future as well.

Not only microfluidics laboratory, I have greatly benefited from Kwang Su Shin and Mrs. Youngshin Ryu who helped my research in an aspect of application with the knowledge of synthetic biology. Aside from aforementioned members and colleagues, I need to send my greatest gratitude to

some of colleagues just popped up in my mind: Dr. Dongmin Kim, Hyun Mo Yang, Seongkyeol Hong, Youngjin Lim, Yunjung Lee, Jongmin Lee, Ji Soo Hong, Jaehoon Kim, Hansol Im, Dong-Kyu Park in UCRF, Mrs. Kyoung-Young Lim and Mrs. So-Hee Eom in the administrative office.

Especially, sincere thanks to my beloved family; my father, Ju-Hwan Lim, for the limitless support of all the decision I have made, my mother, Eun Suk Kim, who spiritually inspired me to keep my study throughout my life. And my younger-sister, Jihye Lim who influences countless things in my life with her extremely strong enthusiasm. Also, there are two more precious names that I should express my huge appreciation, my father-in-law, Jong Su Seo and my mother-in-law, Yong Ju Yoon. They showed me understanding and endless support for my tough times.

Last but not the least, I would like to thank a love of my life: Migyeong Seo. She is the most beautiful and the wisest woman I have ever known. Marrying you is the best decision that I have ever made for my whole life. She has been my greatest inspiration and the most influenced motivation for continuing to improve my knowledge and move my career forward. She is my rock, and I dedicate this work to her for all of the support she has given through all of these years with me. **Love you**.

- END -

Ji Won Lim

Curriculum Vitae
(Jan. 2018, Updated)

Doctor of Philosophy, Ph. D.
Biomedical Engineering Department in School of Life Sciences
Ulsan National Institute of Science and Technology (UNIST)
Rm #706, EB5 (Eng. Bldg. V), 50 UNIST-gil, Ulsan 44919, Republic of Korea
Email: *jiwon@unist.ac.kr* / *bilermugle@gmail.com*
Tel: +82) 52-217-2402 Mobile: +82) 10-2779-1770

RESEARCH INTERESTS

The long-term research vision is to develop micro/nanofluidics and BioMEMS technologies for miniaturized analytical systems, smart biomedical devices, and multi-functional microfluidic platforms such as ***high-throughput screening applications***.

The current research interests are as follows:

- High-throughput Screening (HTS) Technology
- Micro-/Nanofluidics: Small Chip, but Big World!
- Synthetic Biology: Beyond Screening, More New Things

EDUCATION

Ph.D. in Biomedical Engineering
Ulsan National Institute of Science and Technology, Ulsan, KOREA, Feb. 2018.
"Microfluidic Approaches for Quantitative Analysis and Screening of Synthetically Engineered Microbes" (Advisor: Taesung Kim)

M.S. in Biomedical Engineering
Ulsan National Institute of Science and Technology, Ulsan, KOREA, Feb. 2014.
"Microdroplet in a Cavity Array for High-Throughput Screening and Bio-technological Applications" (Advisor: Sung Kuk Lee)

B.S. in Chemistry
Kangwon National University, Chuncheon, KOREA, Feb. 2012
Study Abroad. Washington Semester Program, American University, USA, Dec. 2010, *Fully Funded ($20,000)*

WORK EXPERIENCES

Research Assistant: Mar. 2014 – Dec. 2017
Biomedical Engineering, Ulsan National Institute of Science and Technology, Ulsan, KOREA

Research/Teaching Assistant: Mar. 2012 – Feb. 2014
Biomedical Engineering, Ulsan National Institute of Science and Technology, Ulsan, KOREA

Teaching Assistant: Mar. 2010 – Jun. 2011
Chemistry Department, Kangwon National University, Chuncheon, KOREA

Abroad Research Internship: Sep. 2009 – Dec. 2009
Alter Consulting-LLC, Washington D.C. 20011. USA.

Served as Mandatory Military Service: Dec. 2005 – Dec. 2007
Marine Corps, Pohang, KOREA

AWARD, HONORS, SCHOLARSHIP & CERTIFICATES

Graduate - UNIST

- The Best Paper Oral Presentation Award at KSME* Conference 2016
- The Best Poster Presentation Award at KSME* Conference 2014
- Excellent Student Oral Presentation Award at KMB** 2013

* *KSME (Korea Society of Mechanical Engineering)*
** *KMB (Korea Society of Microbial Biology)*

Undergraduate - Kangwon National University

- Quarter Tuition Scholarship (*Approximately $500-700 for Every Semester)*, Kangwon National University, Chuncheon, KOREA, Mar. 2004 – Feb. 2012
- Best Marine Sergeant in Division, Pohang 1st Marine Division, Dec. 2007
- Fully Funded Scholarship (*$20,000 for a semester* from SAF Foundation KOREA), Washington Semester Program, American University, Sep. 2010
- National Funded Student for a semester (*Approximately $2,000*) from Korea National Scholarship Foundation (KOSAF), May. 2011
- BK21 Student English Presentation Award (*$1,000 for Top 5 Students*), Kangwon National University, Dec. 2011
- Self User Certificates for Analytical Instruments (GC/MS/HPLC), Nov. 2011

JOURNAL PUBLICATIONS

- Impact Factor (IF) and Cited Times (CT) are based on Web of Science at the present.
- '+' indicates that the authors contributed equally.

1. **Ji Won Lim**, Kwang Soo Shin, Sung Kuk Lee* and Taesung Kim*, High-throughput Screening of acyl-CoA *Thioesterase* Mutant of 10^6 Library using Microfluidic Fluid Array Platform, (*In Preparation*)
2. Juyeol Bae, **Ji Won Lim**, and Taesung Kim*, Reusable and storable whole-cell microbial biosensors with a microchemostat platform for in-situ on-demand heavy metal detection, ***Sensors and Actuators:B***, (Under Revision)
3. Minseok Kim, **Ji Won Lim**, Sung Kuk Lee, and Taesung Kim*, Nanoscale Hydrodynamic Film for Diffusive Mass Transport Control in Compartmentalized Microfluidic Chambers, ***Analytical Chemistry***, 2017, Online Published. (IF=6.32, CT=0)
4. Dong-Joo Kim, Dogyeong Ha, Qitao Zhou, Ashishi Kumar Thokchom, **Ji Won Lim**, Jongwan Lee, and Taesung Kim*, Cracking-assisted Micro-/Nanofluidic Fabrication Platform for Silver Nanobelt Arrays and Nanosensors, ***Nanoscale***, 2017 (IF=7.367, CT=0)
5. **Ji Won Lim**, Kwang Soo Shin, Jaemin Moon, Sun Kuk Lee, Taesung Kim*, A Microfluidic Platform for High-Throughput Screening of Small Mutant Libraries, ***Analytical Chemistry***, 2016, 88(10), pp:5234-5242. (IF=6.32, CT=1)
6. Hyun Ju Kim+, **Ji Won Lim**+, Haeyoung Jeong, Sang-Jae Lee, Dong-Woo Lee, Taesung Kim*, Sang Jun Lee*, Development of a Highly Specific and Sensitive Cadmium and Lead Microbial Biosensor using Synthetic CadC-T7 Genetic Circuitry, ***Biosensors & Bioelectronics***, 2016, 79, pp:701-708. (IF=7.78, CT=2)
7. **Ji Won Lim**, Dogyeong Ha, Jongwan Lee, Sung Kuk Lee, Taesung Kim*, Review of Micro/Nanotechnologies for Microbial Biosensors, ***Frontiers in Bioengineering and Biotechnology***, 2015, 3, Article No.61 (IF=3.02, CT=14)

8. Minseok Kim+, **Ji Won Lim**+, Hyun Ju Kim, Sung Kuk Lee, Sang Jun Lee* and Taesung Kim*, Chemostat-like Microfluidic Platform for Highly Sensitive Detection of Heavy Metal Ions using Microbial Biosensors, ***Biosensors & Bioelectronics***, 2015, 65, pp:257-264. (IF=7.78, CT=26)

CONFERENCE PROCEEDINGS

International Conferences

1. **Ji Won Lim**, Sung-Kuk Lee, Taesung Kim, Microfluidic High-Throughput Screening Device for Small Mutant Libraries, 8th International Conference on Microtechnologies in Medicine and Biology (MMB) 2016.
2. **Ji Won Lim**, Minseok Kim and Taesung Kim, A Microfluidic Platform for Programmable Cell Culture Environments, IBEC 2015.
3. **Ji Won Lim**, Sung Kuk Lee and Taesung Kim, A Large-area Fluid Patterning Platform for High-throughput Screening of Small Mutant Library, microTAS 2015.
4. **Ji Won Lim**, Minseok Kim, Sung Kuk Lee, Taesung Kim, Chemostat-like Microfluidic Platform for Highly Sensitive Detection of Heavy Metal Ions Using Microbial Biosensors, IEEE-SENSORS 2015.
5. Dogyeong Ha, **Ji Won Lim**, Taesung Kim, Live-Cell Printing for Screening of Engineered Bacterial Strains, Biofabrication 2014.
6. **Ji Won Lim**, Taesung Kim, Sung Kuk Lee, Agitation Programmable Picoliter Droplet Arrays For HTS of Recombinant Escherichia Coli, MicroTAS 2013. (**Marked as Top 15% Rated Proceeding**)

Domestic Conferences

1. Juyeol Bae, **Ji Won Lim**, Taesung Kim, A Microchemostat Platform for Reusable *in situ* Whole-cell Microbial Biosensors, KSME 2017.
2. **Ji Won Lim**, Sung Kuk Lee, Taesung Kim, Microfluidic high-throughput Screening Device for Small Mutant Libraries of Recombinant *Escherichia Coli*, Microbial Biotechnology Conference 2016.
3. **Ji Won Lim**, Sung Kuk Lee, Taesung Kim, Microfluidic High-throughput Screening Device for Small Mutant Libraries of Recombinant *Escherichia coli*, KSME 2016. (***The Best Paper Oral Presentation Award***)
4. **Ji Won Lim**, Sung Kuk Lee, Taesung Kim, A Fluid Array Platform for High-throughput Screening of Small Mutant Libraries, KMEMS 2016.
5. **Ji Won Lim**, Sung Kuk Lee, Taesung Kim, Characterization of Fluid Patterning Platform for High-throughput Screening of *Escherichia coli*, KSME, 2015.
6. **Ji Won Lim**, Sung Kuk Lee, Taesung Kim, High-throughput Screening of Recombinant *Escherichia coli* using Fluid Patterning Technology, KMEMS, 2015.
7. **Ji Won Lim**, Minseok Kim, Hyun Ju Kim, Sang Jun Lee, Taesung Kim, Chemostat-like Microfluidic Platform for Highly Sensitive Detection of HMIs Using Microbial Biosensors, KSME, 2014.
8. **Ji Won Lim**, Sung Kuk Lee, Taesung Kim, Fluid Patterning for High-throughput Screening of Synthetic Microbes, KSME, 2014.
9. **Ji Won Lim**, Sung Kuk Lee, Taesung Kim, Fluid Patterning for High-throughput Screening of Synthetic Microbes, KSME-spring, 2014. (***The Best Poster Presentation Award***)
10. **Ji Won Lim**, Taesung Kim, Sung Kuk Lee, Agitation Programmable Picoliter Bioreactor in Droplet Array for HTS of Recombinant *Escherichia coli*, The Korean Society for Microbiology and Biotechnology 2013. (***Excellent Student Presentation Award***)

11. **Ji Won Lim**, Taesung Kim, Sun Kuk Lee, Agitation Programmable Picoliter Bioreactor in Droplet Array for HTS of Recombinant *Escherichia coli*, KSME-spring, 2013.

PATENTS (Registered)

1. Biosensor for Detecting Heavy Metals using a Microbe by Taesung Kim, **Ji Won Lim**, Minseok Kim, *Registration Number: 10-1724015 (03.31.2017)*
2. Microfluidic Cultivating Apparatus and Manufacturing Method for the Same and Method for Screening Microfluidic using the Same Device by Taesung Kim, **Ji Won Lim**, *Registration Number: 10-1782105 (05.13.2016)*

REFERENCES

Graduate - UNIST

- Taesung Kim, Associate Professor in Mechanical Engineering, Ulsan National Institute of Science and Technology. Tel) 82-052-217-2313. Email: tskim@unist.ac.kr
- Sung Kuk Lee, Associate Professor in Chemical Engineering, Ulsan National Institute of Science and Technology. Tel) 82-052-217-2574. Email: sklee@unist.ac.kr
- Cheol-min Ghim, Associate Professor in Physics Department, Ulsan National Institute of Science and Technology. Tel) 82-052-217-2517. Email: cmghim@unist.ac.kr

Undergraduate - American University, Kangwon National University

- Jeffrey Sosland, Assistant Professor in School of Professional and Extended Studies, American University. Tel) 1-202-895-4922. Email: sosland@american.edu
- Hyonseok Hwang, Associate Professor in Chemistry Department, Kangwon National University. Tel) 82-033-250-8497. Email: hhwang@kangwon.ac.kr

-- END --